N° d'ordre :
N° de série :

UNIVERSITE KASDI MERBAH OUARGLA
FACULTE DES SCIENCES APPLIQUEES
DEPARTEMENT DE GENIE MECANIQUE

Thèse

Présentée pour l'obtention du diplôme de

Doctorat en sciences

Spécialité : Génie Mécanique

Présenté par:

Messaoud SANDALI

Thème

Contribution à l'étude d'amélioration des performances thermiques des séchoirs solaires utilisant différentes techniques d'apport de chaleur

Soutenue publiquement le : 13/06/2019
Devant le jury composé de :

Boubekeur Dokkar	**Professeur**	**Université Kasdi Merbah Ouargla**	**Président**
Hosine Benmoussa	**Professeur**	**Université Elhadj Lakhder Batna**	**Examinateur**
Rachid Saim	**Professeur**	**Université Abou bakr Belkaid Tlemcen**	**Examinateur**
Abdelghani BOUBEKRI	**Professeur**	**Université Kasdi Merbah Ouargla**	**Directeur de thèse**

Order number:
Serial number:

A thesis submitted to the University Kasdi Merbah Ouargla for the degree of Doctor of Philosophy (PhD) in The Faculty of Applied Sciences, Mechanical Engineering Department

Presented by:
Messaoud SANDALI

Theme

Contribution to the performance improvement study of solar dryers using different heat supply techniques

Discussed publicly on: 13/06/2019
Before the jury composed of:

Boubekeur Dokkar	**Professor**	**Kasdi Merbah Ouargla University**	**Chairman**
Hocine Benmoussa	**Professor**	**Elhadj Lakhdar University**	**Examiner**
Rachid Saim	**Professor**	**Abou Bakr Belkaid University**	**Examiner**
Abdelghani BOUBEKRI	**Professor**	**Kasdi Merbah Ouargla University**	**Supervisor**

Thanks

The work presented in this thesis was carried out within the Laboratory of Development of New and Renewable Energies in Arid Zones (LENREZA), faculty of sciences and technology and taterials sciences, university of Kasdi Merbah Ouargla. On this occasion, I would like to express my warmest thanks to the director and all members of the LENREZA laboratory.

I would like to thank in a very special way my PhD supervisor, **Pr. Abdelghani Boubekri** for his patience, understanding, advice and the confidence he always showed me during the realization of this work. I also thank very much **Dr. Djamel Mennouche** for his help and advice during the period of the experimental work of our study.

I am very appreciative to the honor we have done to **Mr. Dokkar Boubekeur** of Kasdi Merbah Ouargla University for having accepted to preside over the jury; that he finds here my deep gratitude and my sincere thanks.

My thanks also go to the examiners of our thesis **Mrs Benmoussa Hocine** and **Saim Rachid** for having devoted time to the examination of this work. I am very sensitive to the honor they gave me by participating in the jury of our thesis. Whose they find here the expression of my gratitude!

I would like to thank also all those who supported and helped me to perform this work. Finally, I intend to dedicate this work to my parents and all the members of my family, as well as to the entire drying team of LENREZA laboratory.

ملخص

تقدم هذه الأطروحة دراسة تجريبية وتحليلية للأداء الحراري لمجفف شمسي مباشر. لقد تم بحث ومناقشة تقنيات مختلفة للإمداد بالحرارة باستخدام المبادل الحراري والتخزين الحراري الكامن والتخزين الحراري الحساس خلال هذه الأطروحة. تم وضع المبادل الحراري فوق الصفيحة الماصة التي تواجه الثقوب وذلك لإتاحة اختراق الهواء. وعلاوة على ذلك ، أجريت محاكاة عددية وتمت مقارنة النتائج مع التجريبية. تم دمج طبقة مسطحة من مادة تغيير الطور (PCM) تحت لوحة الامتصاص بهدف تخزين الطاقة الحرارية الكامنة جزئيًا. تم دمج PCM بسماكات مختلفة وخصائص فيزيائية مختلفة. وقد تم اختبار تقنية أخرى لإمدادات الحرارة التي تركز على تخزين الحرارة الحساسة عبر طبقة من وسط مسامي مكسور (سرير من الصخور) فوق لوحة الامتصاص. تم تنفيذ العديد من عمليات المحاكاة الرقمية باستخدام طريقة الحجم المحدودة باستخدام نموذج ثنائي غير مستقر تم تنفيذه على برنامج CFD Fluent. وأظهرت النتائج أن دمج المبادل الحراري يحسن أداء مجفف الشمسي بشكل كبير. بعد غروب الشمس وطوال الليل ، تظل درجة حرارة هواء التجفيف مهمة ومستقرة تقريبًا بمتوسط قيمة 46 درجة مئوية. يضمن التكامل بين المبادل الحراري استمرارية عملية التجفيف في الليل وحتى خلال الأيام الملبدة بالغيوم. علاوة على ذلك، أظهرت النتائج من حالة طبقة MCP تحسنا ملحوظا في السلوك الحراري، خصوصا في الفترة بعد الغروب. خلال الساعات غير المشمسة، سيوفر السائل PCM الحرارة للامتصاص؛ إنها الحرارة المفيدة للسائل المبرد. لذلك، فإن سائل نقل الحرارة لا يزال يوفر الحرارة بعد غروب الشمس. ومع ذلك، فإن درجة حرارة تجفيف الهواء تزداد بمقدار 4 درجات مئوية مع دمج وسط مسامي. تم إجراء تحليل اقتصادي للمجفف الشمسي عن طريق حساب تكلفة دورة الحياة (LCC) ، واستحقاق دورة الحياة (LCB) وفترة الاسترداد. هذا التحليل يثبت جدوى مجففنا الشمسي. ومع ذلك ، فقد تم اختيار تقنية استخدام مبادل الحرارة الجوفية باعتبارها الأهم بسبب فترة الاستثمار (0.9 سنة) التي تم الحصول عليها باستخدام هذه التقنية.

الكلمات المفتاحية: *مجفف شمسي مباشر ، مبادل حراري ، ماء جوفي حراري ، وسط مسامي ، مواد تغيير الطور ,تحليل اقتصادي*

Résumé

Cette thèse présente une étude expérimentale et numérique de la performance thermique d'un séchoir solaire direct. Différentes techniques d'apport de chaleur utilisant un échangeur de chaleur, un stockage de chaleur latente et un stockage de chaleur sensible ont été étudiées et discutées dans cette thèse. L'échangeur de chaleur a été placé délibérément au-dessus de la plaque absorbante afin de permettre la pénétration de l'air. De plus, une simulation numérique a été faite et les résultats ont été comparés à ceux de l'expérimental. Une couche plate de matériau à changement de phase (MCP) a été intégrée sous la plaque absorbante dans le but de stocker partiellement de l'énergie thermique à chaleur latente. Le MCP a été intégré avec différentes épaisseurs et différentes propriétés thermo-physiques. Une autre technique d'apport de chaleur basée sur le stockage de chaleur sensible a travers de l'intégration d'une couche plate d'un milieu poreux fracturé (lit de roches) au-dessus de la plaque absorbante a été testée. Plusieurs simulations numériques utilisant la méthode des volumes finis à l'aide d'un modèle instationnaire bidimensionnel implémenté sur le logiciel CFD Fluent ont été réalisées. Les résultats ont montré que l'intégration de l'échangeur de chaleur améliore considérablement les performances du séchoir solaire. Après le coucher du soleil et durant toute la nuit, la température de l'air de séchage reste importante et presque constante avec une valeur moyenne de 46 ° C. L'intégration de l'échangeur de chaleur assure la continuité du processus de séchage dans la nuit et même dans les journées nuageuses. De plus, les résultats du cas de l'intégration d'une couche de MCP ont montré une nette amélioration du comportement thermique, en particulier après le coucher du soleil. En dehors des heures ensoleillées, le MCP liquide fournira de la chaleur à l'absorbeur; c'est la chaleur utile du liquide de refroidissement en circulation. Par conséquent, le fluide caloporteur fournit toujours de la chaleur après le coucher du soleil. Cependant, la température de l'air de séchage augmente avec une valeur de 4 °C avec l'intégration du milieu poreux. Une analyse technico-économique du séchoir solaire a été réalisée en calculant le coût du cycle de vie (LCC), bénéfice du cycle de vie (LCB) et la période de récupération. Cette analyse prouve la faisabilité de notre séchoir solaire; Toutefois, le technique de l'apport de chaleur utilisant l'échangeur de chaleur à eau géothermique a été choisie comme la plus importante due a la période de retour d'investissement (0.9 an) obtenue avec l'utilisation de cette technique.

Mots clés: *Séchoir solaire direct, échangeur de chaleur, MCP, eau géothermique, milieu poreux, matériau à changement phase, analyse économique.*

Abstract

This thesis presents an experimental investigation and simulation study of the thermal performance of a direct solar dryer. Different techniques of heat supply using heat exchanger, latent heat storage and sensible heat storage have been investigated and discussed throughout this thesis. The heat exchanger was placed deliberately above the absorber plate facing the holes so as to enable the air penetration. Moreover, numerical simulation was carried out and results were compared with the experimental. A flat layer of phase change material (PCM) has been integrated below the absorber plate with the aim of partially storing latent heat thermal energy. The PCM has been integrated with different thicknesses and different thermo-physical properties. Another technique of heat supply focusing on the storing of sensible heat throughout integration of a flat layer of a fractured porous medium (rocked bed) above the absorber plate has been tested. Several numerical simulations using the finite volume method using a two-dimensional unsteady model implemented on CFD Fluent software have been carried out. The findings showed that the integration of heat exchanger improves significantly the solar dryer performance. After sunset and throughout the night, the drying air temperature remains important and almost steady with an average value of 46 °C. The integration of the heat exchanger ensures the continuity of drying process at the night and even during cloudy days. Furthermore, the results from the case of integration of a layer of MCP showed a marked improvement in thermal behavior, especially in the period after sunset. During non-sunny hours, liquid PCM will provide heat to the absorber; it is the useful heat of the coolant in circulation. Therefore, the heat transfer fluid still provides heat after sunset. However, the temperature of drying air is increased by 4°C with integration of porous medium. A technical-economic analysis of the solar dryer was done by computing life cycle cost (LCC), life cycle benefit (LCB) and payback period. This analysis proves the feasibility of our solar dryer; however, the heat supply technique of heat exchanger with geothermal water was chosen as the most recommended one forasmuch to the short payback period (0.9 year) obtained after using it.

Keywords: *Direct solar dryer, heat exchanger, PCM, geothermal water, porous medium, phase change materiel, economic analysis.*

Contents

CHAPTER I: Review study on the solar drying process and solar dryer's improvement

CHAPTER II: Improvement of a direct solar dryer performance using a geothermal water heat exchanger as supplementary energetic supply. An experimental investigation and simulation study

Chapter III: Thermal Behavior Modeling of a Cabinet Direct Solar Dryer as Influenced by Sensible Heat Storage in a Porous Medium

Chapter IV: Latent heat storage technique applied to a direct solar dryer

CHAPTER V: Comparative mixed mode solutions and technical-economic study

Nomenclature

Signification	**Symbols**	**Units**
Solar Dryer Width	W	M
Solar Dryer Length	L	M
Insulation Thickness	Hi	M
Glass Cover Thickness	Hg	m
Absorber Thickness	Ha	m
Air Inlet Thickness	Hl	m
Chimney Diameter	Ec	m
Chimney Length	Lc	m
Dynamic Viscosity	μ	kg/m.s
Density of Fluid	ρ	kg/m^3
Pressure	P	Pa
Permeability of the Porous Medium	K	m^2
Particle Diameter	d_p	m
Porosity of the Medium	ϕ	-
Inertia Coefficient	C	-
Thermal Conductivity of the Medium	λ_m	W/m.K
Average Ambient Temperature	$\bar{T}_{ao}$	K
Temperature Amplitude	$\bar{T}_{ar}$	K
Maximum Solar Intensity	$\hat{G}_{sun}$	W/m^2
Time in Hours	τ	-
Time of Sunrise	a	-
Time of Sunset	b	-
Heat Exchanger	HE	-
Solar Water Heater	SWH	-
Phase Change Material	PCM	-
Porous Medium	PM	-
Heat Transfer Coefficient	h_v	W/m^2K
Temperature	T	K
Heat Generation	S_T	K

General Introduction

Nowadays, the needs for dried agricultural production, marine products and medicinal plants have increased considerably in the world [1]. Renewable energy can play an important role to meet its world demand. Actually, solar energy is most reliable and eco-friendly. It can be used in different ways as solar PV or solar thermal for pumping and drying crops in agricultural sectors [2]. It is an effective alternative source of energy that is relatively preferred to other sources because it is free, abundant and non-pollutant in nature compared with higher prices of fossil fuels [3-4]. It is a permanent and environmentally compatible source of energy in the world. Agricultural and marine products for storage must first be dried to preserve the quality of the final products [5]. In the method of production of crop, treatments of post harvest are highly requested by thermal means in several applications of food engineering. Actually, heat treatments are preferred because they can avoid the chemical treatments side effects [6]. Between all sources of renewable energy, such as air, wind, and water, the one which has the least impact on the environment is the solar energy [7].

The application of solar energy was seen since the existence of human being on the earth. Nowadays, the way of life of the people is dependent on the energy production and utilization; and hence, the demand and supply of energy is increasing in modern communities. At present, 77% of the world's energy is supplied by fossil fuels, which release polluting and greenhouse gases, degrades ozone layer and excessively threatens environment. Moreover, in order to maintain an unharmed environment, considering alternate energy sources has become an essential task [8].

Along with air and water, food is a basic need for all human beings. Food problem appears in most developing countries mainly due to the inability to conserve food surpluses rather than due to low production. Agricultural production is usually more than the consumption needs, resulting in wastage of food excesses during the short harvest periods and scarcity during post-harvest period [9].

Various drying techniques are employed to dry different food products. Each technique has its own advantages and limitations. Choosing the right drying techniques is thus important in the process of drying of the perishable products. To reduce its dependence on solar radiation for operation and to improve the quality of drying, a biomass stove was incorporated with solar drier.

Solar dryers are generally classified as direct, indirect and mixed mode. Air circulation through the dryer is provided either natural or forced (with a fan). Naturally convection solar dryers are generally inefficient because air circulation is quite low. Some studies have revealed that the use of solar chimneys can improve the flow of air (flow and velocity) through the solar dryer. This technique has become the real heat engine in most natural convection solar dryers.

The major limitation of using solar dryers comes from the discontinuous nature of solar energy. This latter is an energy supply in which the intensity depends on the place, the time of day, the season and the weather conditions. As a result, it is often necessary to integrate new techniques of heat supply to reduce the effects of discontinuity and improve the efficiency of solar dryers.

In this perspective, the present work is particularly interested in the numerical simulation of the thermal behavior of a direct solar dryer with no load. Numerical simulations were performed using the finite volume method using a two-dimensional unsteady model implemented on CFD Fluent software. The characteristics of the laptop used in these numerical simulations are:

-Processor: Intel (R) Core (TM) i5-2430M CPU @ 2.40GHz

-RAM: 4, 00 Go

-ROM: 500 Go

To better understand the scope of the treated subject, this thesis is structured in five chapters.

The first chapter presents a brief and recent bibliographic synthesis on solar drying systems and the different technologies used to improve their thermal performance. The contents of this chapter were inspired from the similar previous studies.

The second chapter presents an experimental investigation and simulation study of the thermal performance of a direct solar dryer with integration of heat exchanger as a supplementary heat supply. The experiment was performed in laboratory of development of new and renewable energies in arid zones (LENREZA). The heat exchanger is connected with two different sources of heat; geothermal water and solar water heater in order to evaluate the effect of each one on the thermal performance of the solar dryer.

The third chapter presents a simulation study of the thermal performance of a direct solar dryer with integration of a porous medium for storing of sensible heat. The effect of the nature, the thickness and the porosity of the porous medium on the

thermal performance of the solar dryer is presented and discussed throughout this chapter.

The fourth chapter presents a simulation study of the effect of the integration of a flat layer of phase change material (PCM) on the performance of a direct solar dryer. The effect of the nature and the thickness of the phase change material is studied and presented too.

The fifth chapter includes a comparative study as a first part in order to analyze and to choose between the different techniques of heat supply used in this work, and a technical-economic study as a second part in order to evaluate the benefit of the solar drying system.

A general conclusion illustrates the strong points of this work which is focused on the thermal performance of a direct solar dryer and presents the perspectives which may constitute the favorable continuation of our study.

Chapter I:

Review study on the solar drying process and solar dryer's improvement

I.1 Introduction

This chapter presents a review of the previous works dealing with the improvement of solar dryers' efficiency. This study is aimed thus to determine the different techniques and factors which can highly improve the thermal performance of solar drying systems. The effect of some parameters such as operating conditions, geometrical conditions, adding of reflectors, heat exchanger and heat pump, photovoltaic source, air circulation mode, and phase change material on the efficiency of solar drying system was considered and discussed.

I.2 Solar drying process

Drying is one of the important post-handling processes of agricultural production [4-10]. It has been applied since immemorial times to preserve agricultural products [11-12]. It is known as the process of removing moisture from a product and can be implemented in two steps. In the first step, the moisture inside the product is brought to the surface and dried in air at a constant rate as water vapor. The second step involves a slow drying rate, and its process is related to the properties of the product to be dried [13-15]. Moreover, drying extends the shelf life of product and provides a light-weight product for transportation and reduces storage capacity [14]. Open-air drying is the most commonly used procedure, especially in tropical and subtropical places. However, a lot of disadvantages are usually found: product damage caused by rodents, insects and birds; product degradation due to direct exposure to rain, sun light, storms, and dew; contamination with particles and gases due to air pollution; possible cracking of the product and loss of germination capacity [12-16].

Controlled drying is applied generally in industrial drying process. Warm air in such processes is usually provided by burning of fossil fuels, and large quantities of fuels are used along the world for this objective. The high cost of fossil fuels, and the environmental impacts of their use has put severe constraints on their consumption. Most rural locations of developing countries suffer from non-access to grid electricity. Supplies of other non-renewable sources of energy are unreliable, unavailable and too expensive for many farmers. In such places, crop-drying systems that make use of electrically operated heaters, fans and other accessories are inconvenient [17].

I.3 Solar drying applications

The application of solar drying in industrial sectors can be investigated for different materials, such as brick, biomass, cement, polymers, textile, paper and allied products, and timber as well as for different processes, such as drying of porous materials, pharmaceutical processes, and wastewater treatment. In this time, the use of solar dryers in wastewater treatment reduces the duration and the expenses of the conventional drying process [13]. Solar dryers can be proved to be very useful devices from the energy preservation point of view. They circumvent some of the major disadvantages of classical drying [4]. Solar dryers have one of the most promising applications of solar energy technology. In solar dryers, solar energy was used as supplemental sources or as the sole sources of the needed heat, and the air flow can be generated by natural or forced convection. The technical directions in the development of solar dryers are integrated storage, compact collector design, high efficiency and long-life drying system. Water based collectors can also be used whereby water to air heat exchanger can be used. The hot drying air can be forced to flow in the water to air heat exchanger. The hot water reservoir acts as heat storage source of the solar dryers. The heat pump drying system can be effective use for as part of solar drying systems. Therefore, innovative applications of photovoltaic system for simultaneous production of electricity and heat are suitable as standalone applications and totally operated on solar energy [16].

I.4 Classification of solar dryers

Solar dryers may be broadly classified into different types. Basically, four types of solar dryers have been successfully employed for the drying of horticultural produce. They are direct solar dryers, indirect solar dryers, mixed mode solar dryers and hybrid solar dryers [14]. In fact, the operation of these dryers is primarily based on the principle of natural or forced air circulation mode.

I.4.1 Direct solar dryer

In direct solar dryers, product is exposed directly to sunlight so that it can be simply dehydrated. In this type of solar dryers, a black painted heat absorbing plate is provided that can collect and absorb the sunlight and converts it into heat. The product to be dried is placed directly on the absorber plate. This dryer may has glass lid covers and vents in order to increase thermal efficiency [8]. The solar dryer cabinet is a kind of direct solar dryer as shown in Fig I.1.

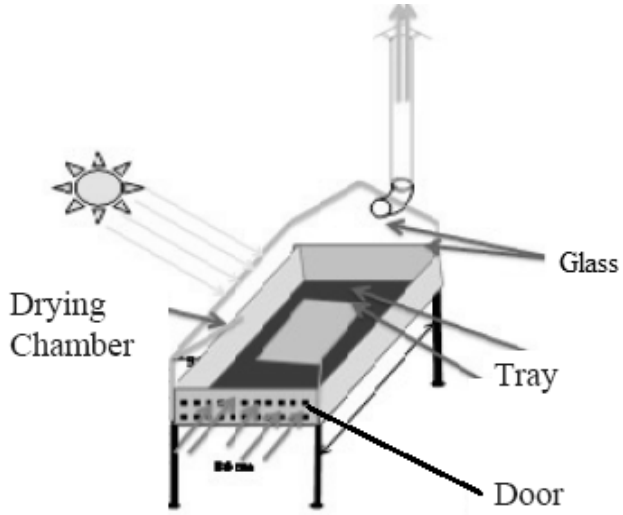

Fig I.1 Direct solar dryer [3].

I.4.2 Indirect solar dryer

Indirect solar dryers are consisted of a solar collector and a drying chamber. In the solar collector, the black painted heat absorbing surface heats the ambient air, instead of direct exposure of product to sunlight. The heated air is subsequently passed through the product which is placed inside drying room, takes the product moisture and exit through the chimney [8]. A diagram of an indirect solar dryer is shown in Fig I.2.

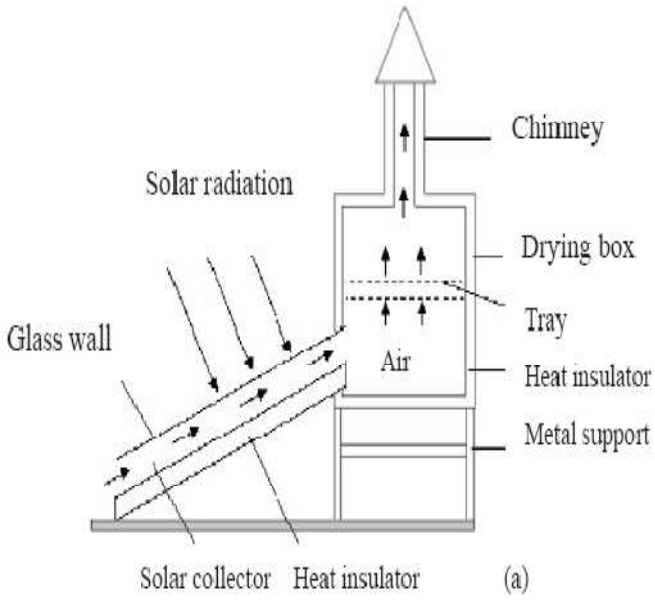

Fig I.2 Indirect solar dryer [6].

I.4.3 Mixed mode solar dryer

The mixed-mode solar dryer is a combination of indirect and direct solar dryer. This works under the combined action of the solar intensity incident on the product to be dried and the air preheated in solar collector provides the heat needed for the drying process [8]. A diagram of a mixed-mode solar dryer is shown in Fig I.3.

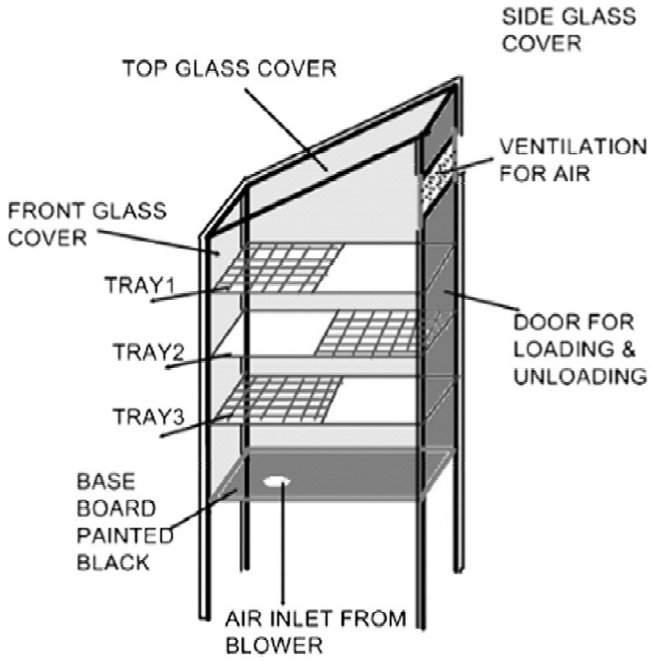

Fig I.3 Mixed-mode solar dryer [8].

I.4.4 Hybrid solar dryer

In the hybrid solar dryer, several sources of energy can be used along with solar energy to ensure suitable drying conditions (Fig I.4). Moreover the drying process is not dependable only on the solar intensity. The blower can be used for proper air movement in hybrid solar dryer which can be run on by a photovoltaic system. Hybrid solar drying system can control drying of any agricultural product efficiently and also helps to preserve the suitable quality of the product [8].

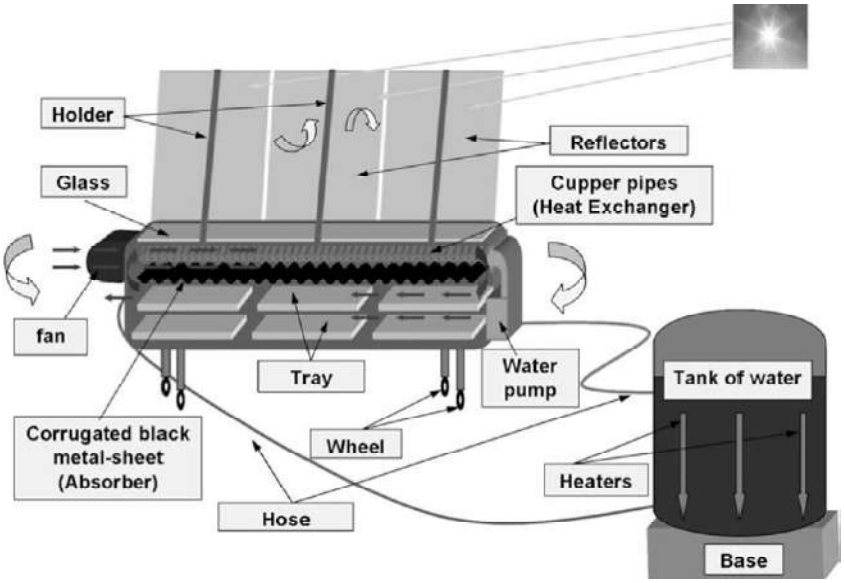

Fig I.4 Schematic diagram of a hybrid solar dryer [54].

I.5 Drying technologies and method

Different solar dryers for food drying have been evaluated and constructed. They are available in different sizes and designs based on drying capacity. To evaluate a solar dryer, it is essential to test its performance with the other solar dryers. The obtained results give the needed information to the manufacturers, users and researchers.

Ramana et al [18] presented the status of drying technologies in developed countries. Development and performance evaluation of different types of solar dryers were presented. Various types of dryers like natural convection and forced convection dryers, direct and indirect dryers, integral dryers, greenhouse dryers, cabinet dryers, tunnel dryers, mixed mode dryers were reviewed. Pirasteh et al [19] presented a review on the development of the solar drying application. They classified solar drying application into two main categories, that is, industrial and agricultural. It was concluded that solar energy enables the industries and agricultural sectors to improve their energy stability, modify their energy requirement, and increase energy sustainability which lead to the improvement in the system efficiency. Mustayen et al [20] presented a performance study of different solar dryers. They discussed the indirect, direct, and mixed mode, active, and passive solar dryers that have shown potential in drying of agricultural products. Direct solar dryer is found to be suitable for small farmers in rural areas where the electrical power is not available. The indirect-type natural convection solar dryer is useful for drying fruits and vegetables in rural areas. The mixed-mode solar dryer is readily available, cheap, and can be easily made by local farmers. The

natural convection solar dryer is more advantageous and applicable than other types. The forced convection dryer is used in small firms with limited financial support from large industrial sectors. Shobhana et al [21] tested thermally various solar dryer designs operated for natural and forced convection. The steady state mathematical model based on heat balance concept of solar dryer without load is applied to identify the dimensionless parameter called no-load performance index (NLPI). By comparison between the dryers, it was found that the mixed mode dryer exhibits maximum value of NLPI followed by indirect ones for both natural and forced convection. Tchamye Boroze et al [22] presented the inventory and comparative characteristics of solar dryers used in the Sub-Saharan zone. Thermo-economic analysis was carried out to determine which dryers were most successfully adopted. The criteria used to compare the dryers were the drying time, the dryer mass capacity, the treated product flow and the dryer efficiency. The results showed that most of the dryers found in the field and also studied beforehand were indirect solar dryers, but they did not satisfy the users because of their low capacity and over-long drying time. The cause of dissatisfaction of the users is that the acquisition and development of the dryers were greatly influenced by social, economic and physical criteria. Pangavhane et al [23] presented a review of research and development work on solar dryers for grape drying. It was found that to improve the acceptability of the solar dryer among the farmers, it is necessary to develop a large scale solar dryer, which is economically favorized. Forced convection and thermal energy storage system are necessary to continue drying process and for assuring reliability and better control respectively. Mennouche et al [3] proposed and investigated a new postharvest method using a laboratory scale direct solar dryer in order to valorize hard Deglet-Nour dates. Dates samples were soaked in distilled water than dried by solar drying mean. They proposed three drying enhancements methods to improve the quality of date: drying under shade (DUS), drying with photovoltaic powered ventilation (DSV) and combination drying method (DCM). It was found that the drying with solar ventilation mode (DSV) and (DCM) were classified in favorable operating conditions needed for the studied case. The combination drying method was selected as the most adequate process to realize the processing time and quality criteria.

I.6 Factors and techniques used for improving solar dryers' efficiency

Thermal performance of solar drying systems depends on a lot of factors and techniques which can affect the drying process. Determination and definition of these factors helps to improve the efficiency of solar dryers such as the insurance of the continuity of the drying

process in the night with preserving the good quality of the dried products. Below, several studies list and mention the major factors and techniques which can improve the efficiency of solar drying systems.

Mojgan Zarezade et al [24] identified the effective factors and risks which may impact on the use of solar dryers. Factor analysis (FA) methodology was performed using SPSS software. Results of analysis reveal that there are three risk types and six major factors impacting the process of constructing, designing and implementation of solar dryers. It can be concluded that those six factors regarding solar dryer implementing; such as geographical situation, performance (quality and speed of drying), infrastructures (private investors, sufficient knowledge…etc), financial support, cultural and political (project delivery and economic conditions), and social (farmer knowledge about solar dryers). The risks impact on the construction and implementation of solar dryers can be categorized into three major categories; external risks, construction risks, and financial risks.

Crops are dried for long-term storage. Drying is a important process in preserving foods to make it available to consumers during the whole year; however, many factors affect the drying process [25]. The main factors affecting efficiency of drying are presented in the following parts.

I.6.1 Operating conditions

Xiao et al [26] studied the effect of drying temperature, air velocity, and sample thickness on thin-layer air impingement drying characteristics and quality of American ginseng slices. It was found that thin-layer air impingement drying enhances drying rate dramatically compared with other drying methods. Drying temperature, air velocity and sample thickness affected on the rehydration rate and the drying time of dried slices. Sarsavadia [27] studied the effect of the air flow rate (2.43, 5.25, 8.09 kg/min), air temperature (55, 65, 75°C) and fraction of recycled air (up to 90%) on the energy requirement of drying. The dryer was consisting of a solar air heater having corrugations and triangular fins to the absorber plate. The energy required for drying of onion slices from initial moisture content of 86% to final moisture content of 7% was found between 23.548 and 62.117 MJ/kg water. It was found that the savings in total energy due to fraction of recycled air were determined at 65 and 75°C air temperature for the above three air flow rates. The total energy required for drying of onion slices increased with increase in airflow rate and decreased with increase in drying air temperature. Manaa et al [28] studied the solar drying of tomato in the arid area. The experiments were performed with a forced convection indirect solar dryer. The experiments

showed the influence of the variety of tomato on drying curves, the temperature of the drying air and the size of the cut slices. The obtained results showed that the water content and the speed of drying were affected by different parameters (the air speed, the air temperature, the pretreatment and the thickness of the product). The increase in the drying air temperature and the reduction thickness of the slices increase the drying speed and decrease the drying time. The effect of the air velocity is less in comparison with the effect of the temperature. Shafiq et al [29] studied experimentally a direct and an indirect solar biomass dryer, in terms of its optimal configuration, drying capability and suitability of usage for different conditions. The results show that the level of air flow, the manner of which sunlight is absorbed and climatic conditions affect the drying rate.

I.6.2. Geometrical factor

Several types of solar dryers with air based solar collectors had been constructed, tested and developed in various countries, yielding varying degrees of technical performance. These designs have been constructed in different geometries in order to enhance the drying time and the dried product quality.

A foldable solar grape dryer was developed and fabricated by Nair and Bongirwar [30]. The side walls of the dryer are fabricated using aluminum sheet and painted black from outside. The dryer is able o dry about 100 kg of grapes at a time. Drying air temperature was found to be twice of the ambient temperature at noon. The main drawback of this dryer is that an increase in outside wind velocity may decrease the inside temperature because heating takes place on the outer surface of the dryer (Fig I.5).

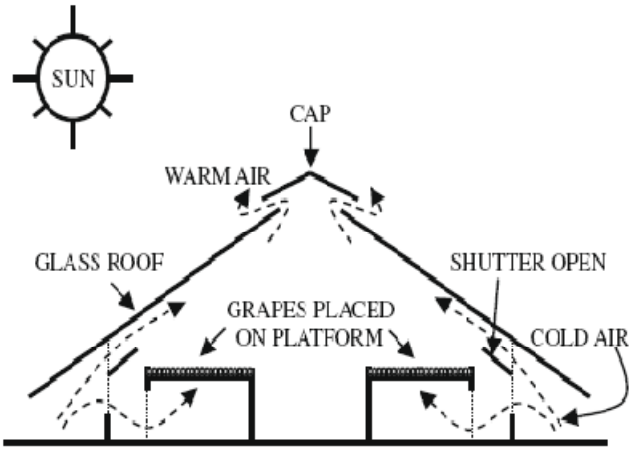

Fig I.5 Glass roof solar dryer [30].

El-Sebaii et al [31] studied an indirect natural circulation solar dryer with chimney, which is often known as an indirect passive solar dryer (Fig I.6). It consists of a solar collector, a drying chamber and a chimney. The solar collector with an area of 1.0 m^2 uses a black painted plate 0.002 m thick as an absorber. A glass covers of 0.005 m with an air gap of 0.08 m for the air to enter. The insulation layer with thickness of 0.08 m is provided at the bottom to minimize heat losses from the back of the dryer. The drying room with size 1.0 m×1.0 m×1.5 m was made from wood and fixed with a matte black painted galvanized iron cylindrical chimney of height 0.5 m and diameter of 0.1 m. It was found that the chimney increases the buoyant force imposed on the air stream to provide a greater air flow velocity which forms one side of moisture removal.

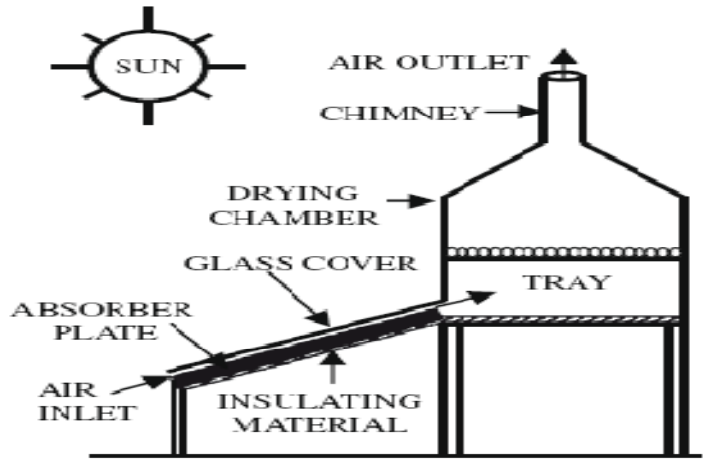

Fig I.6 Indirect natural convection solar dryer with chimney [31].

Pangavhane et al [32] presented a new multipurpose natural convection solar dryer. This solar dryer consists of a solar flat plate air heater, flexible connector, reducer with plenum chamber, drying chamber and chimney as shown in Fig. 7. The air duct beneath the absorber is made using an aluminum sheet which air is passed through. The U-shaped corrugations are placed in the absorber plate parallel to the air flow direction. The space between the box and the bottom of the air duct is filled with glass wool insulation. For loading and unloading the trays, a door is provided at the rear end of the drying chamber. A chimney is provided at the top of the drying room to create the required draft through it. The drying air flow rate increases with an increase in ambient temperature by the thermal buoyancy in the collector. The efficiency of the collector of this solar dryer is found to be varied from 26% to 65% while the drying period of chemically treated grapes is found to be within 4 days;

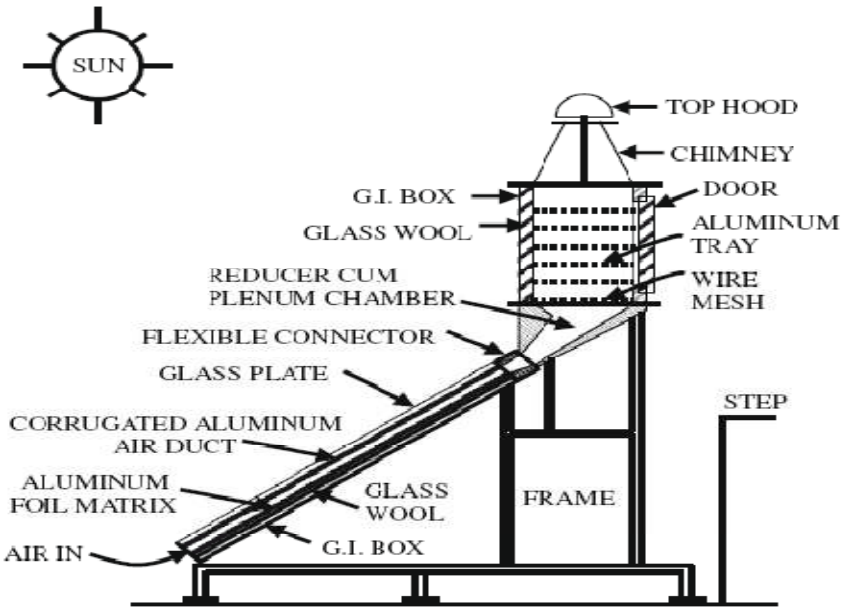

Fig I.7 Multipurpose natural convection solar dryer [32].

Abene et al [33] studied a solar air flat plate collector with obstacles (Fig I.8).This system is an indirect blow-dryer that operates in the forced convection mode. The system consists of a solar collector acting as a hot air generator, a fan and a drying unit. The solar collector has a transparent cover of thickness 1 cm at the top, an absorber plate of aluminum sheet with a thickness of 0.4 mm and obstacles of 2 cm height fixed to a thin plate are placed on an insulator of polystyrene. It was found that the presence of obstacles in the air stream helps to extract maximum quantity of heat from the absorber. Hence, the entering air temperature to the drying chamber through the collector increases.

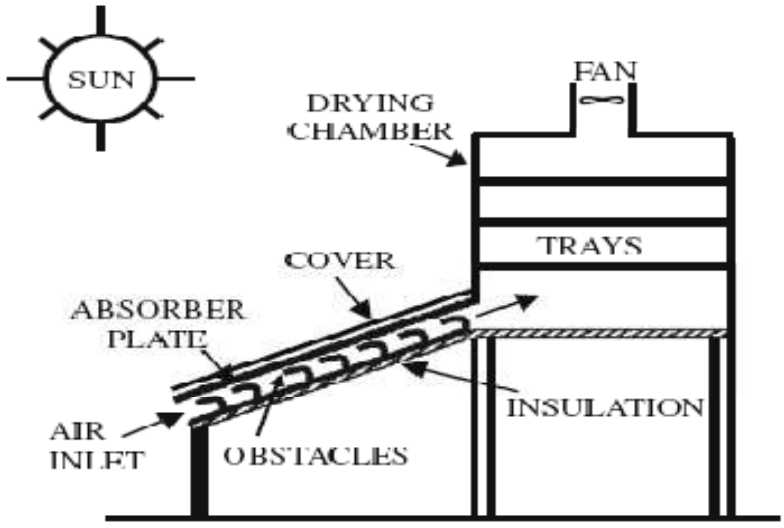

Fig I.8 Solar air collector with obstacles [33].

Adolfo et al [34] constructed an indirect solar dryer where they have the ability of directing the flow of hot air from the solar collector inside the drying room determining the adequate zone to which they want to direct the drying agent (Fig I.9). The connection between the solar collector and the drying room is via a very low thermal conductivity neoprene hose. As in all indirect solar dryers, air enters the system through the base of the coil and raises its temperature through natural convection towards the upper part of the same; this is the function of the solar collector. While hot air through the drying chamber is directed using the entrance too preferentially as the type of product that is wanted to dry and the speed which required all process.

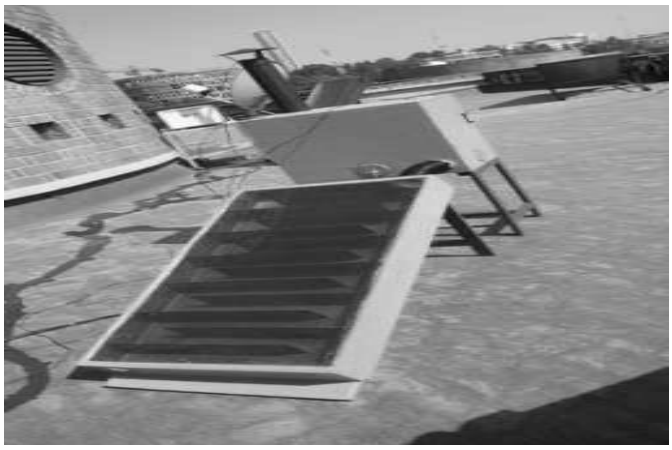

Fig I.9 Indirect solar dryer with variable steering flow [34].

Sahin et al [35] studied the effect of solar-assisted spouted bed and open sun drying on the drying rate and quality parameters of pea. The solar-assisted spouted bed dryer, used in the experiments, consisted of a solar air heater to provide hot air and air blower to provide spouting column for drying of sample (Fig I.10). The obtained results showed that the drying rate for solar assisted spouted bed was about 3.5 times of drying rate for open sun drying. It was found also that the air temperature changed between 20°C and 27.4°C during open sun drying while temperature of the inlet air of solar-assisted spouted bed dryer varied between 35.3C° and 65.5C°. The drying rate was much higher and therefore the drying time was lower for drying in solar assisted as compared to open sun drying.

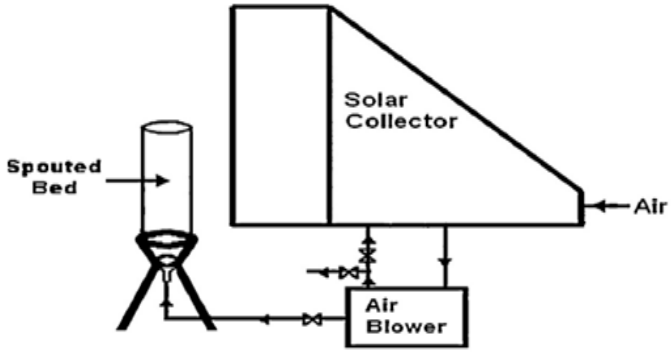

Fig I.10 Schematic diagram of solar-spouted bed dryer [35].

Lamnatou et al [36] developed a new solar dryer by using an evacuated-tube collector. The results showed that the warm outlet air of the collector reaches a suitable temperature levels for drying of agricultural products without the need of preheating. Thus, the solar collector was used as the heat source for a drying room in the frame of the development of a new indirect solar dryer. The proposed dryer has a capacity for drying a larger quantity of products due to the high efficiency given by the solar collector.

Duran et al [37] studied a passive solar dryer that includes a chimney and a wind turbine to improve the air flow rate. The drying room area is 2 m^2 to obtain charqui. The obtained results showed that the drying time was reduced to less than two sunny days with improving of the final quality in relation to the traditional charqui. To find the optimum mass air flow, it is suitable to use simulation study of the passive solar dryer. The provided air flow rate by both devices was complimented, allowing the drying process to be continued during the night when the ambient relative humidity was low by using the wind extractor.

I.6.3 Adding of concentrators and reflectors

Ringeisen et al [38] studied the effect of adding a concave solar concentrator built from low-cost, locally available materials to a typical Tanzanian solar dryer (Fig I.11). The concentrator was built from a wooden L-shaped frame. They fabricated two identical solar dryers; one is for the control and the other for testing the solar concentrator. Relative humidity, solar radiation, and temperature were measured outside as well as within each of the dryers to determine how the affect of addition a solar concentrator on the drying rate of tomatoes in solar dryers. It was found that the concentrator proved to be effective, reducing drying time by 21% by increasing drying air temperature which can reduce the relative humidity. An additional study on the quality of the fresh and dried tomatoes found that the

titratable acidity, pH, lycopene, color, Brix, and vitamin C determined there was no difference in quality between tomatoes dried without and with the concentrator.

Fig I.11 Dryer 2 (left) is exposed to the concave solar concentrator. Dryer 1 (right) is the control [38].

James Stiling et al [39] used the concentrating solar panels (CSP) in a mixed-mode solar dryer to improve the process of solar drying Roma tomatoes (Fig I.12). Solar panels were used to maximize incident solar radiation on the solar dryer, one of the dryers used a mobile and an easily adjustable flat (CSP). The results showed that the temperature inside the dryer used (CSP) was approximately 10°C higher than the one in the dryer without CSP. CSP increase the drying rate with decreasing of total drying time with 27% as compared to the dryer without CSP. With using CSP, the faster achieved drying rate, under both sunny and simulated cloudy conditions, shows the ability to dry products to acceptable moisture content in a reasonable time, with the objective of decreasing postharvest loss.

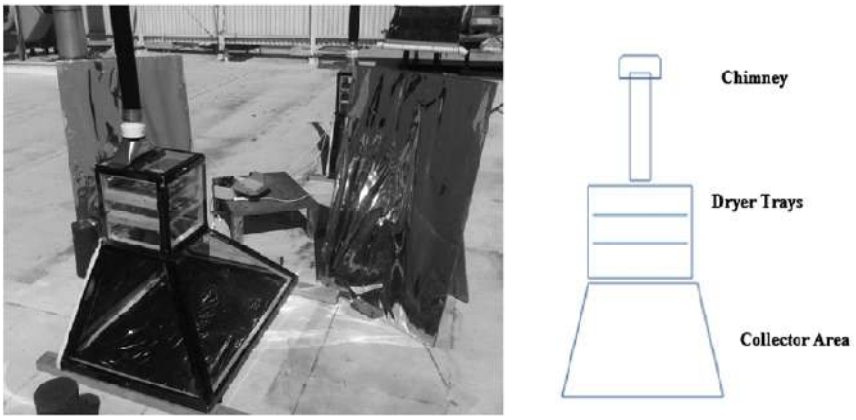

Fig I.12 Solar dryer and two concentrating solar reflection panels used in drying experiments [39].

Subarna et al [40] studied the influence of adding reflectors on the performance of solar dryer. The drying system was an indirect, natural convection batch-type solar dryer fitted with North–South reflectors as shown in. It was found that with using reflectors, the collector efficiency without load was improved from 40% to 58.5% under peak solar irradiation conditions during a typical day. The desired extent of drying (12%, wet basis) of 'papad' – a popular Indian wafer – could be achieved within 5h in this static dryer.

I.6.4 Photovoltaic source

Sevik [41] investigated experimentally a system in drying of various agricultural products under different climatic conditions (Fig I.13). To determine the effects of PID control on the system, and to evaluate the drying behavior of various products at 50°C with different mass flow rate for a drying analysis, he studied how to keep a constant drying air temperature with PID to obtain a homogeneous air temperature inside the drying room. The average obtained thermal efficiency of the solar collector was varied between 16% and 79%. The given results showed that the solar collector, PV unit, HP unit, can work in coordination with each other and give a dried product having good physical and chemical properties.

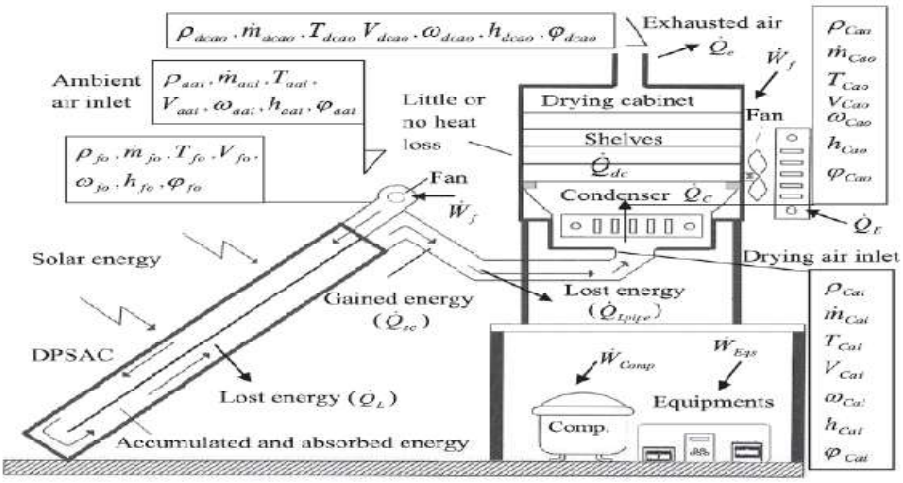

Fig I.13 Energy balance of the dryer [41].

Y. Li et al [42] investigated experimentally a solar assisted heat pump in-store drying system (Fig. 14). The system consists of heat pump, fans, flat-plate air collectors, grain stirrer and air ducts is proposed to make full use of incident solar energy and to reduce the electricity consumption. It was found that the solar assisted heat pump drying system improved the performance of the in-store drying process. The achieved average temperature rise for the granary inlet air was 8.9 °C. The uniformity of grain moisture content was improved and the

drying rate was increased. Moreover, the good quality of the grain was maintained and the level of electricity consumption was reduced too.

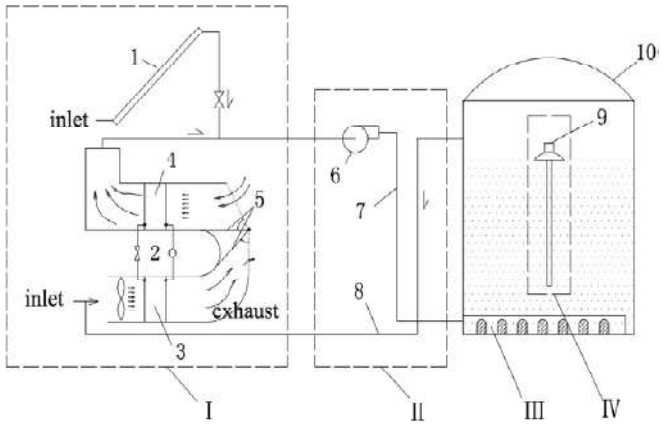

Fig I.14 Schematic diagram of the solar assisted heat pump in-store drying system. 1: solar air collector, 2: air source heat pump, 3: evaporator, 4: condenser, 5: movable diaphragm, 6: supply fan, 7: ventilation supply tube, 8: air recycle tube, 9: grain stirrer, 10: Granary [42].

Seyfi Sevik [43] studied experimentally a new design solar dryer using double-pass solar air collector, photovoltaic unit and heat pump. The solar dryer performance has been tested for drying of carrot. The double-pass solar collector (DPSC) has provided the requirement heat energy for performing the drying process. The thermal performance of solar collector was varied from 60% to 78%. Carrot slices were dried at 220min by using solar collector in solar heat pump dryer. It was found that the system (solar-heat pump dryer) can be easily operated without the need to the heat pump under normal ambient air conditions (average temperature 30°C and average relative humidity 30%). The solar collector can be used efficiently in several thermal applications such as greenhouse heating, space heating and air preheating. Aušra Cipliene et al [44] studied experimentally the use of hybrid solar collector (Fig I.15) for drying process. The solar dryer was developed containing two different solar collectors: the air type solar collector with an area of $12m^2$ for heating the product, and the flat plate solar collector with an area of $8m^2$ for accumulation of the converted heat energy. The results showed that by combining of two different solar collectors, the solar energy for drying could be used continuously and permanently by employing the accumulation energy, in order to ensure stability of the drying process by compensation of the solar radiation variability.

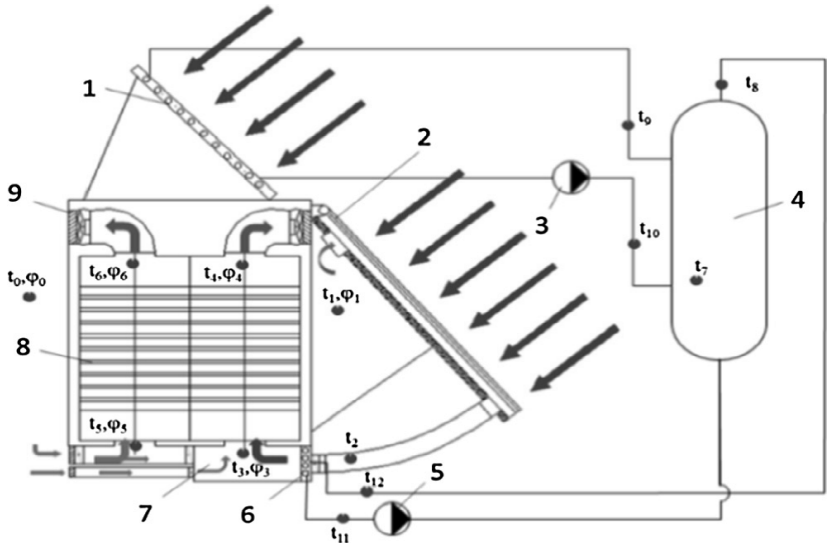

Fig I.15 Basic scheme of the dryer for medicinal plants: 1 – flat-plate type solar collector (8 m^2 area), 2 – air-type solar collector (12 m^2 area), 3 and 5 – a pump; 4 – a tank with water for heat storage; 6 – heat exchanger; 7 – air mixing chamber; 8 – drying chambers; 9 – fan [44].

Chouicha et al [6] studied a solar hybrid drying of sliced potatoes by forced convection in an indirect solar dryer using extra energy via a heater by joule effect generated by photovoltaic modules. The obtained results showed that with the use of one solar panel, the reached final water content of the potato was (xf= 0.13kg w/kg d.m) and the obtained drying time was 3h. While in case of using two panels, the drying time was found 2h45mn. Tsamparlis [45] studied a hybrid solar dryer which consists of a solar heating unit and a drying room as shown in (Fig I.16). Heating unit is organized into two units with two flat plate collectors and 10 evacuated tube collectors in each one. The heating unit is detachable from the drying room which makes it possible to be used for other heating applications when the dryer is not operating. Drying room is divided into two parts; the upper one consists of electric heaters, a fan and a system for modulating velocity of drying air. This dryer is equipped with two fans, one of which is used to drive pre-heated air from the solar unit into the drying room and another is located in the drying chamber for maintaining air circulation within the drying cabinet. The obtained results showed that the dried grapes obtained from this dryer have a good quality, and that the drying time of grapes is significantly reduced to around 30–40 h.

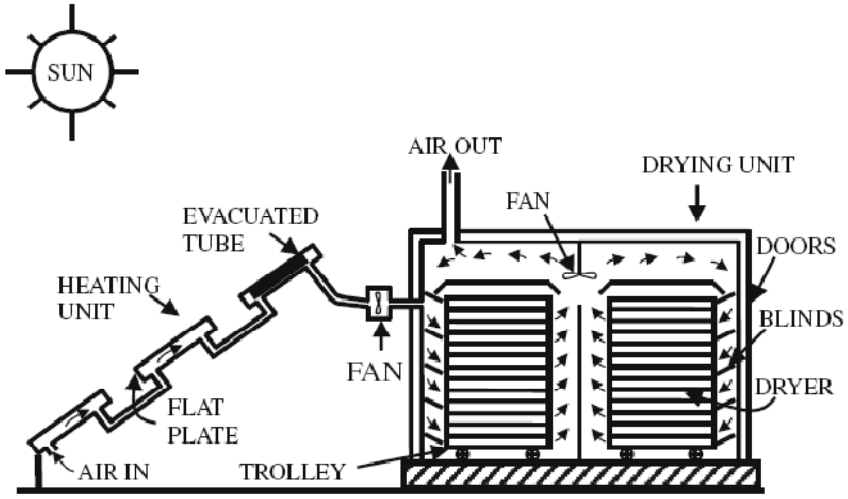

Fig I.16 Hybrid solar dryer [45].

Amer et al [46] examinated an integrated solar system used for drying chamomile (Fig. 17). This system consists of heat exchanger, reflector, collector, main drying chamber below collector, additional drying chamber and an electric heater immersed in the water tank. It was found that this system operated about 30-33 h to reduce the moisture contents of product from 72-75%--6% (wb) compared to 60 h to reduce it to 9-10% (wb) using open sun drying. This system can store the solar energy into water during sun-shine hours and use this energy at cloudy days or after sunset to raise the temperature of drying air.

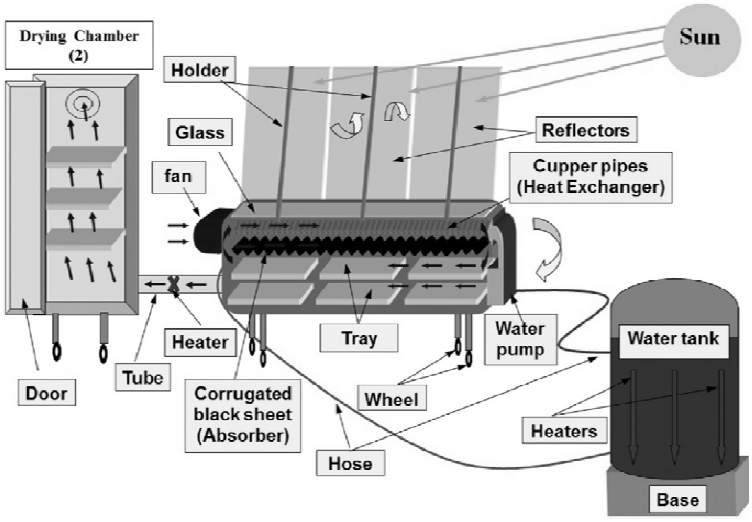

Fig I.17 Schematic diagram of the components of the integrated solar dryer system [46].

I.6.5 Forced air circulation mode

Several designs of forced convection solar drying systems had been constructed, tested and developed. Direct mode forced convection solar drying systems essentially consists of a fan / blower to force the drying air circulated through the product, and a drying room covered with a transparent sheet. While the indirect-mode forced solar drying systems essentially consists of a drying chamber, an air heater and a blower/ fan to duct the heated air to the drying room.

Ben Salma et al [47] studied the development of solar dryer by using forced convection. The drying unit is composed mainly of a drying chamber and a solar collector. The solar collector collected the solar radiations and converted them into heat; its thermal efficiency was reached 80%. The heat transfer in the drying room with the product is generated by forced convection, which is created by an electric fan. It was found that a combination between forced and natural convection is too interest, through the use of a fan, to control precisely the quality of the drying process. The drying rate is proportional to both drying temperature and drying air velocity. The importance of using baffles in the solar collector is to increase its efficiency even with low air flow rate.

Ahmed Fudholi et al [48] tested an indirect forced convection solar drying system for drying of palm oil fronds. It was found that drying of 100kg of palm oil fronds reduced the moisture content from 60% to 10% in 22h. The thermal efficiencies of the solar collector, drying system and pick-up were found about 31%, 19% and 67% respectively. The improvement potential of solar drying system for palm oil fronds ranged from 8W to 455W while the efficiency of the collector was ranged from 9% to 48%.

Varun et al [49] evaluated the dryer performance under natural and forced convection modes. In forced convection, it reached an average drying temperature of 40°C, while in natural convection; the hot air reached an average drying temperature of 45°C. It was found that in natural convection the mass of tomatoes was reduced from 1800g to 180g, while in forced convection; it was reduced from 1800g to 140g. The comparison between those two modes show that forced convection removed more moisture from tomatoes as compared to natural convection, because of in forced convection, the heat transfer rate is more than in natural convection.

Mumba [50] studied a solar grain dryer with photovoltaic powered air circulation. The use of photovoltaic solar cells is to supply the fan by electrical power. This solar dryer can dry 90kg of maize grain per batch from an initial moisture content of 33.3% dry basis to fewer than 20% dry basis in one dry. The drying air temperature has been controlled to be ranged in

60± 3°C. The solar dryer was found to be very effective with many benefits, such as improving of the dried product quality and protection of drying environment. It was found that this kind of dryer is suitable for rural zones where fossil fuel and electricity are either extremely expensive or nonexistent.

I.6.6 Adding of other components

I. 6.6.1 Heat pump

Seyfi sevik et al [51] proposed a simple and cost effective solar heat pump system (SAHP) with flat plate collectors and a water source heat pump for drying Mushroom. The use of solar energy and heat pump systems can be done separately or together. It was found that this system is sustainable, cheap and has a good quality of dried product. The results showed that drying process can be continued with solar energy in daytime while the heat pump system can be used in other times (at nights). The drying process used SAHP is found to be much more quickly than the open sun drying. Fadhel et al [52] presented a review on advanced solar assisted chemical heat pump dryer. A solar assisted chemical heat pump dryer is a new solar drying system, which has contributed to better quality dried products and better cost-effectiveness as well as saving energy. The solar collector is designed to provide thermal energy in a reactor so a chemical reaction will take place. The integration of solar thermal system to the chemical heat pump would assist in expanding the use of chemical heat pump also for several applications in the tropical region. Mohanraj [53] studied the energy performance of a solar-ambient hybrid source heat pump drier (SAHSHPD) for drying under hot-humidity weather conditions. The results showed that the coefficient of performance (COP) of the SAHSHPD was varied between 2.31 and 2.77 with an average value of 2.54. The quality of the product obtained dried under SAHSHPD was found to be higher by comparison with other drying methods.

I.6.6.2 Heat exchanger

Misha et al [54] studied drying of Kenaf core fiber at low solar radiation using a solar solid desiccant dryer and heat exchangers. The system was equipped with electrical heater to maintain the temperature of hot air high if the solar radiation becomes low. The desiccant wheel system is used as a heat source to supply dry and hot air for the drying room. It was found that this system reduced the drying time by 24% from 20.75h to 15.75h compared to open sun drying because it was used even in the absence of solar radiation to continue the

drying process. The obtained results showed that the solar-assisted solid desiccant dryer can operated even at low solar radiation for drying of kenaf core fiber.

Alejandro et al [55] doubled the thermal conductivity of cans filled with paraffin wax by adding 5% w/w of aluminum wool. They used a heat exchanger for accumulating the solar energy, this exchanger is composed by 48 cans filled with 9.5kg of paraffin wax mixed with aluminum wool. The conductivity of this mixture could be augmented by increasing the percentage of aluminum strips. The time needed to melt the wax completely in sunny day is 3 hours. During a period of 2h, the temperature with 3.5m^3/h air flow rate increased from 20 to 40°C. This application can be used in drying process.

Amer et al [56] studied a hybrid solar dryer that consists of solar collector, reflector, drying chamber, and heat exchanger with heat storage unit (Fig I.18). The heat energy was stored in water inside the heat storage unit by the effect of solar radiations and electric heaters. The results showed that the drying process can be continued at night by using the heat energy stored in the water tank. It was found also that the efficiency of the solar dryer was raised by recycling about 65% of the drying air.

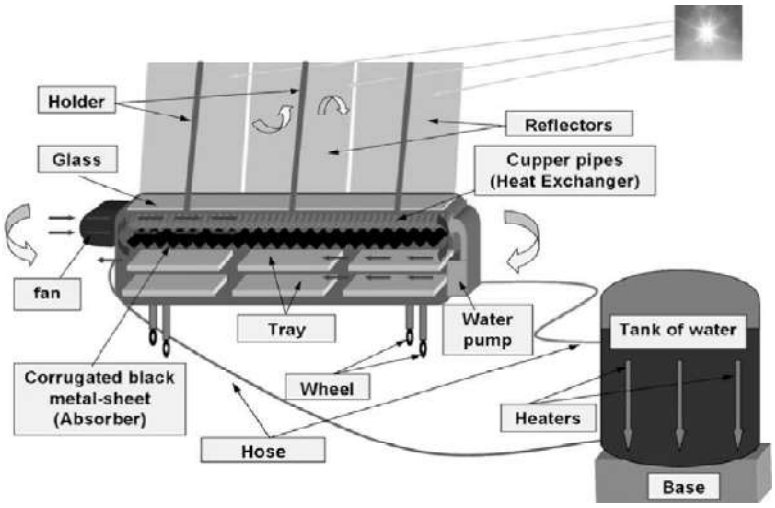

Fig I.18 Schematic diagram of a solar hybrid dryer [56].

I.6.7 Using of geothermal water

The intercalary continental aquifer generally called Albian aquifer constitutes the main geothermal resource in the South of Algeria. Additionally it represents the biggest water reserve in the word. The use and the exploitation of the Albian water have started since 1960 in the regions of southern Algeria. However, this operation is confronted with various problems, the most of which is the scaling and corrosion in pipes and the rising of

groundwater [57]. The main utilizations of the hot water in Algeria are balneology, space and greenhouse heating. For some practical reasons, Ouargla and Touggourt (north-eastern region of the Algerian Sahara) have been chosen for the experimental greenhouses/geothermal heating systems. Algeria is divided into three geothermal zones according to some geological and thermal considerations: (1) The Tlemcenian dolomites in the northwestern part, (2) carbonate formations in the northeastern part and (3) the sandstone Albian reservoir in the Sahara [58].The Albian water temperature varies from 30 °C to 80 °C respectively from West to East. The depth of this geological layer increases towards Northeast direction; until it reaches up to 2500 m depth at the Northeast periphery such as in Biskra and El Oued regions [57]. In the South of Algeria, the Albian sandstone formation extends on 600,000 km2, and forms the geothermal Saharan reservoir. This reservoir is confined in its Northeastern part and deeps to 1500-2600m. The total flow rate from exploiting wells is about 10m3/s and the mineralization is around 2g/L. Generally, the geothermal water is cooled before its utilization for domestic and agricultural purposes due to its high temperature [59]. An analysis of 41 hot waters sampled from different regions shows that the pH values varied from 6.5 to 8.5 and more than 90% of the samples exhibited high salinity (550-5,500 mg/L). Most of the samples belong to the sodium-chloride water type [58]. The Albian water is a huge source of energy without restraint and that for a long time. Yet the geothermal water is not highly used in drying technology [60-61].

Solar drying has always been a technique of great interest to preserve and stabilize agricultural products such as fruits, vegetables and medicinal plants. The researches on solar drying systems covered a wide range of processes depending on the dried product, the operating region climate and the nature of the application [62-66]. In open sun drying processes, products are subjected to rain, wind, and dust. They are exposed to birds, insects and rodents. Substantial losses take place during this drying processes and the food quality may be seriously tarnished [67-74]. Some of these problems have been overcome using a direct solar dryer. In the direct solar drying systems, crop is exposed directly to sunlight to be dehydrated. In this type of systems a black painted surface holding the crop to be dried is placed inside in order to convert the sunlight into heat. These dryers may have glass lid covers and vents in order to increase efficiency [75]. Direct solar dryer is simple equipment that can be built by village artisans, using locally existing materials and allows a hygienic drying. They are also easy to manipulate and maintain. Many researches and performance studies have been reported on this kind of dryers [76–78].

The use of geothermal energy for heating application is an important technique. Several research works are made to investigate this process. Indeed, Boughanmi et al [79] examined the performance of a new conic helicoidal geothermal heat exchanger (CHGHE) for greenhouse heating in the north of Tunisia. This geometry was intended to reduce the used area and the operating cost compared to horizontal and vertical. They found that the geothermal system insured a quantity of heat equal to 692.208 kW corresponding to a temperature increase of 3°C under greenhouse for an optimal water flow rate of 0.6 kg/s. Calise et al [80] analyzed a novel hybrid solar–geothermal polygeneration system producing energy and water. The plant was made on purpose to supply electrical, thermal and cooling energy and fresh water for a small community, connected to a district heating and cooling network. The obtained results showed that global exergy efficiency varies between 16% and 20% during the ‘‘Cooling Mode" and between 40% and 50% during the ‘‘Thermal Recovery Mode" operation. Bououd et al [81] presented a modeling and parametric studies of a water-to-air heat exchanger in which the hot water-coming from solar concentrators heats the air injected into a thermal chamber to dry the clay bricks. The obtained results showed that the heat exchanger performance could be improved by fulfilling certain conditions and modifying the different geometrical parameters. Calise et al [82] studied a geothermal energy system for wastewater sludge drying and electricity production in a small island. They found that this system reduces wastewater sludge to be disposed and transported by 73.3%. Using of geothermal energy to produce heat for sludge drying saves 58.6*103 Sm3 of natural gas and 115 tons/year CO2 emissions. Daneshipour et al [83] investigated the application of the CuO water and Al2O3 water nanofluids as the working fluids of a geothermal borehole heat exchanger. The obtained results show that the CuO water gives higher extracted heat than the alumina-water. Husham Abdulmalek [84] studied the effect of tube diameter on the design of heat exchanger in solar drying system. Furthermore, they presented the difference between using electrical heater and solar heat source in terms of design aspect. They found that the increasing of tube diameter increases the heat transfer area of both electrical heater and heat exchanger. Focaccia et al [85] studied the using of shallow geothermal energy for industrial applications. The results showed that these industrial processes can be advantageous when a low-enthalpy shallow geothermal heat source is used, especially in combination with thermal energy storage methods. Ghasemkhani et al [86] studied the effect of using a simple heat exchanger on the exergetic performance parameters of a rotating-tray air dryer. They found that the exergetic efficiency of drying process was significantly improved from a minimum value of 23.0% to a maximum value of 96.1% by using the heat exchanger. Moreover, the

incorporation of heat exchanger did not negatively affect the quality of dried product. Al-Hinti et al [87] studied the ground temperature profile in Zarqa, Jordan for geothermal heat pump applications. It is found that despite the cyclic nature of the seasonal and daily variations of the ground surface and ambient temperatures, the underground temperature variations decreases with depth and stabilizes throughout the year at around 21°C starting from a depth of 5 m below the surface. Ambriz-Diaz et al [88] presented an analysis for the sequential production of electricity, ice and drying of agricultural products, by the concept of cascade for medium and low temperature geothermal energy. The thermal cascade is composed at the first level by an Organic Rankine Cycle (ORC) for production of electricity, in the second thermal level, by an absorption refrigeration cycle for production of ice, and in the third level includes a dehydrator for drying of agricultural products such as avocado, green chile and tomato. They proposed five integration alternatives and five different modes of operation of the system. The alternatives have different features for the activation of the first thermal level of the cascade, different nominal capacities of electricity production, cold, and quantity of product to be dehydrated. The obtained results show that the dehydration process improves drastically the economic profits of all alternatives, especially for dehydration of tomato, achieving simple payback periods of around one year, overall energy efficiency of up to 17.84%. Agra et al [89] studied the heat capacity ratio and the best type of heat exchanger for geothermal water providing maximum heat transfer. They found that effectiveness of heat exchanger increases as capacity ratio decreases. The best type of heat exchanger giving maximum heat transfer can be determined using ε*Cr curves for geothermal applications while (ε) is the effectiveness of heat exchanger and (Cr) is the capacity ratio of hot and cold streams. Navarro and Gomez [90, 91] presented a mathematical model to determine ε-NTU relations for cross-flow heat exchangers with complex flow arrangements and presented the ε-NTU curves for several complex circuit arrangements. Ezzat et al [92] investigated the energy and exergy analysis of a new geothermal–solar energy based system. Their system was aimed to produce five output commodities; refrigeration for industry, heating air for residential application, hot water for domestic use, drying food and finally electricity. The overall energy and exergy efficiencies are found to be 69.6% and 42.8% respectively. While the overall energy efficiency of the system appears to be about five times more than the energy efficiency of the basic geothermal cycle.

In other researches, several techniques were used to improve solar dryer performance such as S. Misha et al [93] who studied the drying of Kenaf core fiber at low solar radiation using a solar solid desiccant dryer and heat exchangers. The solar energy was used to heat water using

solar collector and transfer heat to the air via heat exchanger. The distribution of hot water ratio via heat exchangers 1 and 2 can be adjusted to find the optimum performance of the dryer. The desiccant wheel system is used as a heat source to supply hot and dry air for the drying room. It was found that this system reduced the drying time by 24% from 20.75h to 15.75h compared to open sun drying because it was used even in the absence of sunshine to continue the process of drying. The air flow rate provided by both devices was complimented, allowing the drying process to continue at night when the ambient relative humidity was low by using the wind extractor. A new postharvest method was proposed and investigated by Mennouche et al [94] using laboratory scale direct solar dryer in order to valorize hard Deglet-nour dates. They proposed three drying enhancements to improve the quality of date: drying under shade (DUS), drying with photovoltaic powered ventilation (DSV) and combination drying method (DCM). It was found that the treatment with solar ventilation drying mode (DSV) and (DCM) were considered as favorable operating conditions for the studied case. The combination drying method was selected as the most adequate process to realize the quality criteria and processing time.

In other work, Reyes et al [95] doubled the thermal conductivity of cans filled with paraffin wax by adding 5% w/w of aluminum wool. They designed a heat exchanger for solar energy accumulation, composed by 48 cans filled with 9.5kg of paraffin wax mixed with aluminum wool. The time needed to melt the wax completely in sunny day is 3h. During a period of 2h the temperature, of 3.5m3/h air flow rate, increases from 20°C to 40°C by 3000kJ of the accumulated energy. This application can be used in drying processes. The thermal conductivity of the mixture could be augmented by increasing the aluminum strips percentage. A new hybrid solar dryer was studied by Amer et al [96]; the system consists of solar collector, reflector, heat exchanger with heat storage unit, and drying room. The heat energy was stored in water inside the heat storage unit during sun-shine time and with electric heaters. Drying was also carried out at night with stored heat energy in water. The heat was collected during the time of sun-shine and with electric heaters located at water tank. The results showed that the efficiency of the solar dryer was raised by recycling about 65% of the drying air. In order to improve the efficiency of a direct solar dryer, Sandali et al [97] studied the effect of adding a porous medium as a sensible heat storage medium on the thermal performance of a direct solar dryer. Different kinds of materials with different thickness have been tested. The obtained results show that the drying air temperature is increased by 4°C with integration of porous medium.

I.6.8 Using of porous medium

Having a solar energy storage system is very important in energy conversion and is responsible for performing the drying process of many agricultural products even when direct sunlight is very low or not available. Although many agricultural food products, such as grains, fruits, and vegetables are often dried under the open sun, this method can lead to reduce the quality and quantity of the final product. The energy storage system acts as a key issue to be addressed to allow intermittent energy sources, typically renewable sources, to match energy supply with demand. There are several technologies for storing energy in several forms including thermal, electrical and mechanical energy. Several research works have explored different techniques for accelerating the solar drying of various agricultural products by considering the possible use of thermal storage materials, and developed drying models to predict the drying curves of the dried materials. Sopian et al [110] evaluated the performance of a solar drying system equipped with a double-pass collector with an integrated storage system. This system consists of a blower, auxiliary heater, solar collector and drying room. The lower channel of the solar collector is filled with porous media that act as heat storage systems. Drying time is found to be 7 hours. The system efficiency is around 25–30%, and evaporative capacity is 1.26kg/h. Furthermore, the auxiliary heater is used while low solar radiation conditions, particularly in the evening and in morning. El-Sebaii et al [31] investigated an indirect natural convection solar dryer with storage material and chimney used for drying grapes. The solar dryer consists mainly of a solar collector coupled with drying chamber. In order to obtain heated air even after sun set, the gap between the absorber plate and the insulation layer was filled with sand as a sensible heat storage material. The obtained results showed a significant improvement of the dryer thermal performance. The sensible heat storage material (sand) which is placed in the solar collector provided a drying air temperature at the inlet of the drying chamber with a range of 45.5-55.5 °C. Tiwari et al [111, 112] evaluated experimentally a crop dryer cum water heater and crop dryer rock bed storage. They reported that the energy balance equations for each component of the system have been used to predict the analytical results. On the basis of the analytical results, it was observed that the drying time is significantly reduced on using the water and the rock best as storage media. The system can be used to provide hot water in case the drying system is not in operation. The water heater below the air heater systems will act as a storage material for drying the crop during off-sunshine hour. Comparative performance of coriander dryer coupled to solar air heater and solar air heater rock bed storage was studied by Chauhan et al [113]. They

concluded that the average moisture content of the grains in the grain bed can be reduced from 28.2% (db) to 11.4% (db) in 27 cumulative sunshine hours (i.e. 3 sunshine days) by using the solar air heater only; whereas, by using the solar air heater during sunshine hours and the rock bed energy storage during off-sunshine hours the same amount of moisture can be evaporated in 31 cumulative hours (18 sunshine and 13 off sunshine hours).

I.6.9 Using of phase change material (PCM)

Several previous works which studied the use of PCM to store solar energy such as Çakurak et al [117] who studied the drying kinetics of seeded grape in solar dryer with PCM-based solar integrated collector. The system consists of an expanded-surface solar air collector, a solar air collector with phase change material and drying room. The phase change material has been used to perform the drying process even after sunset. The advantage of drying at night makes the proposed system a promising dryer based on less drying time and lower moisture value. It has been found that drying time decreases when drying air velocity increases and the drying process has occurred in decreasing drying period. Shalaby et al [118] investigated a novel indirect solar dryer implementing phase change material (PCM) as energy storage medium. The system consists of PCM storage units in order to store the solar energy which can be used after sunset. It was found that with using PCM, the temperature of the drying air is higher than the ambient temperature by 2.5-7.5°C after sunset for five hours. This novel drying system can successfully maintain the desired drying temperature for seven consecutive hours every day. Dilip Jain et al [119] studied the performance of an indirect solar crop dryer with phase change material. The system consists of a solar collector, packed bed energy storage material (paraffin wax), drying plenum with crop trays and natural ventilation system. The packed bed solar energy storage with a capacity of 50kg of PCM was combined with the solar dryer. The phase change material stores the solar energy during sunshine hours and releases it after the sunset, which can maintain the continuity of the drying process for next 5-6 hours. After sunshine period, it was found that the temperature of the drying room was observed with 6°C higher than the ambient temperature. Shalaby et al [120] reviewed the previous works on solar drying systems which used the phase change material (PCM) as an energy storage medium. The results showed that the PCM reduces the heat losses and improves the thermal efficiency of drying systems. It was concluded that such materials as expanded graphite, graphite, carbon fibers and high thermal conductivity particles can improve the efficiency of solar energy devices using paraffin wax as thermal

energy storage medium. Srivastava et al [121] investigated the using of Lauric acid as a phase change material to store solar energy. They studied the effect of inlet air velocity and inlet air temperature on the charge and discharge time, during the charge period, only the effect of inlet air velocity was taken into consideration. They concluded that thermal energy storage is the most effective use of solar energy to resolve the discrepancy between the energy supply and demand in solar heating applications. Dina et al [122] evaluated the efficiency of solar dryer integrated with desiccants thermal energy storage for drying cocoa beans. They tested two types of desiccants, molecular sieve $13\times(Na86[(AlO_2)86.(SiO_2)106].26H_2O)$ and $CaCl_2$. It was found that during sunshine hours, the air temperature in drying chamber varied from 40°C to 54°C and higher than ambient temperature by 9-12°C. It was concluded that a solar dryer integrated with desiccant thermal energy storage makes drying more effective in term of specific energy consumption and drying time. Reyes et al [123] studied Mushrooms dehydration in a hybrid-solar dryer using a phase change material. The system consists of a solar panel, paraffin wax and electric resistances. It was found that the use of solar energy reduces the electric energy consumption. Incorporating phase change material contributed significantly to improve the global thermal efficiency of the drying system. Agarwal et al [124] studied the shell and tube type latent heat storage (LHS) as a solar dryer. The heat transfer characteristics of the latent heat storage system have been evaluated during charging and discharging process using air as heat transfer fluid (HTF). The effects of temperature and flow rate of heat transfer fluid on the charging and discharging process of LHS have been studied. It was found that (HTF) is suitable to supply the hot air for drying of food product during non-sunshine hours or when the solar radiation is very low. Ayadi et al [125] investigated the performance of a solar collector and a storage system for a drying unit. They evaluated the performance of the storage system and the collector without drying energy supplement. Experimental results show that the efficiency of the solar collector at flow rate of 0.024kg/s is 30.52% and the temperature difference created by the storage system is about 10°C with efficiency more than 60% and 90% respectively during charging and discharging process. Lalit M. Ball et al [126-127] presented a review of solar dryer with thermal energy storage systems for drying agricultural products. The results showed that with the using storage unit, agricultural materials can be dried at night, while night drying was not possible with a normal solar dryer without using energy storage system. The solar energy storage system can reduce the time between energy supply and energy demand, furthermore, it play an important role in energy conservation. Consequently, solar dryer with thermal energy storage unit is very beneficial for the energy conservation as well as for the humans.

I.7 Theoretical study on the phase change materials

I.7.1 Definition of phase change materials

PCM are materials that accumulate energy when changing from solid to liquid state (melting heat), and turns it over when changing from liquid to solid state (solidification heat). Phase change heat exhibits a high heat density and a minimum temperature variation during fusion and solidification periods [123]. A phase change material is a solid which stores energy by melting upon the application of heat. The melting temperature may be fixed or vary over a small range. The stored energy is recovered upon solidification of the liquid [128].

I.7.2 Classification of phase change materials

During the last four decades many phase change materials, with a wide range of melting/freezing point, have been identified and studied extensively. These materials include organic (e.g., paraffins, fatty acids), inorganic (e.g., salt hydrates, metallic) and eutectics (e.g., mixture of organic and/or inorganic materials)[129].

I.7.3 The most used and important PCMs

The most important PCMs include Glauber's salt, calcium chloride hexahydrate, sodium thiosulfate penthydrate, sodium carbonate decahydrate, fatty acid, and paraffin waxes. These applications are listed by Zalba et al [130]. Both fatty acids and paraffin are cheap, readily available, and melt at different temperatures.

I.7.4 Desirable properties of phase change materials

Kenisarin et al [132] determined the most desirable properties for choosing the best phase change material and which are listed below:

- A high value of the heat of fusion and specific heat per unit volume and weight,
- A melting point which matches the application,
- A low vapor pressure (1 bar) at the operational temperature,
- A chemical stability and non-corrosiveness,
- A PCM should not be hazardous, highly inflammable or poisonous,
- A PCM should have a reproducible crystallisation without degradation,
- A PCM should have a small supercooling degree and high rate of crystal growth,
- A PCM should have a small volume variation during solidification,

- A high thermal conductivity,
- A PCM should be of abundant supply and at a low cost.

The main criteria that govern the selection of phase change heat storage materials are given by Abhat. A [133]:

- Possess a melting point in the desired operating temperature range (temperature range of application).
- Possess high latent heat of fusion per unit mass, so that a smaller amount of material stores a given amount of energy.
- High specific heat to provide additional significant sensible heat storage effects.
- High thermal conductivity, so that the temperature gradients for charging and discharging the storage material are small.
- Small volume changes during phase transition, so that a simple container and heat exchanger geometry can be used.
- Exhibit little or no subcooling during freezing.
- Possess chemical stability, no chemical decomposition and corrosion resistance to construction materials.
- Contain non-poisonous, non-flammable and non-explosive elements/compounds.
- Available in large quantities at low cost.

It is desirable to select the thermal energy storage based on the following criteria: cost, efficiency, environmental impact, life cycle cost, safety, and the required space [134]. Bal LM et al [127] found that the PCM to be used in the design of thermal-storage systems should possess desirable thermo-physical, kinetics and chemical properties which are as follows:

I.7.4.1. Thermal properties

- Suitable phase-transition temperature (melting temperature) in the desired operating temperature range.
- High sensitive heat capacity and latent heat of fusion per unit volume to minimize the physical size of the heat storage container.
- High specific heat to provide for additional significant sensible heat storage.
- High thermal conductivity of both solid and liquid phases to assist the charging and discharging of energy of the storage systems.

I.7.4.2. Physical properties

- High density, so that a smaller container volume holds the material.
- Small volume changes on phase transformation.
- Low vapor pressure at operating temperatures to reduce the containment problem.
- Congruent melting (phase stability) of the phase change material for a constant storage capacity of the material with each freezing/melting cycle.

I.7.4.3. Kinetic properties

- High nucleation rate to avoid super cooling of the liquid phase.
- High rate of crystal growth, so that the system can meet demands of heat recovery from the storage system.

I.7.4.4. Chemical properties

- Long-term chemical stability.
- Complete reversible freeze/melt cycle.
- No degradation after a large number of freeze/melt cycle.
- Compatibility (non-corrosiveness) with materials of construction.
- Non-toxic, non-flammable and non-explosive materials for safety.

I.7.5 Applications of PCMs in thermal energy storage systems

Murat Kenisarin et al [132] listed the different applications of PCM in thermal energy storage systems:

- Cooling of heat and electrical engines
- Cooling: use of off-peak rates
- Cooling: food, wine, milk products (absorbing peaks in demand), greenhouses
- Heating and hot water: using off-peak rates
- Medical applications: transportation of blood, operating tables, hot–cold therapies
- Passive storage in bio-climatic building/architecture (HDPE, paraffin)
- Safety: temperature level maintenance in rooms with computers or electrical/electronic appliances
- Smoothing exothermic temperature peaks in chemical reactions
- Solar power plants
- Thermal comfort in vehicles
- Thermal protection of electronic devices (integrated in the appliance)

I.7.6 Recent investigations on PCMs

It is found that most organic and inorganic PCMs investigated in the literature are those whose melting temperature is in the range of 30–60C and latent heat of fusion is in the range of 150–250 kJ/kg. The most eutectic PCMs studied in literature has the melting point in the range of 20–60C and latent heat of fusion is in the range of 125–200kJ/kg [129].

I.7.6.1. Organic materials

Most organic PCMs investigated are paraffins and fatty acids. It is found that paraffins have good thermal and chemical stability after number of the thermal cycles. The fatty acids studied widely are stearic, lauric, myristic, capric and palmitic acid. Most of the fatty acids used as PCMs are industrial grade.

I.7.6.2. Inorganic materials

The inorganic materials have not been investigated as heat storage materials to the same extent as the organic ones have. Nagano et al [135] discovered that manganese nitrate hexahydrate could be used as the basis for the development of a new heat storage composition. The melting range for this material varies from 7.7 to 25.3 °C and its heat of fusion is 125.9 kJ/kg. It was observed that salt has a significant degree of supercooling. They also examined the influence of introducing various additives to change the melting temperature, the heat of fusion and the degree of supercooling. For example, they discovered that adding manganese chloride tetrahydrate into Mn(NO3)2 . 6H2O in quantities of up to 10% in weight did not change the heat of fusion value. It can be seen that erythritol have a specific feature is its high-density value. It should be noted that there is also a 10% change in erythritol's volume during the solid-to-liquid transition and therefore the storage vessel and heat exchanges need to be designed to take this into account [136].

I.7.6.3 Eutectic PCM

A eutectic PCM is a combination of two or more compounds which are either organic, inorganic or both. In the last decade, many researchers have shown significant interest in new eutectic type PCMs instead of pure compounds. It is observed that the most of the organic and inorganic eutectics which are proposed as PCMs are made from fatty acids and salt hydrates, respectively [129].

I.7.7 Problems and disadvantage of phase change materials

It is concluded that most of the phase change problems have been carried out at temperature ranges between 8C and 60 °C suitable for domestic heating applications. The major disadvantage, as reported by many researchers has been the low thermal conductivities possessed by many PCMs, leading to low charging and discharging rates (especially for the organic based materials). The development of a latent heat thermal energy storage system therefore involves the understanding of heat transfers/exchanges in the PCMs when they undergo solid-to-liquid phase transition in the required operating temperature range, the design of the container for holding the PCM and formulation of the phase change problem [131]. At present, the cost of PCMs is quite high. For example, paraffin products of Rubitherm GmbH cost 2900–3500 h/ton and the price for a salt hydrate product is 9000–11,000 Australian dollars/ton [132].

I.7.8 Heat transfer in PCMs and enhancement techniques

Several studies have been conducted to study heat transfer enhancement techniques in phase change materials (PCMs) and include finned tubes of different configurations, bubble agitation, insertion of a metal matrix into the PCM, using PCM dispersed with high conductivity particles, micro-encapsulation of the PCM or shell and tube (multitubes).

To ensure long-term thermal performance of any PCM system, the size and shape of the PCM container must correspond to the melting time of the PCM and the daily insulation at a given location, if the source of energy is a solar collector. PCMs are typically placed in long thin heat pipes, cylindrical containers or rectangular containers [131]. In additions, various heat transfer enhancement techniques for paraffin as a PCM thermal storage medium were studied, such as those using fins, pin fins and lessing rings [120]. Despite the fact that paraffin wax is cheap and has moderate thermal energy storage density, its main drawback is the poor thermal conductivity. Fukai et al [137] used carbon fibers as a high thermal conductivity material. They investigated two different enhancement techniques. The first technique uses oriented fibers randomly, while the other is using a fiber brush. The authors concluded that the random type and the fibers' length have little effect on the effective thermal conductivity of the PCM. However, the fiber brush increases the effective thermal conductivities to the maximum expected values. Zhong et al [138], implemented mesosphere pitch based graphite foams (GFs) to increase the thermal diffusivity of paraffin wax. The thermal diffusivity of the Paraffin-GF can be enhanced190, 270, 500, and 570 times as compared with that of pure

paraffin wax. The key factors of such improvement are pore-size and thickness of ligaments of the foam. Small pore size and thicker ligament in the GF improves the composite thermal diffusivity, While, large pore-size and thinner ligament increases the composite latent heat. Results of studies from Morrison and Abdel-Khalik [139] and Ghoneim [140], show that to store the same amount of energy from a unit collector area, rock (sensible heat storage material) requires more than seven times the storage mass of Paraffin 116 Wax (P116-Wax), five times the storage mass of medicinal paraffin and more than eight times the storage mass of Na2SO4-10H2O.

I.8 Conclusion

Throughout this review study which collects the different technologies used to improve the thermal performance of solar drying systems, we have noticed the following remarks:

1. The total energy required for drying of an agricultural product increases with the increase of the air mass flow rate and decreases with the increase of the temperature of drying air.
2. The increase of drying air temperature leads to increase the speed of drying and therefore to reduce the drying time.
3. The drying air flow rate increases with an increase in ambient temperature by the effect of the thermal buoyancy in the solar collector.
4. The chimney integrated in solar dryer increases the buoyant force applied on the air stream to maintain a greater air flow velocity which can form one side of moisture removal.
5. The concentrators found to be effective in reducing of drying time, in increasing of air temperature inside the dryer and reducing relative humidity.
6. The solar air heater is the most important component in the indirect solar drying system; then, the improvement of the solar air heater leads to better thermal performance of the solar drying system.
7. Photovoltaic panels provides electricity source to run electrical components such as the fan or the heat pump. The solar assisted heat pump drying system improves the drying process because this last one can be continued and operated even at night with using of heat pump system. Running fan provides a forced air circulation which removed more moisture from the product as compared to natural convection.
8. Integration of heat exchanger improves the thermal performance of solar dryers.

Chapter II:

Improvement of a direct solar dryer performance using a geothermal water heat exchanger as supplementary energetic supply.

II.1. Introduction

In this chapter, the study of improvement of the thermal performance of a direct solar dryer realized at LENREZA laboratory, University of Ouargla (UKMO) by providing a sufficient drying air temperature to ensure the continuity of drying process even at night and during cloudy days will be presented. A new technique of heat supply using a heat exchanger with geothermal water, applied to the north-eastern regions of Algerian Sahara, was investigated and discussed throughout this paper. The used heat exchanger was fabricated at LENREZA laboratory with specific configuration which makes it easy to install inside the solar dryer.

II.2. Heat exchanger supplied with geothermal water

II.2.1. Experimental set-up

In this study, we describe the characteristics of the various components of the drying system. The main components of the experimental device are composed of energy supply system and direct solar dryer, while the energy supply system is composed of heat exchanger and hot water device.

The experiment was performed in LENREZA laboratory. It started at 09:00am in the first day and finished at 09:00am in the second day. The drying air temperature was measured at different time during the day to evaluate the thermal performance of the solar dryer.

II.2.1.1 Energy supply system description

This system is used in order to insure the continuity of the drying process during the night, or cloudy days. It is a heat exchanger fed by a source of hot water. This system presents a simulation device of heat exchanger supplied with the Albien water. The temperature of the hot water is fixed at 70°C. This temperature is justified by a measurement of temperature in several sites of the Albien water source in Ouargla city [3].

II.2.1.2. Design of the heat exchanger

The heat exchanger was designed following a number of steps as presented below:

- Providing a tube of copper with 25m of length and 9mm of diameter
- Cutting the tube on 24 tube pieces, the length of each one is 85cm
- The tube pieces are arranged in two layers with distance of 4cm, each layer contains 12 tube pieces.

- The distance between the tube pieces of each stage is 5cm.
- The whole of the tube pieces are welded with each other to have the shape of a tubular exchanger (fig II.1).

This tubular heat exchanger is placed above the absorber plate inside the drying room (fig. II.2). During the flowing of the hot water inside the heat exchanger, a heat transfer is produced between the heat exchanger walls and the entering air through the holes located at the door bottom of the dryer; the air temperature increases by the contact with the heat exchanger, prior to exit through the chimney.

Fig II.1 Picture of the heat exchanger.

Fig II.2 Emplacement of the heat exchanger inside the drying room.

II.2.1.3. Device of the hot water source

It is an apparatus consisting of: a 10L capacity tank, a resistance designed to heat the water inside the tank, a thermostat to maintain the water temperature at 70°C and an integrated pump delivering a flow rate of 3 L/min (Fig II. 3). This system supplies the heat exchanger with hot water and then the heat exchanger heats the drying air.

Fig II.3 Picture of the hot water source device.

II.2.1.4. Solar dryer description

The direct solar dryer consists mainly of a drying room, a chimney and a heat exchanger. The chimney with 1m of length and 0.1m of diameter was a galvanized metal cylinder. The drying room is composed of six glass covers, the thickness of each one is 4mm, two of which were placed as a roof of the solar dryer, they were tilted at an angle of 31° (latitude of Ouargla city), and the others were placed at the lateral, the rear and the front sides of the dryer. The drying room was placed on a galvanized metal sheets insulated with polystyrene. The door through which the air gets inside consists of two lines of holes, 0.01m in diameter and 0.05m in inter-axial distance. The base of the drying room is a metal galvanized sheet painted in mat black in order to improve the radiations absorbance. The heat exchanger is placed inside the drying room above the absorber plate. The design schemes of the solar dryer are presented in Figs II.4 and II.5.

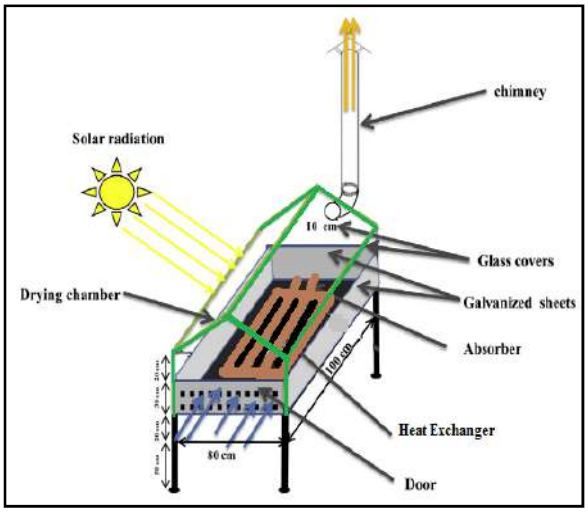

Fig II.4 Picture of the direct solar dryer. **Fig II.5** Schematic diagram of the direct solar dryer.

The geometrical dimensions of the studied problem are presented in the table below:

Designation	Symbols	Values *(m)*
Width	W	0.7
Length	L	1
Insulation Thickness	Hi	0.04
Glass cover Thickness	Hg	0.004
Absorber Thickness	Ha	0.002
Air Inlet	Hl	0.02
Chimney Diameter	Ec	0.1
Chimney Length	Lc	1

Table II.1 Geometrical dimensions of the solar dryer.

Thermo-physical properties of the solar dryer are cited in the next tables:

Physical Properties	Symbols	Values
Density ($kg.m^{-3}$).	ρ	1375
Specific heat ($J.kg^{-1}.K^{-1}$)	C_p	840
Conductivity ($J.m^{-1}.s^{-1}.K^{-1}$)	λ	0.0263

Table II.2 Thermo-physical properties of the glass cover.

Physical Properties	Symboles	Values
Density ($kg.m^{-3}$).	ρ	2719
Specific heat ($J.kg^{-1}.K^{-1}$)	C_p	500
Conductivity ($J.m^{-1}.s^{-1}.K^{-1}$)	λ	237

Table II.3 Thermo-physical properties of the absorber.

Physical Properties	Symboles	Values
Density ($kg.m^{-3}$).	ρ	700
Specific heat ($J.kg^{-1}.K^{-1}$)	C_p	2310
Conductivity ($J.m^{-1}.s^{-1}.K^{-1}$)	λ	0.116

Table II.4 Thermo-physical properties of the insulation

II.2.1.5. Measurements apparatus

To measure the experimental results, a several measurements apparatus were used in this experiment. The global solar radiation was measured with a Pyranometer (type Mod. DS 120) and the output data were posted on an apparatus with numerical display. Temperature measurements were performed using a thermometer (Testo 608-H1). An anemometer (Testo 416) was used to measure the air flow velocity while the mass flow rate measurements were performed with a flow meter (Rotameter DUM-5).

II.2.2. Simulation procedure

In the present study, the numerical simulation has been employed to compare with the experimental results in order to improve the thermal performance of the direct solar dryer.

The governing equations mentioned above were solved with the Fluent CFD software. The geometry of the studied problem which is a direct solar dryer has been created by using Gambit software after that it has been treated under Fluent using the finite volume method with a two-dimensional model.

The configuration adopted in this simulation study was chosen taking into consideration the effect of the solar dryer roof on the thermal and the dynamic aspect which can't be neglected. It was treated as a two-dimensional model instead of 3D model in order to simplify the numerical process. The solar dryer roof with a triangular form was drawn above the drying room in which the thermal and the dynamic aspect in this region can be clearly appeared in the numerical process. This adopted configuration gave the optimal approach comparing with the real configuration of the direct solar dryer used in the experimental study.

The numbers of cells considered in this study were 90532, 93422 and 96312. Therefore, to achieve favorable CPU computation time in the simulation, a number of 93422 had been chosen for this study. The unsteady state numerical simulation was performed using a time step of $\Delta\tau = 60$s, while the max iterations per time step was 5 iterations. A uniform mesh sizes were used for the numerical simulation. The grid in the two directions; horizontal and vertical; was uniformly distributed (Fig. II. 6).

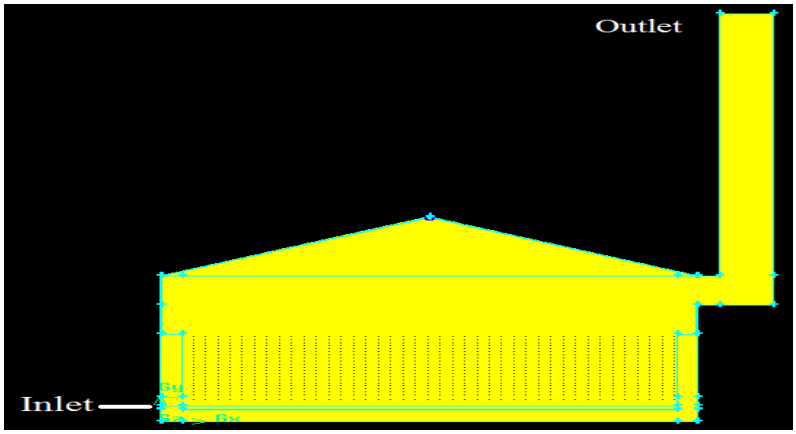

Fig II.6 Meshing of the direct solar dryer with Gambit

The boundary and the initial conditions were considered for Ouargla city, Algeria in November 29-30th, 2017 with the outdoor temperature and solar irradiation variation given by the following empirical equations [98].

$$T_{ao}(\tau) = \bar{T}_{ao} + \bar{T}_{ar} \cos\left(\frac{\pi}{12}(\tau - 14)\right) \quad \text{(II.1)}$$

$\bar{T}_{ao}$=20.5 °C, $\bar{T}_{ar}$ = 5.5 ° C

$$G_{sun}(\tau) = \hat{G}_{sun} \sin\left(\frac{\tau - a}{b - a}\pi\right), \quad a \prec \tau \prec b \tag{II.2}$$

$\hat{G}_{sun}$ = 643W/m^2, a = 07: 00 am, b = 06: 00 pm

II.2.3 Mathematical modeling and boundary conditions

The modeling of the phenomena generated inside the solar dryer is too much recent. So that, inside the drying room, the major part of the volume is occupied by the air. The mass of air plays two important roles in the drying process:

- The transfer of the convective heat flow from the absorber to the dried product.
- The transportation of the product vapor to the outside.

II.2.3.1 Hypothesis

- The flow is supposed two dimensional, unsteady and in turbulent model.
- The flow is supposed incompressible, viscous and Newtonian.
- The thermo-physical properties of the air and the dryer components are considered constant.
- The solar radiation between the internal walls of the solar dryer is neglected.
- The flow of the air is obeyed to the Boussinesq approximation $\rho = \rho_0$ in everywhere exept in the term of gravity where it vary according to the relation:

$$\rho \vec{g} = \rho_0 [1 - \beta(T - T_0)] \vec{g} \tag{II.3}$$

ρ_0: Density at the temperature of reference T_0 and β is the thermal expansion coefficient, evaluated at T_0.

- The porous medium is homogeneous, permeable, and unconsolidated; it is saturated with a unique fluid (air).
- The PCM behaves as an ideal material (no degradation, nor super-cooling).

II.2.3.2 Mathematical model

The following equations of conservation describe the heat transfer inside the solar dryer:

In the air

- of mass:

$$\frac{\partial u}{\partial x}+\frac{\partial v}{\partial y}=0 \tag{II.4}$$

- of momentum along x and y:

$$\frac{(\partial(\rho u))}{\partial t}+div(\rho U u)=div(\mu.gradu)-\frac{\partial P}{\partial x} \tag{II.5}$$

$$\frac{(\partial(\rho v))}{\partial t}+div(\rho U v)=div(\mu.gradv)-\frac{\partial P}{\partial y} \tag{II.6}$$

- of energy:

$$\rho_f c_f \frac{\partial T}{\partial t}+\rho_f c_f\left(u\frac{\partial T}{\partial x}+v\frac{\partial T}{\partial y}\right)=\frac{\partial}{\partial x}\left(\lambda_f \frac{\partial T}{\partial x}\right)+\frac{\partial}{\partial y}\left(\lambda_f \frac{\partial T}{\partial y}\right) \tag{II.7}$$

In the solid medium

- of energy:

$$\rho c\frac{\partial T}{\partial t}=\frac{\partial}{\partial x}\left(\lambda\frac{\partial T}{\partial x}\right)+\frac{\partial}{\partial y}\left(\lambda\frac{\partial T}{\partial y}\right) \tag{II.8}$$

II.2.3.3 Boundary and initials conditions

- *The inlet of the solar dryer:*

  The ambient temperature and the atmospheric pressure are assessed at the inlet of the solar dryer.

  $T_{inlet}=T_a$, $p_{inlet}=10^5 Pa$

- *The outlet of the chimney:*

  The atmospheric pressure is assessed at the outlet of the chimney:

  $p_{outlet}=10^5 Pa$

- A dynamic condition in the wall (u=v=0) is imposed in all the internal walls of the dryer.
- *The lateral walls of the dryer:*

The externals laterals surfaces of the solar dryer are exposed to the convection (convective losses). The thermal flow lost by convection may be evaluated by:

$$-\lambda_w \frac{\partial T}{\partial n} = h(T_w - T_a) \quad \text{(II.9)}$$

T_w : Is the temperature of the external walls and T_a is the ambient temperature.

h : Is the heat transfer coefficient with the ambient air; it is considered constant and evaluated starting from the correlation of Watmuff et al [99].

$$h = 2.8 + 3V_v \quad \text{(II.10)}$$

V_v : is the wind velocity, it was found equal to 3 m/s (average wind velocity measured during the period of the experiment at the study site).

- *Glass cover:*

A heat transfer combined convection-radiation is assessed on the external wall of the glass cover:

$$-\lambda_g \frac{\partial T}{\partial n} = h(T_g - T_a) + \varepsilon_v \sigma (T_v^4 - T_{sky}^4) \quad \text{(II.11)}$$

The sky temperature is calculated using the correlation of Swinbank [100]:

$$T_{sky} = 0{,}0552 T_a^{1,5} \quad \text{(II.12)}$$

II.2.4. Results and discussion

II.2.4.1. Experimental results

Fig. 6 displays the daily solar radiation and the ambient temperature variation versus local time during the 24 hours of the day 29-30/11/2017. It is noted that the maximum solar radiation value reached 643 W/m^2 at 13:00, then it gets decreasing till became zero after the sunset at 18:00. It is also important to note that solar radiation intensity affects directly the ambient temperature. This result reveals, as expected, that the instantaneous drying air temperature depends upon the solar radiation evolution.

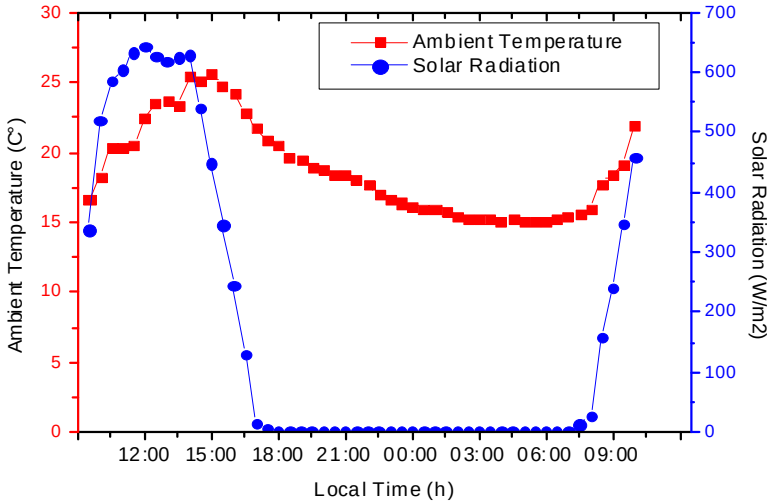

Fig II.6 Recorded daily solar radiation and ambient temperature evolution.

Fig II.7 shows that the drying air temperature in the solar dryer without using the heat exchanger reached 41°C exceeding the ambient temperature by 15°C. After the midday, the ambient temperature starts to decrease because of the decreasing of the solar radiation leading to a decrease in the drying air temperature till becomes the same as the ambient temperature by the sunset meaning that the solar dryer efficiency depends on the solar intensity variation as the only source of heat in this case. This comment has been mentioned by Mennouche et al [94]. The drying process in this case stops with the sunset because of the absence of the heat source and then the solar dryer efficiency will be worthless.

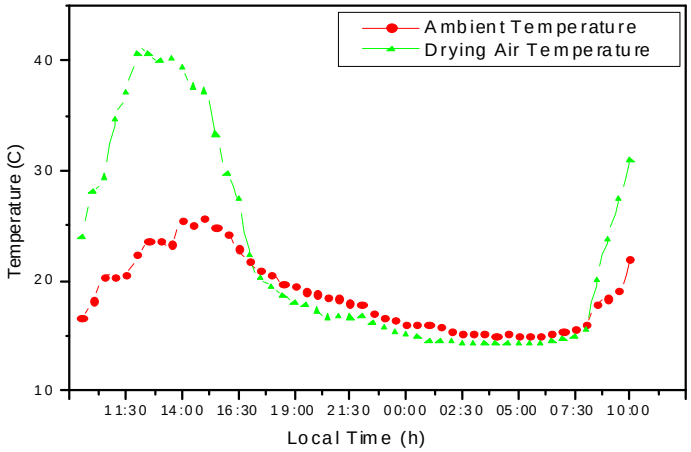

Fig II.7 Experimental measurements of the drying air temperature in the solar dryer without heat exchanger.

Fig II.8 illustrates the drying air temperature evolution of the solar dryer during 24h. It is noticed that with the integration of the heat exchanger inside the solar dryer, the drying air temperature increases with time and with the increasing of solar radiation until reaches the

maximum value 58°C at 13:00. After noon, the solar radiation starts decreasing until becomes zero at 19:00 as the drying air temperature becomes 47°C. After sunset and throughout all the night until the sunrise, the drying air temperature remains important and almost steady with an average value of 46°C exceeding the ambient temperature by 30°C. The obtained result after using the heat exchanger show a significant improvement in the solar dryer thermal performance by comparison with some previous similar results such as what is found by Sandali et al [97] who integrated a sensible heat storage medium to improve the thermal performance of a direct solar dryer. However, they found that the temperature of drying air is increased by 4°C with integration of porous medium. The heat exchanger keeps the drying air temperature high and sufficient to continue the drying operation even in the night as reported by S. Misha et al [93] and Varun et al [101] who used an air heater as a source of heat to improve the thermal performance of a solar dryer, whereas they found that the drying air temperature reached 45°C after using the air heater.

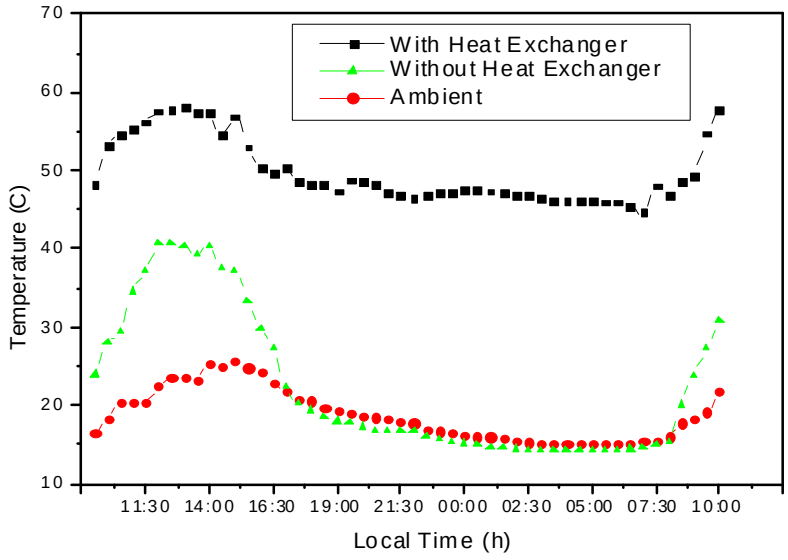

Fig II.8 Experimental measurements of the drying air temperature in the solar dryer with and without heat exchanger.

Fig II.9 shows the variation in the water temperature between the inlet and the outlet of the heat exchanger. The water enters with 3 L/min and with a fixed temperature of 70°C then it releases the heat by convective transfer. At midday, the solar radiation and the ambient temperature remain very high which reduces the convective heat transfer between the exchanger and the circulating air. Consequently the water temperature is reduced only by 1°C at the outlet. After midday, the solar radiation starts to decrease and hence its heating effect

on the drying air declines. Accordingly the heat exchanger effect on drying air becomes predominant and heat convective transfer exchanger-air is enhanced. The heat transferred from water to drying air reduces water temperature from 70°C at the inlet to 67°C at the outlet. After midnight, the ambient temperature gets too cold, thus the transferred heat quantity is increased and the outlet water temperature becomes 66°C. With the sunrise of the second day, the solar radiation restarts its effect on the drying air which reduces the heat transfer exchanger-air.

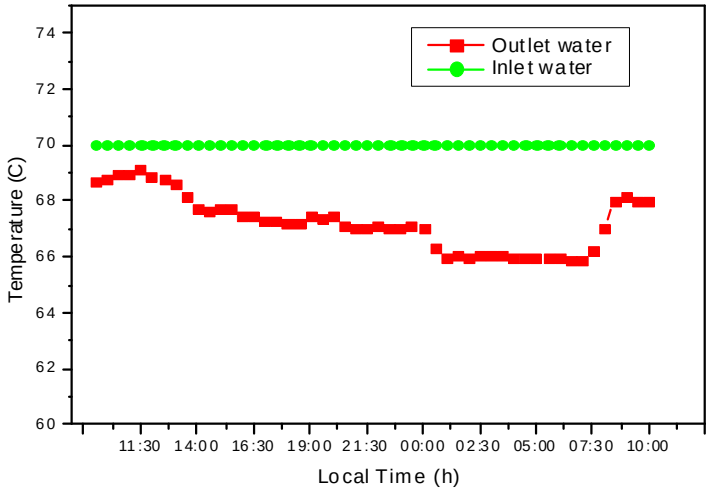

Fig II.9 Measured variation of the heat exchanger water temperature.

II.2.4.2 Simulation results

In this part of study, the simulation results are presented to highlight the thermal aspect of the studied problem and to compare with the experimental one.

Fig II.10 shows the temperature evolution inside the solar dryer without using the heat exchanger. It is noticed that the drying air temperature of the solar dryer increases with time and with increasing solar radiation. At first, the solar radiation level at 07:00 is still very low causing low ambient air and absorber plate temperatures. After, the solar radiation begins to increase till reaching its maximum value 643W/m^2 at 13:00 leading to a rise of the absorber plate and the drying air temperatures up to 81°C and 41°C respectively. This is the maximum drying air temperature produced by the solar dryer without using the heat exchanger. After noon, the solar radiation starts to decline and hence both the absorber plate and drying air temperatures were brought down. After sunset, the heat transfer stopped because of no solar radiation. The data obtained from the CFD modeling software showed good correlations with the experimental results. Hence CFD FLUENT may be used as a drying optimization tool as stated by Mathioulakis et al [102].

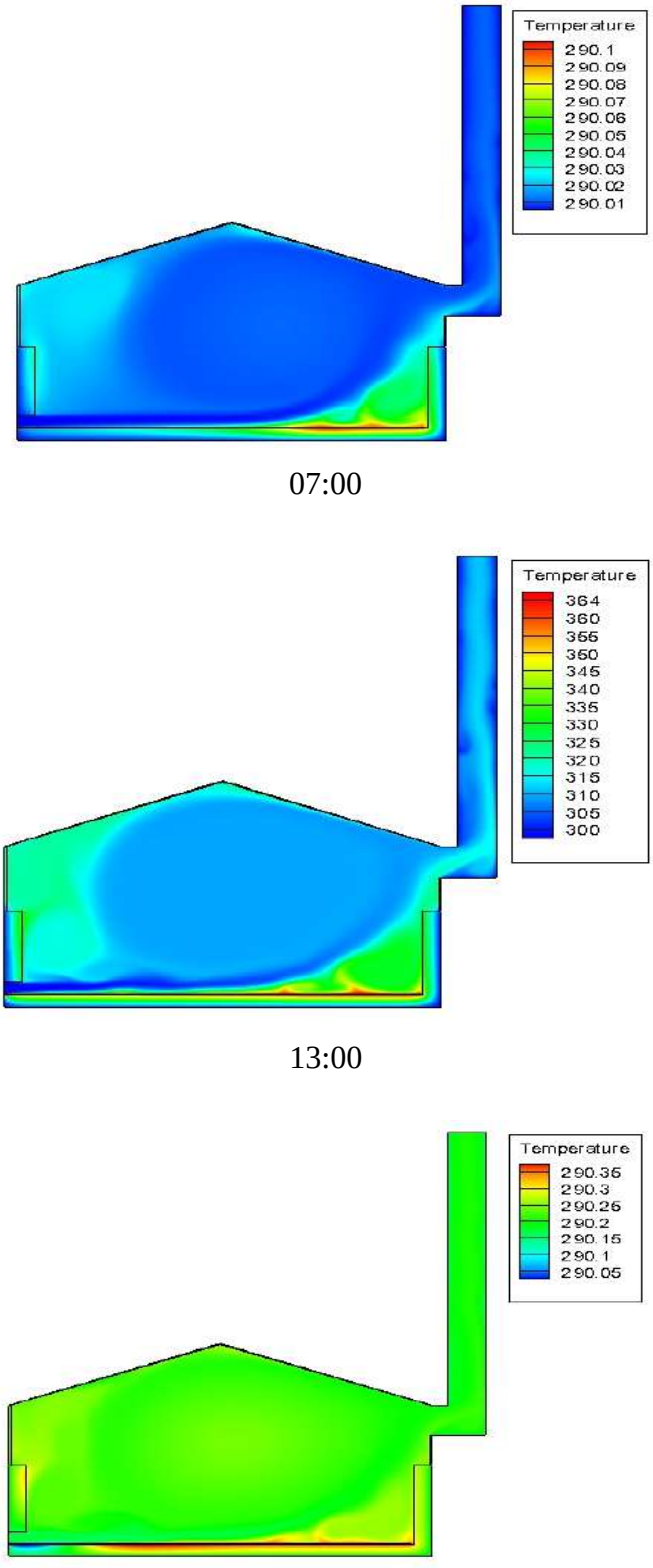

Fig II.10 Temperatures counters of solar dryer without heat exchanger at different time.

Fig II.11 shows the temperature evolution inside the solar dryer with integration of the heat exchanger. At 07:00, it is noticed that the air enters at low temperature of 17°C. After, it becomes gradually warmer under the effect of heat convection when passing through the heat exchanger using the circulating hot water. The drying air temperature at this time reaches 48°C owing to the heat exchanger effect only. As illustrated at 13:00, the drying air temperature reaches a maximum temperature of 57°C due to the presence of two heat sources namely absorber plate and heat exchanger. After sunset, because of no solar radiation, the absorber plate has no heating effect on the drying air. At this time, the only remaining heat supplying source in the solar dryer is the heat exchanger whose temperature is fixed at 70°C. For instance, at 00:00, the inlet air temperature is 17°C, but after passing through the heat exchanger, it becomes 49°C. This temperature is sufficiently large to continue the drying operation overnight. The use of the heat exchanger with geothermal water decreases the drying time and extends the drying operating of the solar dryer. The addition of an auxiliary source of heat highly improves the performance of the solar dryer as found by Hossain et al [103].

The obtained results show a significant similarity with the previous studies as what it was found by Sevik et al [104] who proposed a simple and cost effective solar heat pump system (SAHP) with flat plate collectors and a water source heat pump for drying Mushroom. They found that drying process can be continued with solar energy in daytime while the heat pump system can be used in other times (at nights).

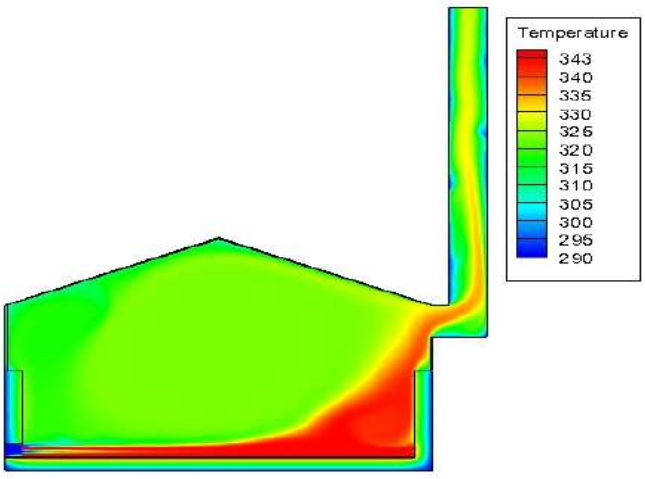

07 :00

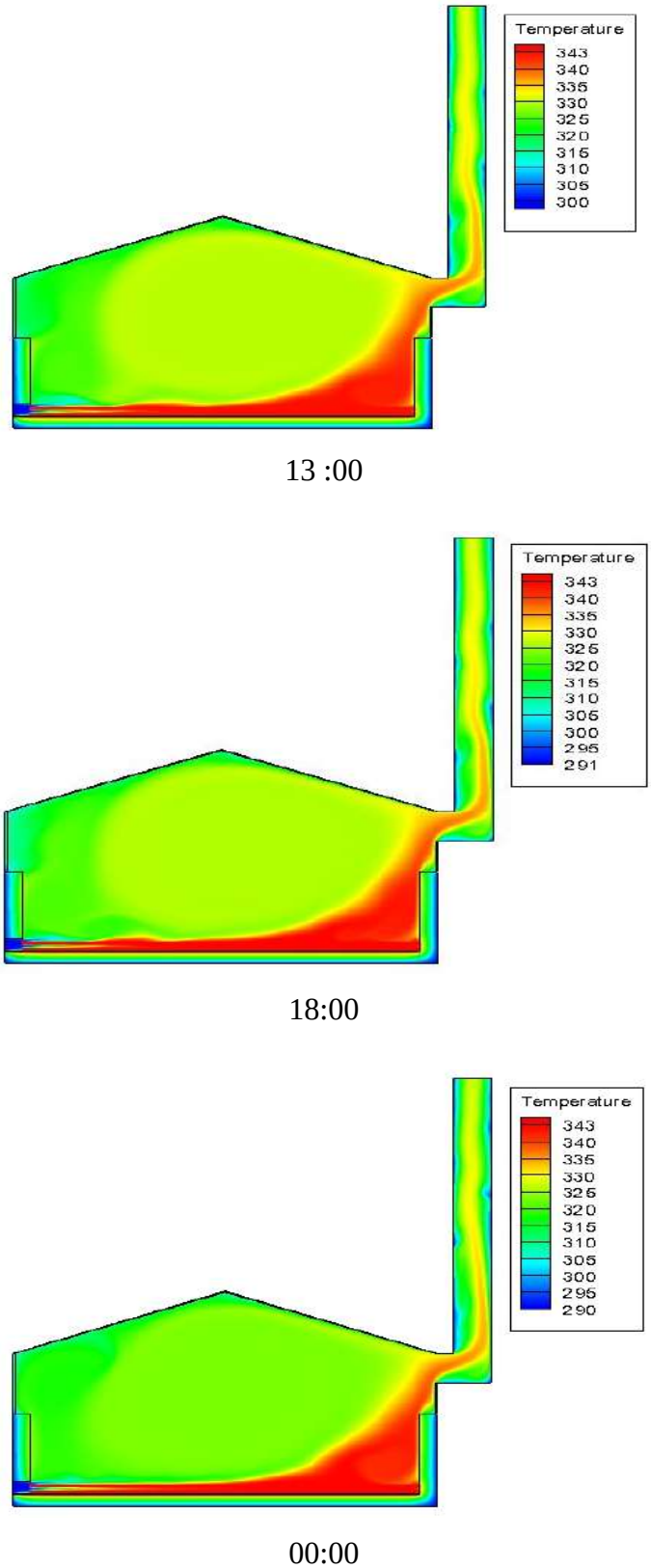

Fig II.11 Temperatures counters of solar dryer with heat exchanger at different time.

Fig II.12 shows that the axial air velocity is almost uniform in the middle of the solar dryer where the dried products will be placed in; ranging between 0.05 and 0.15 m/s. This uniformity and stability of the drying air velocity makes the drying process and drying time easy to control and can help also to keep the same final state of the same dried product. In this context, Xiao et al [105] and Sarsavadia et al [106] found that the stability of the drying air velocity has an important influence on the drying process. By other side, small areas appear in dark blue color indicating the presence of recirculation zones of fluid particles.

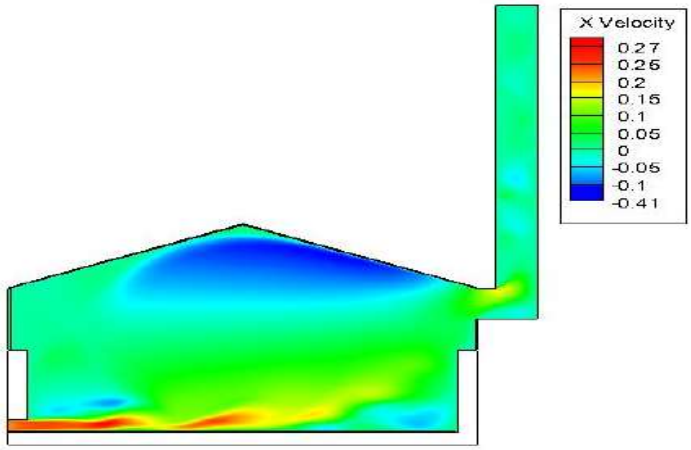

Fig II.12 Axial velocity evolution of the drying air in the solar dryer without heat exchanger.

Fig II.13 shows that the axial velocity is almost constant and homogeneous too, even during the integration of the heat exchanger inside the solar dryer, because it was set up horizontally in the same direction of the air trajectory and hence drying air passes easily and freely with no obstacles. It should be noted in such situation that the low values observed in the drying air velocity confirm that the drying mode would be mainly controlled by a natural convection.

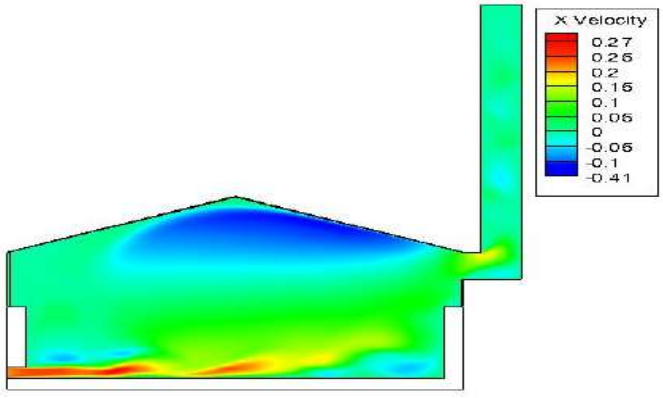

Fig II.13 Axial velocity evolution of the drying air in the solar dryer with heat exchanger.

Fig II.14 shows a comparison between the simulation and the experimental results. It is noticed that from 10:00 to 03:00pm the difference in temperature between the simulation and the experimental results is almost steady (2°C), however it is ranged between 1°C and 3°C from 15:00 to 10:00 of the second day, which are small differences with no significant impact on the drying process and product quality. The remarked approach between the simulation and the experimental results approve the adopted simulation model presented in this study. The fluctuations remarked in the level of the experimental results are explained by the influence of the wind velocity (Fig II.15) which was not steady and then can affect the stability of the drying air temperature as it is confirmed by Nair et al [107].

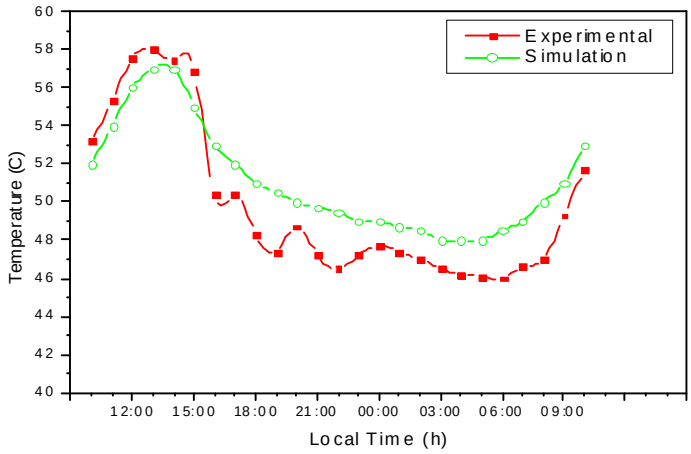

Fig II.14 Comparison between the experimental and the simulation results.

Fig II.15 shows the variation of the wind velocity during the day of the experiment. It appears that the wind velocity is almost constant with a value of 4 ms^{-1} over the interval of time from the morning till 16:00, after that it starts to vary and it ranges between 1-5.5ms^{-1}. This variation negatively affects the stability of the drying air temperature, because that convection heat transfers between the solar dryer and the ambient depends on the wind velocity as mentioned by Naphon [108]. The wind velocity affects the entry air speed which leads to the fluctuations observed on the drying air temperature. This result is consistent with what it was reported by Sallam et al [109] who found that climatic conditions such as wind velocity affects the stability of the thermal performance of solar dryer.

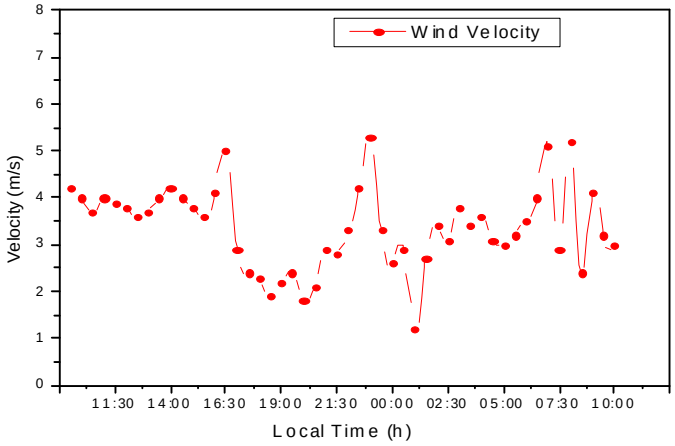

Fig II.15 Evolution of the wind velocity.

II.3. Heat exchanger supplied with the solar water heater

In such region where there is no available geothermal water source, it is really important to think about another source of heat which can be used after sunset. Solar water heater store the solar energy in form of sensible heat using water which is circulated throughout a solar collector and then store it inside the storage tank to use it after sunset. In this part of chapter, the heat exchanger is connected with a solar water heater which is made in one piece (the solar collector and the storage tank are assembled in one component). In which the storage tank is placed above the absorber plate as shown in Fig II.16.

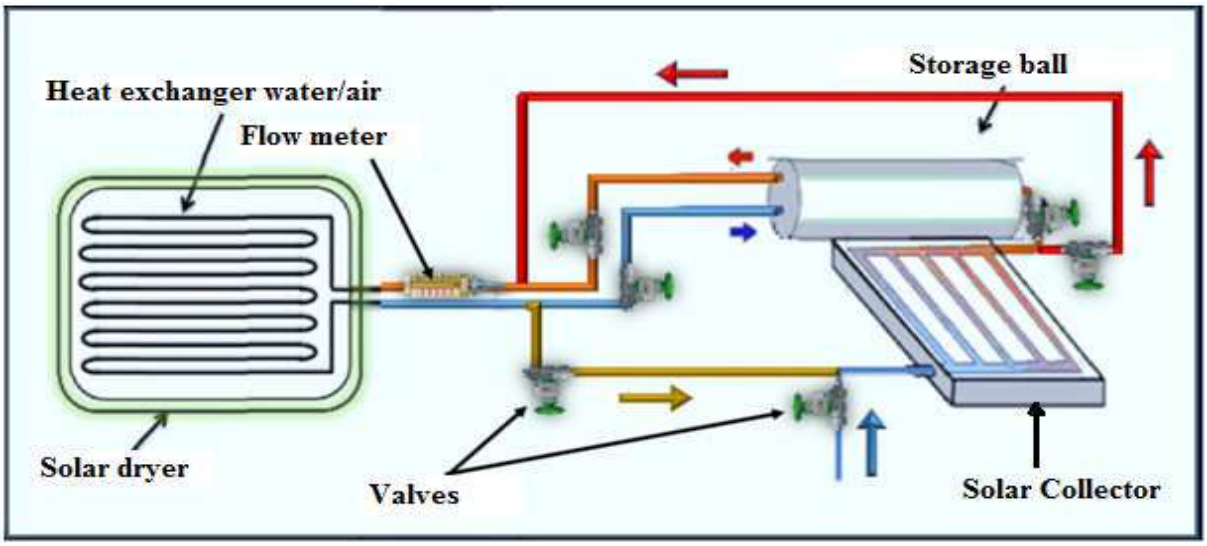

Fig II.16 Representation of the process circuit.

In this case, the solar water heater is fed by a source of cold water, in which the output of the solar collector, is connected on the one hand with the heat exchanger (direct connection)

and on the other hand, it is connected with the storage tank. At 18:00h; where the solar radiation become very low; the supply with cold water of the solar water heater is stopped and the direct connection with the heat exchanger is replaced by a supply from the storage tank (tank connection).

Fig II.17 shows the experimental results of the drying air temperature of the solar dryer without and with heat exchanger supplied by the solar water heater. It appears that there is no big difference in temperature (almost 1°C) in the period from the morning till the midday which means that there is no effect of the heat exchanger on the solar dryer temperature in this period. In this period, the solar dryer is still low but in progress and the solar collector of the system works on heating the water circulated through it. At 13h00, the solar radiation reaches its maximum value and the water circulated inside the heat exchanger will be very hot under the effect of the solar collector which leads to increase the drying air temperature (55°C as the maximum reached value). After 13h00, the solar radiation starts to decrease and the temperature of the circulated water decrease too which leads to decrease the drying air temperature (37°C at 18h00). At 18h00, the solar radiation becomes very low and then the heat exchanger supplied by the storage tank instead of the solar collector. The temperature of the drying air starts to increase under the effect of the hot water which comes from the storage tank and circulates inside the heat exchanger. It ranges between 40°C and 41°C from 19h00 till midnight, and then it starts to decrease with a very slow way. With using solar water heater, drying process can be continued 6h after sunset. The solar water heater system stores the hot water inside the storage tank and acts as a source of heat after sunset.

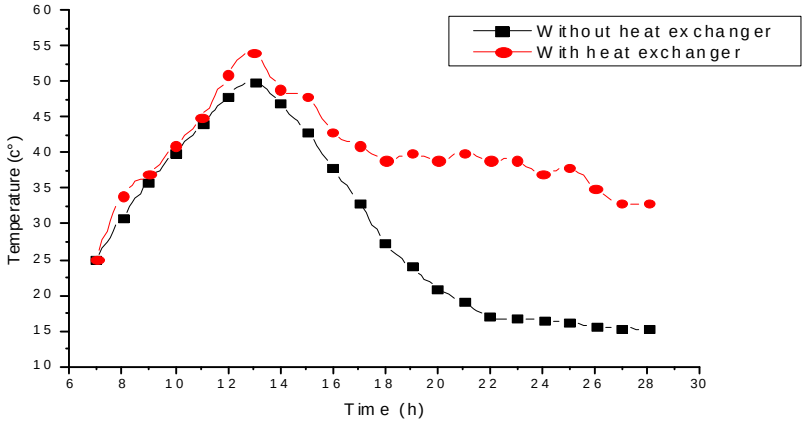

Fig II.17 Experimental measurements of the drying air temperature in the solar dryer with and without heat exchanger supplied by the solar water heater system.

Fig II.18 shows a comparison between the simulation and the experimental results. It is noticed that the difference in temperature of drying air between the simulation and the experimental results is ranged between 1°C and 4°C in the rare cases. This small difference

has no significant impact on the drying process and the product quality. The remarked approach between the simulation and the experimental results approve the adopted simulation model presented in this study. The fluctuations remarked in the level of the experimental results are explained by the influence of the climatic conditions which are not controllable contrary to the simulation procedure which can affect the stability of the drying air temperature.

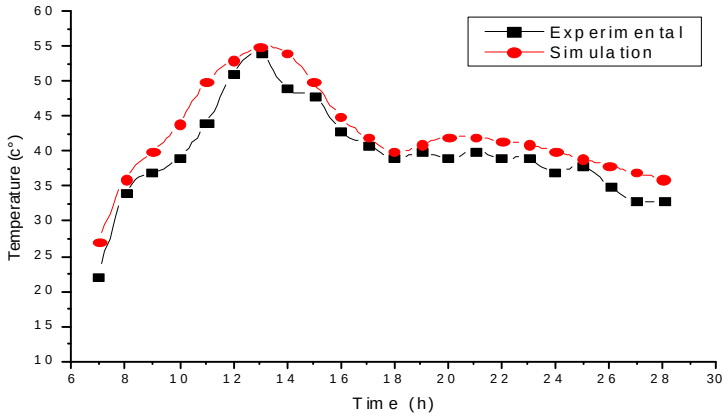

Fig II.18 Comparison between the experimental and the simulation results.

II.4 Conclusion

The presented work concerns an experimental study aiming to improve the thermal performance of a direct solar dryer with integration of geothermal water heat exchanger properly tested in the arid north-Saharan regions of Algeria. The heat exchanger generates the heat from the circulated hot water and acts as a permanent source of heat. The obtained results in this study showed a significant improvement of the thermal performance of the direct solar dryer, especially after sunset. With integration of heat exchanger inside solar dryer, the smallest obtained experimental value of drying air temperature was found 46°C, while the highest one was 58°C. After sunset and throughout all the night until the sunrise, the drying air temperature remains important and almost steady with an average value of 46°C and exceeds that in case of solar dryer without heat exchanger by 30°C. The integration of the heat exchanger inside solar dryer ensures the continuity of drying process at the night and even during cloudy days. In addition to the importance of the obtained results relating to the improvement of the drying system with a supplementary thermal source, the present study, in case of large application, can provide tap water with satisfactory and moderate temperature as preferred by the consuming citizens. The problem of discontinuity of drying process has been resolved by using this technique.

Chapter III:

Thermal Behavior Modeling of a Direct Solar Dryer as Influenced by Sensible Heat Storage in a Porous Medium

III.1 Introduction

Numerical simulation method has been employed to improve the thermal performance of cabinet direct solar dryer. This chapter focused on the numerical simulation of a direct solar dryer with integration of a flat layer of fractured porous medium above the absorber plate in the aim to store thermal energy in form of sensible heat. Several calculations were conducted, using the finite volume method with a two-dimensional unsteady model implemented in the Fluent CFD software. The porous medium has been integrated with different thickness to show the influence of the medium thickness on the thermal performance of solar dryer. Different kinds of materials have been tested and studied. The effect of porosity of porous medium has been studied.

III.2 Models and approximation

III.2.1 Physical Model

The geometry of the considered problem is shown in figure III.1. It is a laboratory scale direct solar dryer with integration of porous medium above the absorber plate. Therefore, This solar drier consists of four components; the insulation which decreases the heat losses, the absorber plate to absorb solar radiations and then to heat the drying air, the glass cover for allowing the transmission of solar radiations through it and the solar chimney for air outlet. In this study, the air enters with low temperature (ambient temperature), and while passing across the porous medium it get heated and its temperature increase under the effect of convective heat transfer.

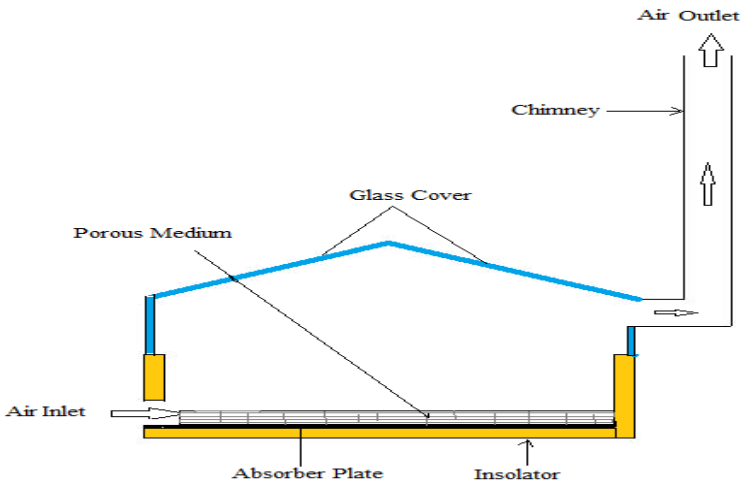

Fig III.1 Schema of direct solar dryer with integrated porous medium.

The thermo-physical properties of the materials used as porous medium are presented in table III.1.

Material	**Thermal conductivity** ***(w/m-K)***	**Density** ***(kg/m-3)***	**Specific heat** ***(J/kg-K)***
Gravel	2	2200	1100
Steel Wool	3.76	7700	452
Stone	0.12	700	1200

Table III.1 Thermo-physical properties of materials [114-116].

III.2.2 Flow Model

The following equations of conservation describe the thermo-convective transfer inside the solar dryer:

In the air

- of mass:

$$\frac{\partial u}{\partial x}+\frac{\partial v}{\partial y}=0 \qquad \text{(III.1)}$$

- of momentum along x and along y:

$$\frac{(\partial(\rho u))}{\partial t}+div(\rho U u)=div(\mu.gradu)-\frac{\partial P}{\partial x} \qquad \text{(III.2)}$$

$$\frac{(\partial(\rho v))}{\partial t}+div(\rho U v)=div(\mu.gradv)-\frac{\partial P}{\partial y} \qquad \text{(III.3)}$$

- of energy:

$$\rho c\frac{\partial T}{\partial t}+\rho c\left(u\frac{\partial T}{\partial x}+v\frac{\partial T}{\partial y}\right)=\frac{\partial}{\partial x}\left(\lambda\frac{\partial T}{\partial x}\right)+\frac{\partial}{\partial y}\left(\lambda\frac{\partial T}{\partial y}\right) \qquad \text{(III.4)}$$

In the solid medium

- of energy:

$$\rho c_s \frac{\partial T}{\partial t} = \frac{\partial}{\partial x}\left(\lambda_s \frac{\partial T}{\partial x}\right) + \frac{\partial}{\partial y}\left(\lambda_s \frac{\partial T}{\partial y}\right) + S_T \quad \text{(III.5)}$$

In the porous medium

The flow in the porous medium is governed by the Brinkman-ForchHeimar Extended Darcy model in which the government equations may write as follow*:*

- of mass:

$$\frac{\partial(\rho u_f)}{\partial x} + \frac{\partial(\rho v_f)}{\partial y} = 0 \quad \text{(III.6)}$$

- of momentum along x and along y

$$\frac{\rho}{\phi}\frac{\partial u_f}{\partial t} + \frac{\rho}{\phi}\left(u_f \frac{\partial u_f}{\partial x} + v_f \frac{\partial u_f}{\partial y}\right) = -\frac{\partial P}{\partial x} + \frac{\partial}{\partial x}\left(\mu \frac{\partial u_f}{\partial x}\right) + \frac{\partial}{\partial y}\left(\mu \frac{\partial u_f}{\partial y}\right) - \frac{\mu u_f}{K} + \frac{\rho C \phi}{\sqrt{K}}\left|\vec{u_f}\right| u_f \quad \text{(III.7)}$$

$$\frac{\rho}{\phi}\frac{\partial v_f}{\partial t} + \frac{\rho}{\phi}\left(u_f \frac{\partial v_f}{\partial x} + v_f \frac{\partial v_f}{\partial y}\right) = -\frac{\partial P}{\partial x} + \frac{\partial}{\partial x}\left(\mu \frac{\partial v_f}{\partial x}\right) + \frac{\partial}{\partial y}\left(\mu \frac{\partial v_f}{\partial y}\right) - \frac{\mu v_f}{K} + \frac{\rho C \phi}{\sqrt{K}}\left|\vec{v_f}\right| v_f \quad \text{(III.8)}$$

$$K = \frac{d_p^2 \phi^3}{175(1-\phi)^2} \quad \text{(III.9)}$$

$$C = \frac{1.75}{\sqrt{175}} \phi^{-3/2} \quad \text{(III.10)}$$

- of energy:

$$(\rho c)_m \frac{\partial T}{\partial t} + (\rho c)_m \left(u_f \frac{\partial T}{\partial x} + v_f \frac{\partial T}{\partial y}\right) = \frac{\partial}{\partial x}\left(\lambda_m \frac{\partial T}{\partial x}\right) + \frac{\partial}{\partial y}\left(\lambda_m \frac{\partial T}{\partial y}\right) \quad \text{(III.11)}$$

The thermal conductivity of the medium λ_m and the product of density-specific heat of the medium are calculated as follow:

$$\lambda_m = \phi \lambda_f + (1-\phi)\lambda_s \quad \text{(III.12)}$$

$$(\rho c)_m = \phi(\rho c)_f + (1-\phi)(\rho c)_s \quad \text{(III.13)}$$

The simplification hypothesis and boundary conditions are cited in the chapter II.

III.2.3 Daily Ambient Temperature Evolution

The climatic conditions used in this work have been measured in the site of study; Ouargla city, country of Algeria; on a specific day, April 4th, 2017.

Fig. 2 shows the variation in the ambient temperature versus time for a specific day. This variation is mathematically modelled by the following empirical equation [98]:

$$T_{ao}(\tau) = \bar{T}_{ao} + \bar{T}_{ar} \cos\left(\frac{\pi}{12}(\tau - 14)\right) \qquad \text{(III.14)}$$

$\bar{T}_{ao}$=25 °C

$\bar{T}_{ar} = 5\ °C$

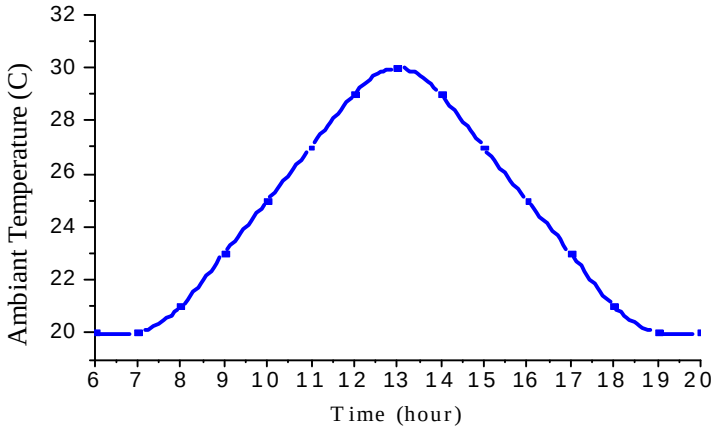

Fig III.2 Daily ambient temperature evolution.

III.2.4 Daily Solar Radiation Evolution

Fig III.3 shows the variation of the solar radiation in function of time. This variation is mathematically modelled by the following empirical equation [98]:

$$G_{sun}(\tau) = \hat{G}_{sun} \sin\left(\frac{\tau - a}{b - a}\pi\right), \qquad a \prec \tau \prec b \qquad \text{(III.15)}$$

$\hat{G}_{sun}$ = 940 W/m^2

a = 07:00

b = 19:00

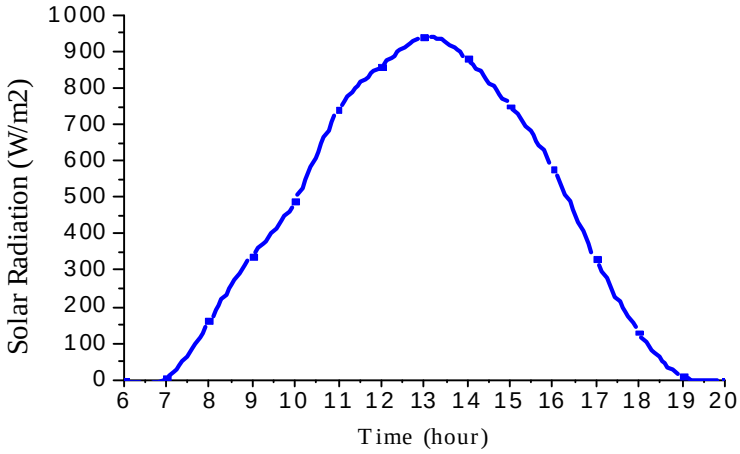

Fig III.3 Daily solar radiation evolution.

III.3 Results and discussion

In this part of work, the study of thermal performance of the direct solar dryer is presented in order to evaluate and to show its thermal performance before integration of porous medium. The contours of air temperature inside solar dryer are presented and discussed. As a second and principal step in this work, the study of solar dryer with integration of porous medium is presented and discussed. A comparative study between the two cases of solar dryer, without and with integration of porous medium, has been done to show the effect of adding a porous medium on the thermal performance of solar dryer.

III.3.1 Solar Dryer without Integration of Porous Medium

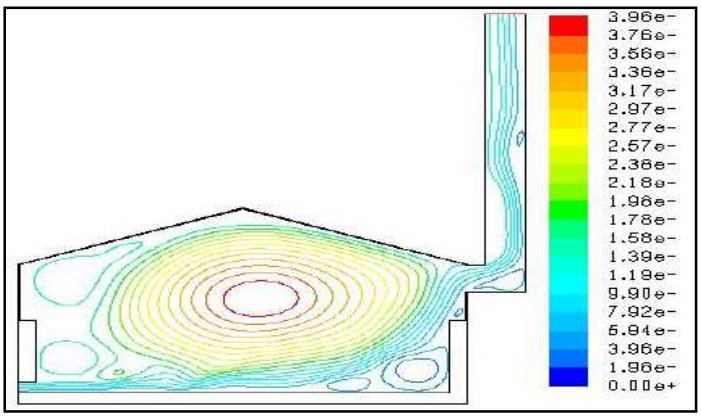

Fig III.4 Contours of stream function

Fig III.4 shows the contours of the stream function. We remark the presence of a recirculation zones in such regions inside the solar dryer. These zones were generated by the presence of a singularity in the air flow.

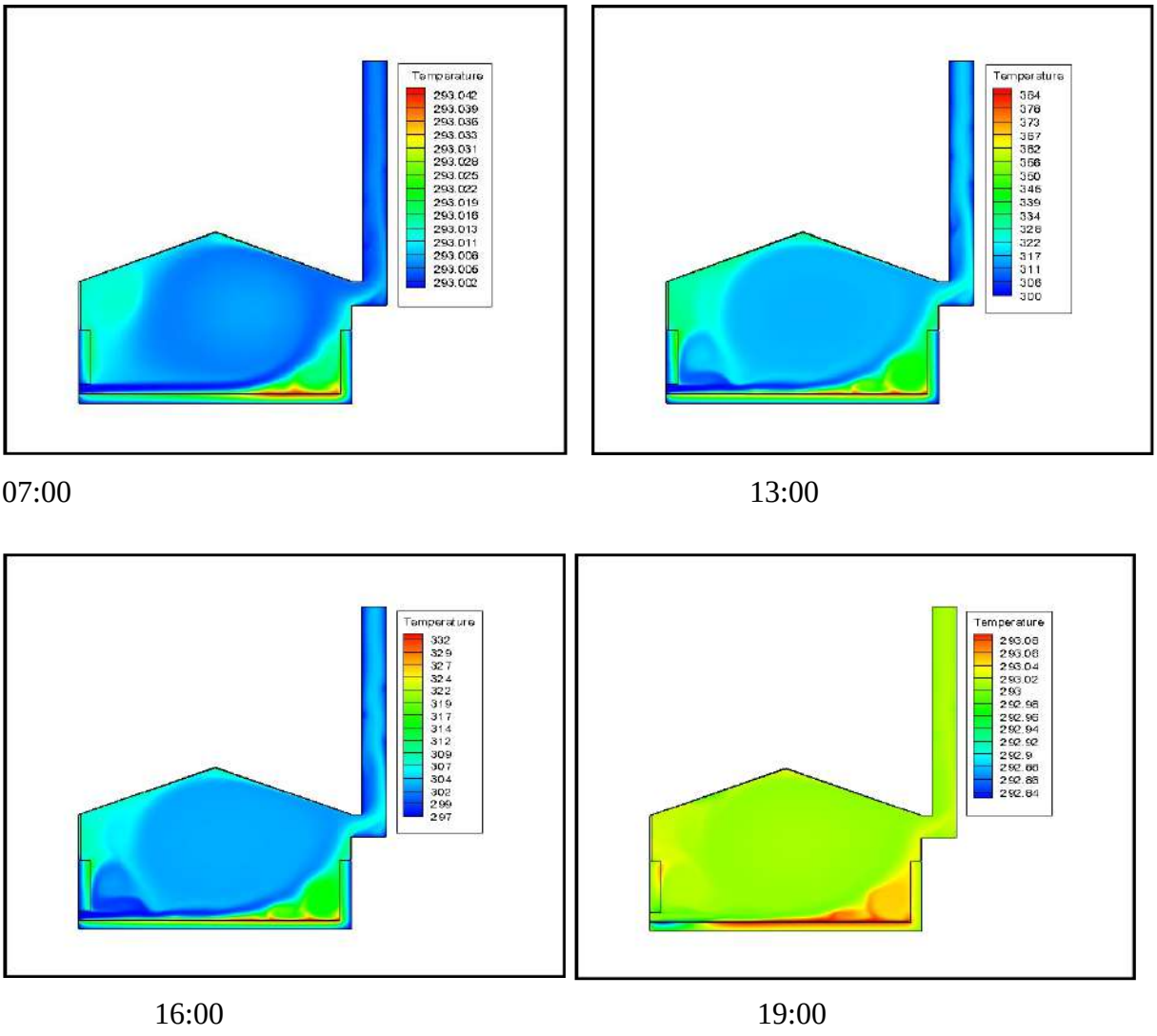

07:00 13:00

16:00 19:00

Fig III.4 Temperature evolution of solar dryer without integration of porous medium.

Fig III.4 shows the temperature evolution of drying air inside solar dryer from sunrise to sunset. At 07:00, the temperature of drying air is still very low and the solar intensity too, it starts to increase with increasing of solar intensity with the passage of time. The solar intensity reaches the maximum value of 940W/m^2 at 13:00 where the temperature of the absorber plate and the drying air were 384K and 323K respectively. After the midday, the temperature of drying air begins to decrease with decreasing of solar intensity; its value at 16:00 was 307K. After sunset, the solar intensity decreases to be zero which make the drying air temperature as the same as the ambient temperature (293K).

III.3.2 Solar Dryer with Integration of Porous Medium (Gravel)

In this part of study, a thin layer of 3cm of gravel has been integrated above the absorber plate as a porous medium. The obtained results are presented below.

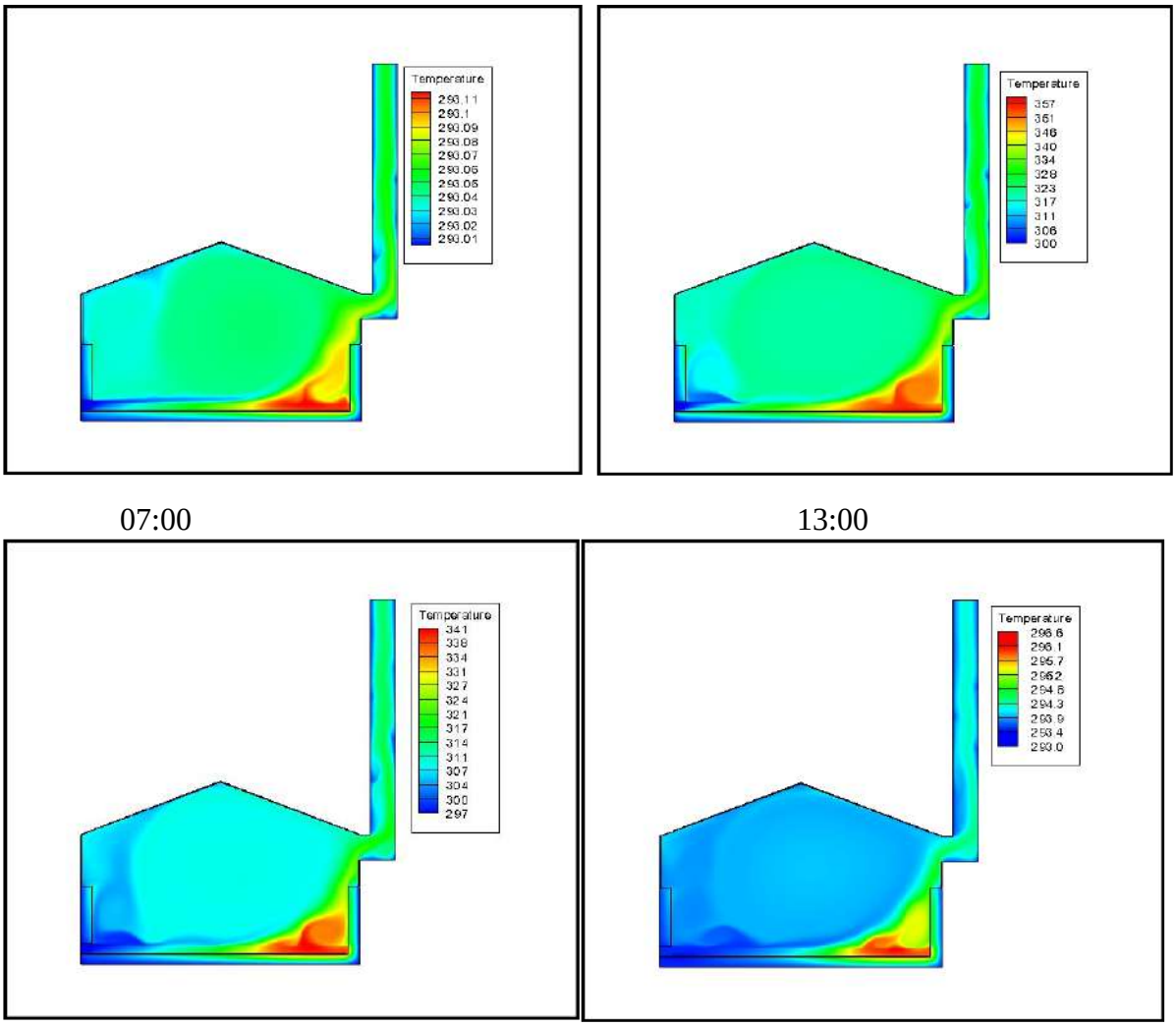

Fig III.5 Temperature evolution of solar dryer with integration of porous medium.

Fig III.5 shows the temperature evolution of solar dryer after adding a thin layer of gravel as porous medium above the absorber plate. The improvement in thermal behaviour of solar dryer after adding the porous medium is clearly observed. The maximum reached temperature of the absorber plate in this case (solar dryer with porous medium) is less than the one in the first case (solar dryer without porous medium), this decreasing in absorber temperature is traduced by the effect of adding of porous medium. The porous medium absorbs the heat stored in the absorber plate by conduction heat transfer which decreases the absorber temperature and makes the porous medium reacts as a source of heat. At 16:00, the drying air temperature is about 310K more than the first case by 4°C, and 300K at 19:00. After midday, the drying air temperature is increased by 4°C with adding of porous medium.

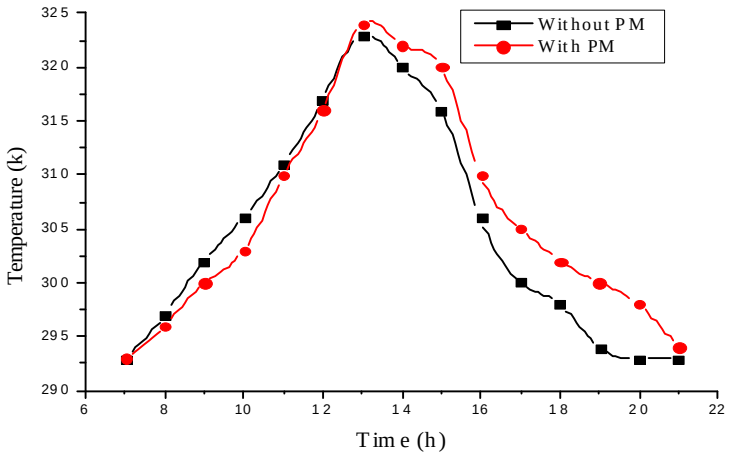

Fig III.6 Temperature evolution of drying air with and without integration of porous medium.

Fig III.6 shows the difference in temperature of drying air in the two cases of solar dryer; with and without porous medium. Before the midday, it is clear that the temperature of drying air in the case of solar dryer without porous medium more than the one in the case of solar dryer with porous medium which means that the integration of porous medium leads to decrease the temperature of drying air. The porous medium spent too much time to warm up and to store the heat because of its low thermal conductivity which bedevils the well functioning of the absorber plate to heat the drying air. After the midday, the porous medium warm up and its temperature increase too. This performs it to heat the drying air passed through it. With integration of porous medium, the temperature of drying air increases by 4°C and extends the functioning of solar dryer by two hours after the sunset. The porous medium in this case reacts as an auxiliary source of heating in addition to the absorber plate. The porous medium creates an area of thermal exchange between the drying air and the materiel which helps to increase the temperature of drying air.

III.3.3 Effect of the porous medium material

Different kinds of porous medium have been tested in order to evaluate their influence on the thermal performance of the solar dryer and to choose the best one that gives the best thermal performance.

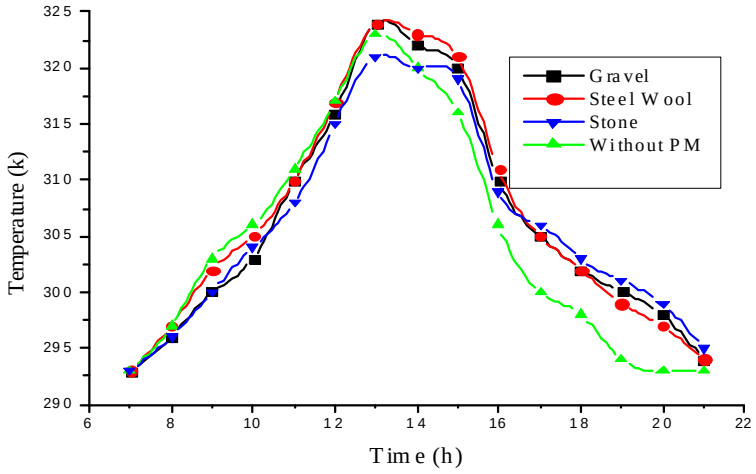

Fig III.7 Temperature evolution of drying air with integration of three different porous medium materials.

Fig III.7 shows the temperature evolution of drying air while using different kinds of porous medium. The maximum reached drying air temperature (324K) is obtained when using steel wool and gravel. However, the maximum obtained temperature while using stone was 321K. The value of the maximum drying air temperature is due to the thermal conductivity of the used material. The thermal conductivity of steel wool and gravel is 3.7W/mK and 2W/mK respectively. However, the thermal conductivity of the stone is 0.12W/mK. After the midday, the way of decreasing of drying air temperature in case of using stone as porous medium is more slowly than the one in the other two cases (gravel and steel wool). After 05:00PM, the drying air temperature in case of using stone becomes the highest one and higher than the case of using gravel and steel wool by 1°C and 2°C respectively. This result is due to the high specific heat 1200J/kgK of the stone comparably with 452J/kgK and 1100J/kgK of steel wool and gravel respectively.

III.3.4 Effect of the Porous Medium Thickness

In this part of work, the effect of porous medium thickness will be presented. The gravel as porous medium has been integrated above the absorber plate in three different thicknesses 2cm, 3cm and 4cm. The temperature evolution of drying air is presented below.

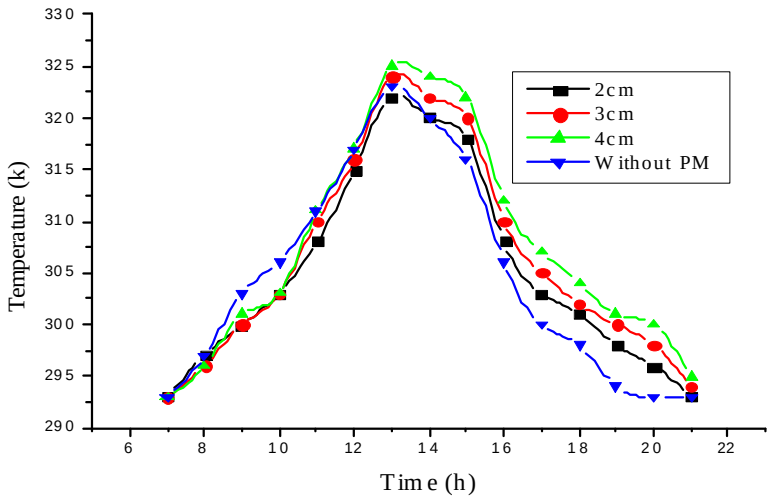

Fig III.8 Temperature evolution of drying air with integration of three different thicknesses of porous medium.

Fig III.8 shows the temperature evolution of drying air in case of integration of porous medium with three different thicknesses 2, 3 and 4cm. Before the midday, it is remarkable that the temperature of drying air in case of solar dryer without porous medium is higher than the one when using porous medium. This remark is traduced by negative influence of porous medium before it warming up. After the midday, the porous medium warms up and affects positively on the process of heating of the drying air. It is well obvious that whenever the thickness of porous medium increases, the temperature of drying air increases too; an extreme relationship between them. The increasing of the porous medium thickness conducts to extent the staying time of drying air inside the porous medium and leads to increase the thermal exchange area between the drying air and the porous materiel which helps to increase the temperature of drying air. The increasing in the thickness of the porous medium by 1cm leads to increase the temperature of drying air by 2°C.

III.3.5 Effect of the Porous Medium Porosity

The effect of the porous medium porosity on the thermal performance of solar dryer will be presented in order to show the appropriate porosity which is congenial with this kind of study. The tested values of porosity are 0.5, 0.6 and 0.7.

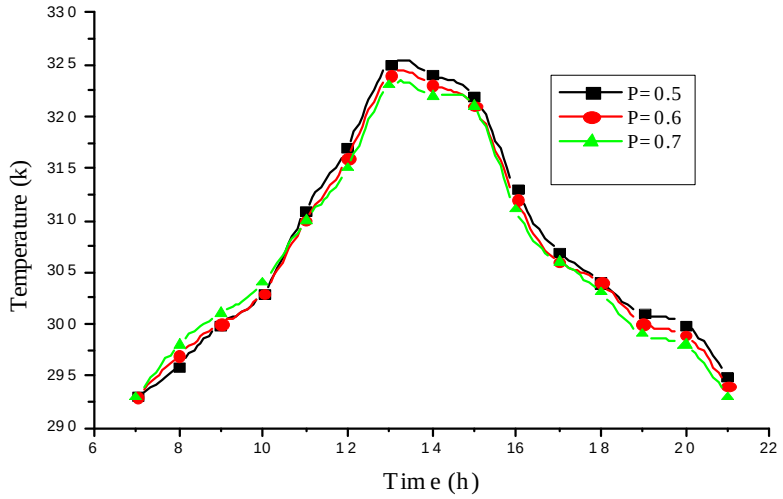

Fig III.9 Temperature evolution of drying air with using different porosities

The effect of the porous medium porosity on the thermal performance of solar dryer is shown in Figure III.9. From sunrise to midday, the temperature of drying air little increases with increasing of the porosity of the medium. However, after midday, the temperature of drying air increases with decreasing of the medium porosity. The porosity is a measure of the void spaces in a material, and is a fraction of the volume of voids over the total volume which means that the increasing of the medium porosity increases the volume of the circulating air inside the porous medium and conversely reduces the volume of the solid materiel which leads to decrease the source of heat and consequently low heating of drying air. The increasing of porosity of the medium by 10% leads to decrease the temperature of drying air by 1°C which is a non significant effect.

The obtained results in this study showed a significant improvement of the thermal behavior, especially after midday. In fact, with integration of porous medium, the temperature of drying air increases by 4°C and extents the functioning of solar dryer by two hours after the sunset. The increase of the porous medium thickness conducts to extent the staying time of drying air inside the porous medium and leads to increase the thermal exchange area between the drying air and the porous materiel which helps to increase the temperature of drying air. The increase of the medium porosity by 10% leads to decrease the temperature of drying air by 1°C, so it is found to be non significant.

III.4 Conclusion

This chapter concerns the contribution to the study of improving the thermal performance of a direct solar dryer which is destined for drying of agricultural products. The concept of ‘sensible heat thermal energy storage’ using different materials reduces the time between energy supply and energy demand, thereby playing a vital role in energy conservation and improves the solar drying energy systems. The porous medium has been used to improve the thermal performance of direct solar dryer. The porous medium stores the thermal energy during sunshine hours and releases the sensible heat during the bad sunny hours. Another technique of solar energy storing and which is highly recommended in drying technology will be presented in the next chapter. This technique is storing of latent heat using phase change material (PCM).

Chapter IV:

Latent heat storage technique applied to a direct solar dryer

IV.1 Introduction

In this chapter, a numerical simulation of the improvement of the thermal performance of the direct solar dryer by the extension of its daily operating time is presented. The present study focused on the study of a direct solar dryer without and with integration of a flat layer of a phase change material (PCM) with the aim of partially storing latent heat thermal energy. Several calculations have been carried out, using the finite volume method using a two-dimensional unsteady model implemented on CFD Fluent software.

IV.2 Models and approximation

IV.2.1 Physical model

The geometry of the considered problem is presented in Fig IV.1. It is a direct solar dryer incorporating a layer of phase change materials (PCM) below the absorber plate. This prototype was made at the level of the laboratory of development of new and renewable energies in arid zones (LENREZA, University of Ouargla, Algeria),

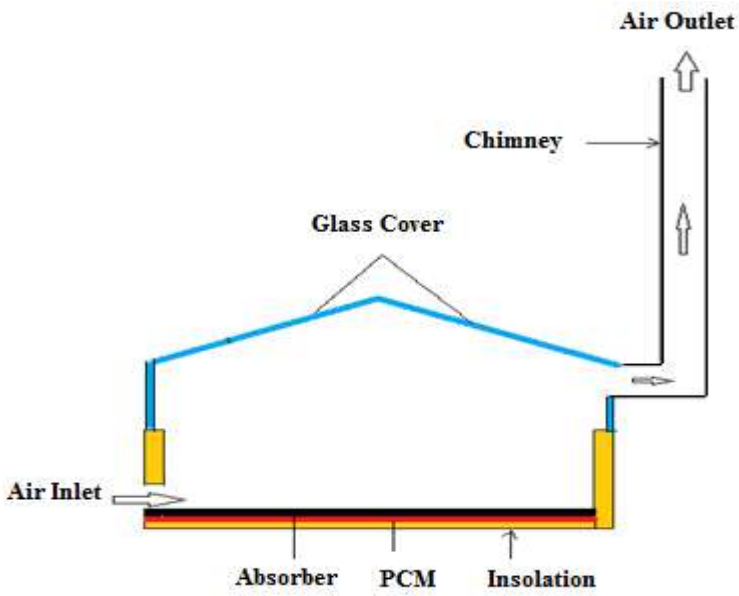

Fig IV.1 Scheme of a direct solar dryer with integration of a flat layer of PCM.

IV.2.2 Flow model

The following equations of conservation describe the thermo-convective transfer inside the solar dryer:

In the air:

- *Of mass:*

$\partial u/\partial x + \partial v/\partial y = 0$ (IV.1)

- *Of momentum according to x and according to y :*

$(\partial(\rho u))/\partial t + div(\rho U u) = div(\mu.gradu) - \partial P/\partial x$ (IV.2)

$(\partial(\rho v))/\partial t + div(\rho U v) = div(\mu.gradv) - \partial P/\partial y + \rho g \beta (T - T_0)$ (IV.3)

- *Of Energy:*

$$\rho c \frac{\partial T}{\partial t} + \rho c \left(u \frac{\partial T}{\partial x} + v \frac{\partial T}{\partial y} \right) = \frac{\partial}{\partial x} \left(\lambda \frac{\partial T}{\partial x} \right) + \frac{\partial}{\partial y} \left(\lambda \frac{\partial T}{\partial y} \right) \quad \text{(IV.4)}$$

U = (u, v) represents the velocity vector, ρ the density, P the pressure, μ the dynamic viscosity of the fluid.

In the solid medium:

- *Of energy:*

$$\rho c \frac{\partial T}{\partial t} = \frac{\partial}{\partial x} \left(\lambda \frac{\partial T}{\partial x} \right) + \frac{\partial}{\partial y} \left(\lambda \frac{\partial T}{\partial y} \right) \quad \text{(IV.5)}$$

In the phase change material (PCM):

The equation of conductive heat transfer is written as following:

$$\rho c \frac{\partial T}{\partial t} = \lambda \left(\frac{\partial^2 T}{\partial x^2} + \frac{\partial^2 T}{\partial y^2} \right) \quad \text{(IV.6)}$$

The equation of the heat transfer in the PCM layer is written as below:

$$\frac{\partial H}{\partial t} = \lambda \left(\frac{\partial^2 T}{\partial x^2} + \frac{\partial^2 T}{\partial y^2} \right) \quad \text{(IV.7)}$$

With

$$H = h + \rho L_{mel} . f(T) \quad \text{(IV.8)}$$

Where h: volume sensible enthalpy (J/m^3): $h = \int_{t2}^{tf} C dt$

L_{mel} : melting latent heat (J/kg)

$f(T)$: Fraction of PCM in the liquid stat

$$f(T)=\begin{cases}0 & T<T_{mel} & solide\\ ]0,1[& T=T_{mel} & melting\\ 1 & T>T_{mel} & liquide\end{cases} \quad \text{(IV.9)}$$

With combination of equation 6 and 7, it comes:

$$\frac{\partial h}{\partial t}=\lambda\left(\frac{\partial^2 T}{\partial x^2}+\frac{\partial^2 T}{\partial y^2}\right)-\rho L_{mel}\frac{\partial f}{\partial t} \quad \text{(IV.10)}$$

$$\rho c\frac{\partial T}{\partial t}=\lambda\left(\frac{\partial^2 T}{\partial x^2}+\frac{\partial^2 T}{\partial y^2}\right)-\rho L_{mel}\frac{\partial f}{\partial t} \quad \text{(IV.11)}$$

The thermo-physical properties of the PCMs used in this study are presented in the table below:

PCM	**Thermo-physical properties**				
	Melting temperature [K]	**Latent heat [KJ/kg]**	**Density [kg/m3]**	**Thermal conductivity [W/m.K]**	**Specific heat [j/kg.K]**
Paraffin	309.7	247	778	0.15	2210
Paraffin	301	244	774	0.15	2160
Paraffin	326,5	266	780	0.21	2500
Paraffin	307	150	1850	0.47	2350

Table IV.1 Thermo-physical properties of PCMs used in the numerical simulation.

The initials and boundary conditions have been cited in the 2nd chapter.

IV.3 Results and discussion

IV.3.1 Evolution of solar intensity in function of time

Fig IV.2 shows the variation in solar intensity in function of time for a typical day. This variation is modeled mathematically by the following empirical equation [98]:

$$G_{sun}(\tau)=\hat{G}_{sun}\,sin\left(\frac{\tau-a}{b-a}\pi\right),\quad a<\tau<b \quad \text{(IV.12)}$$

$\hat{G}_{sun}$: Maximum solar radiation = 940 w/m^2

τ : Time in hour, a <τ< b

a: Sunrise hour: 07h00
b: Sunset hour:19h00

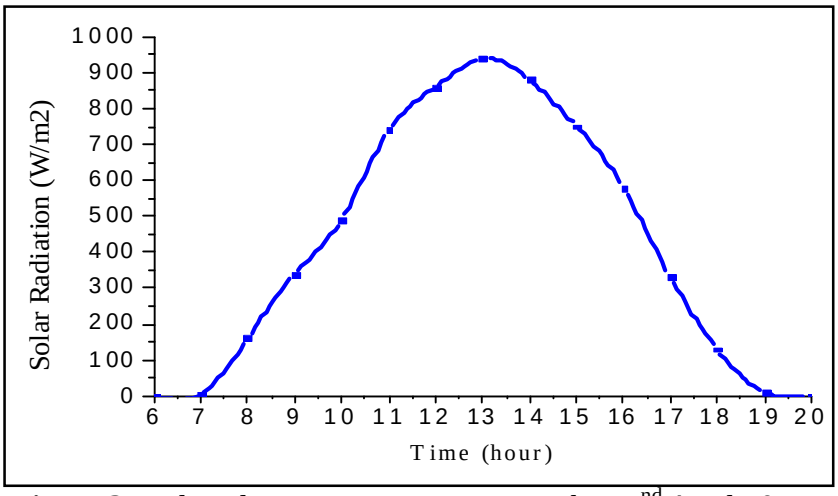

Fig IV.2 Daily solar intensity variation on the 22nd April 2017 .

IV.3.2 Evolution of ambient temperature in function of time

Fig IV.3 shows the variation of the ambient temperature as a function of time for a typical day. This variation is modeled mathematically by the following empirical equation [98]:

$$T_{ao}(\tau) = \bar{T}_{ao} + \bar{T}_{ar} \cos\left(\frac{\pi}{12}(\tau - 14)\right) \quad \text{(III.13)}$$

$\overline{T}_{ao}$: average ambient temperature

T_{ar} : temperature amplitude

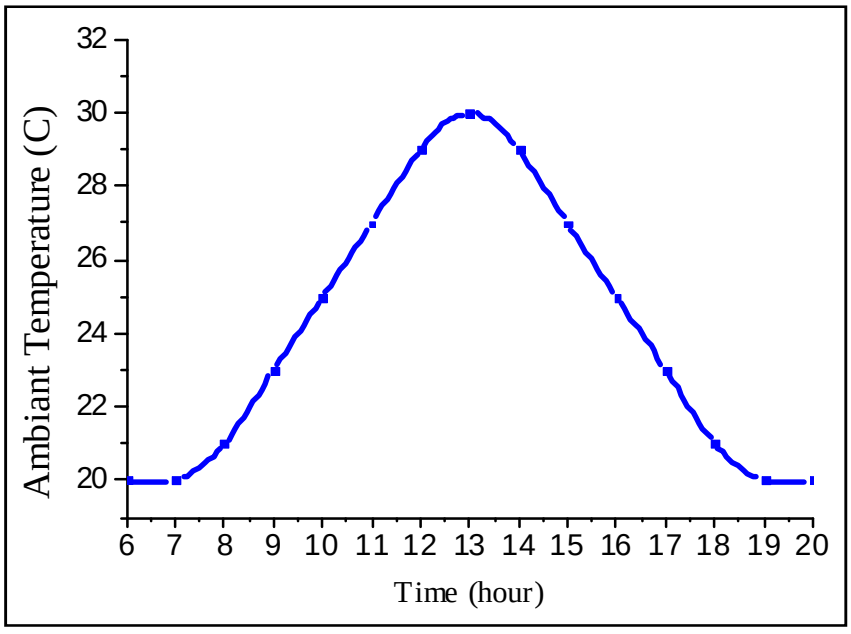

Fig IV.3 Daily ambient temperature evolution.

IV.3.3 Comparison between the simulation and experimental results

In order to have a logical comparison, we carried out a simulation test to record each time the point value of the air temperature in the middle of the solar dryer. This value for regular time intervals was compared to the experimentally measured value for the same time intervals. All of these simulated and calculated values are shown in Fig IV.4. It is clear, taking into account the studied phenomenon that the calculated and measured values are in good agreement with a maximum difference of almost 5°C. This observed discrepancy can be explained by the difference between the actual climatic conditions (fluctuations in solar radiation and the wind speed during the day) and those used by the software calculation, based on a typical regular evolution.

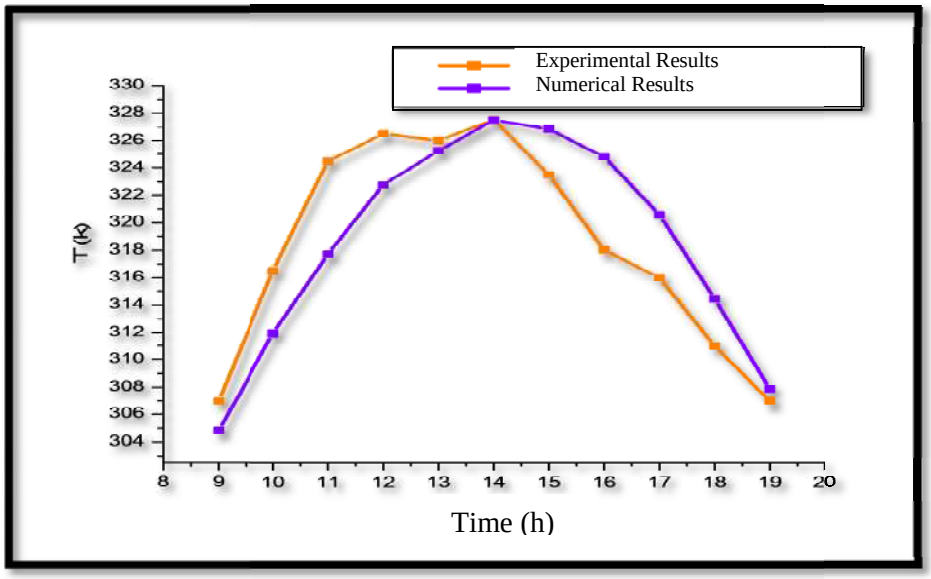

Fig IV.4 Evolution of the drying air temperature of the solar dryer without PCM.

Fig IV.5 shows the distribution of temperature in the direct solar dryer without integration of PCM. After the sunrise, at 09:00, the solar radiation is still not very high and the absorber begins to heat the air circulating inside the solar dryer where we notice that the hottest component is the absorber due to its great absorption coefficient. The lack of homogeneity inside the solar dryer is due to heat transfer with the outside on one side, and on the other side because the temperature of the absorber is still very low (325K) which influences on the good heating of the circulating air. At 12:00, we notice that the air temperature inside the solar dryer is almost homogeneous especially in the drying chamber which leads to obtain good drying results. It is also noted that the temperature of the drying air reaches a higher and acceptable value (324K) for carrying out a drying operation.

At 17:00, we notice that the temperature of the air inside the solar dryer is still homogeneous but it is a little low (315K) because of the decrease in solar radiation. However, the hottest component is always the absorber.

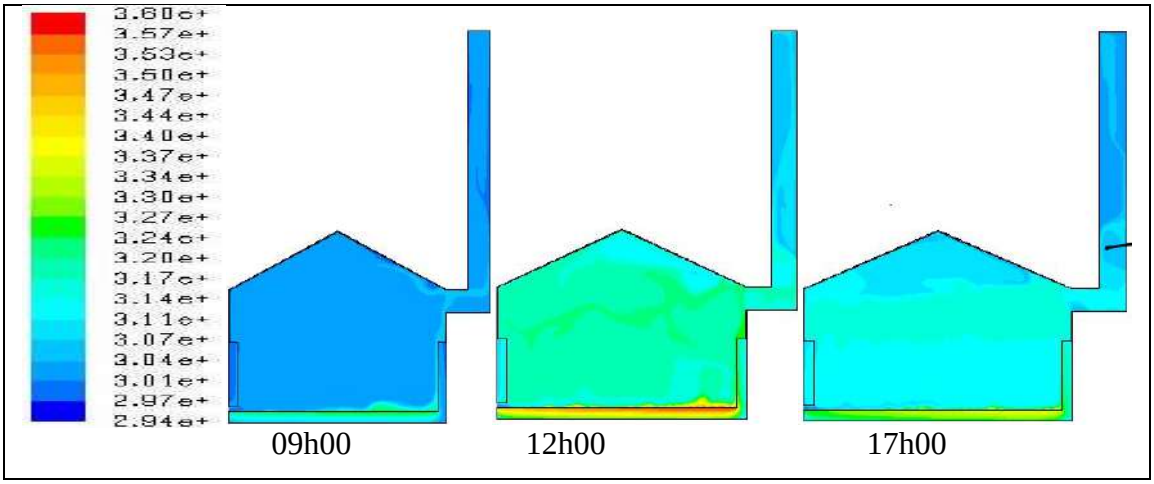

Fig IV.5 Temperature distribution in the direct solar dryer without PCM.

In Fig IV.6, at 09:00, it is noted that the temperature of the air inside the dryer is caused to rise under the effect of solar radiation. With the passage of time and at 12:00, the solar radiation becomes higher which allows to increase the temperature of the air and to generate homogeneity inside the solar drier. Note also that the temperature of the PCM layer is higher compared to that at 09:00. After sunset, at 19:00, we note that the PCM temperature is the largest compared to the other components of the dryer which allows feed the dryer by heat and heating the circulating air. The temperature of the drying air remains homogeneous and sufficient to continue the drying operation under the effect of PCM. During non-sunny hours, liquid PCM will provide heat to the absorber; it is the useful heat of the circulated air. The PCM behaves as a source of heat after sunset.

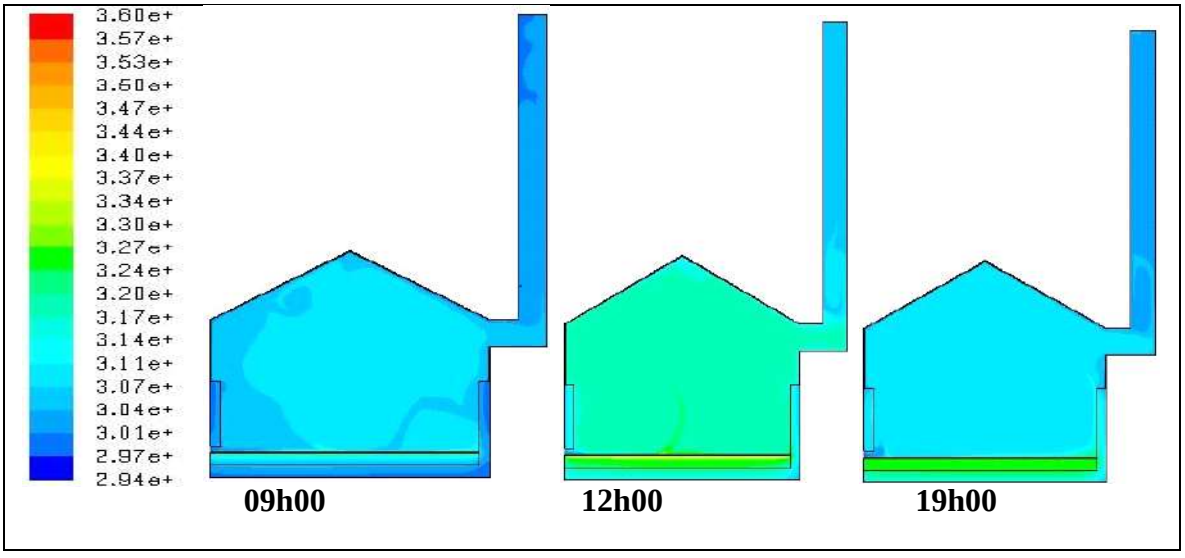

Fig IV.6 Distribution of temperature in the direct solar dryer with PCM.

IV.3.4 Effect of PCM Thickness

To investigate the effect of PCM layer thickness, we incorporated different thicknesses of the PCM layer below the absorbent plate into the direct solar dryer. The PCM used in this case is the one with the 326.5K melting temperature. The thicknesses used in this case are 2cm, 4cm and 6cm. In order to study the influence of the quantities of the PCMs, the obtained results are compared with reference to the case of the solar dryer without PCM. For this we chose to plot the temperature curves of the absorbent plate as a function of time for different thicknesses.

Fig IV.7 shows the variation of the average absorber temperature as a function of time, it is noted that the curve undergoes refraction when the absorber temperature approaches the PCM melting temperature (326.5 K). We Note also that there is a small phase shift, especially at the point of peak moment, between the curves when increasing the thickness of the PCM. The maximum temperature difference of the absorber between the PCM curve and without PCM increases as the thickness of the PCM is increased. It is very clear that from 19h (sunset), the temperatures obtained for the different thicknesses of the PCM are more than that of the case of the dryer without PCM. It can be mentioned, as an indication that at 24h00 there is a temperature difference of 23 °C between the case of the dryer without PCM and the case of PCM with 4 cm of thickness. The best thickness of PCM that gives the best result is the thickness of 4cm, it allows to keep the temperature of the absorber higher after the sunset about 316K to 24h00 and more than the case of the dryer without PCM by 23 °C which allows to extend the operating time of the solar dryer by more than 4 hours after sunset.

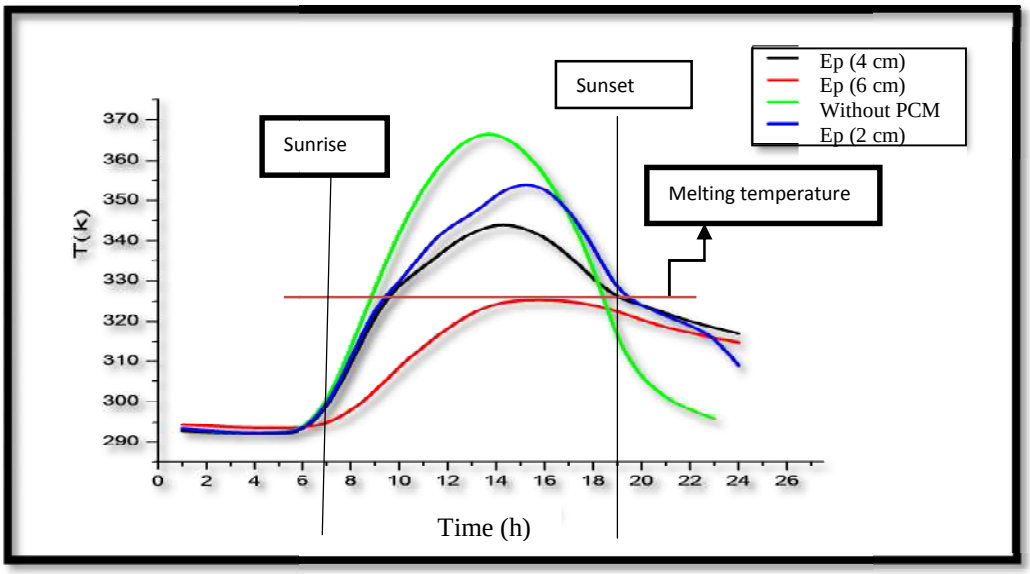

Fig IV.7 Evolution of the absorber temperature of the direct solar dryer with different thicknesses of PCM.

Fig IV.8 shows the evolution of the temperature of the drying air in the direct solar dryer with integration of the different thicknesses of PCM. It is noted that the temperature of the drying air in the case of the solar dryer without PCM reaches the maximum value (327 °C) at 14:00, then it begins to decrease with the passage of time until it becomes equal to the ambient temperature by the sunset. In the case of the solar dryer without PCM, the drying process stops directly with the sunset and the dryer no longer works.

With the integration of the different thicknesses of PCM, we notice before sunset that the temperature of the drying air less than that of the dryer without PCM, this decrease is translated by the influence of the addition of PCM below the absorber. The conductive transfer between the PCM and the absorber led to the decrease of the absorber temperature which brought down the air temperature before the sunset. After sunset, it is noted that the drying air temperature in the case of the PCM dryer is high than that in the case of the dryer without PCM thanks to the integration of PCM below the absorbing plate. The PCM stores heat during the sunny hours to provide it again after sunset. The PCM behaves as a source of heat. By way of example, at 22:00, the drying air temperature in the case without PCM is of the order of 294K, while it is 305K in the case of the dryer with 4cm thickness of PCM. The integration of a 4cm thickness of PCM makes it possible to increase the temperature of the drying air by 11 ° C after sunset.

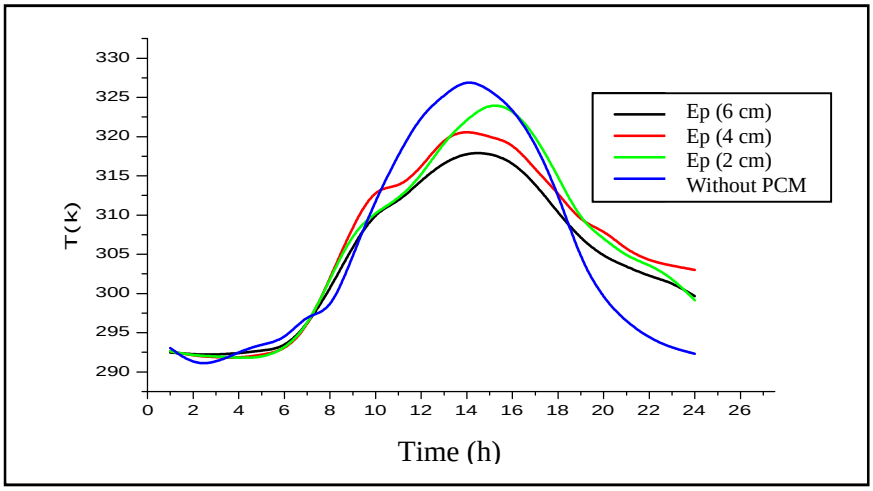

Fig IV.8 Evolution of the drying air temperature of the direct solar dryer with integration of different thicknesses of PCM.

In order to verify the behavior of the PCM in storage and destocking we presented in Fig IV.9 the liquid fraction of PCM as a function of time for different thicknesses. Note that the melting of PCM begins at 09:00 while its solidification begins at 18:00. This figure shows that the refraction of the previous curves is due to the phase change influence of PCM. We also note that for all the studied thicknesses that the total volume of the PCM participates in

the phase change in both directions, which indicates that the maximum possible heat has been extracted.

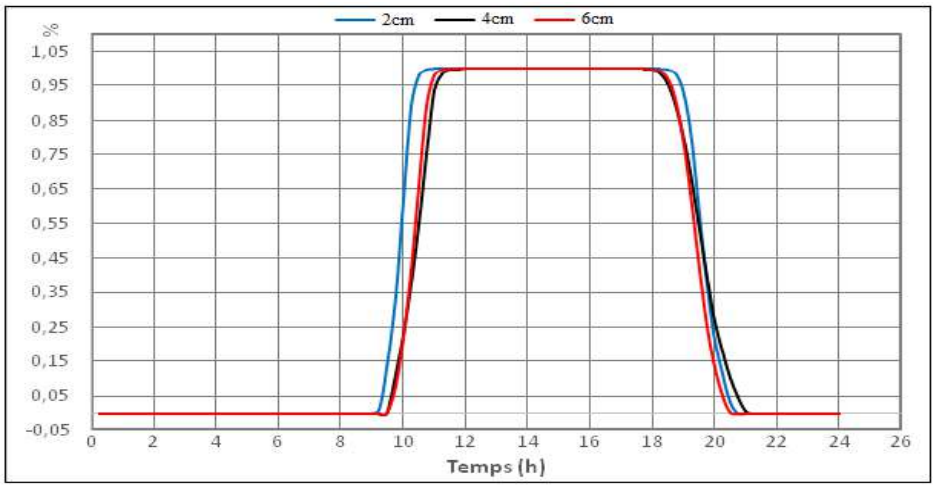

Fig IV.9 Evolution of the PCM liquid fraction.

IV.3.5 Effect of the nature of the phase change material

From the Fig IV.10, it is noted that the curves undergo refractions in different temperatures corresponding to the melting temperature of each PCM. The absorber is in direct contact with the PCM, so during the phase change time the absorber will give a quantity of energy to PCM that uses it later to change its phases. We also note that the phase shift, especially at the point of the peak moment, increases when integrating PCM with low melting temperatures, against it decreases when integrating PCM with stronger latent heat of fusion. The best PCM is the one that gives the highest value of air temperature after sunset. In our study, we noticed that the highest temperature obtained after sunset is found in the case of PCM with 326.5K of melting temperature. So, the choice of the best PCM is fundamentally dependent on the following two parameters: the melting temperature and the latent heat of the material.

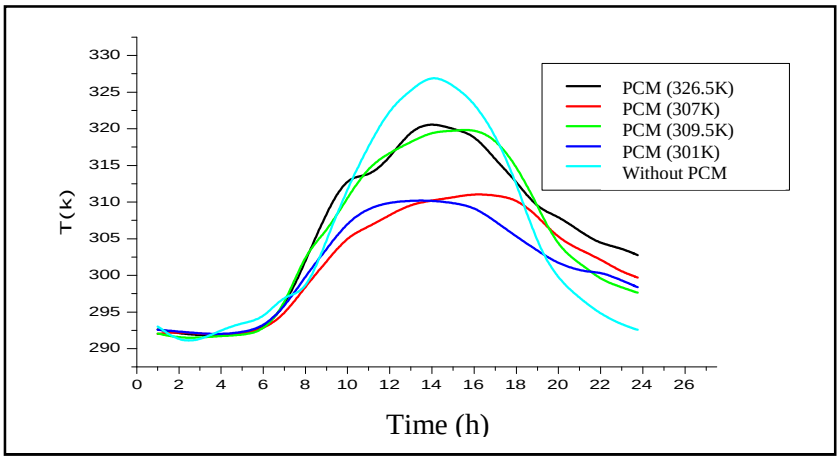

Fig IV.10 Evolution of the drying air temperature of the solar dryer with different kinds of PCM.

IV.4 Conclusion

This chapter is focused on the numerical simulation of the direct solar dryer without and with integration of a flat layer of a phase change material in order to partially store heat energy by latent heat. The results obtained in this study, in the case of absence of PCM, showed the reliability of our simulation model adopted by comparison with the results of the experiment. Furthermore, the results from the case of integration of a layer of PCM showed a marked improvement in thermal behavior, especially in the period after sunset. During non-sunny hours, liquid PCM will provide heat to the absorber; it is the useful heat of the air in circulation. Indeed, among the tested thicknesses, the one of 4cm gave a better thermal contribution for four hours after the sunset, while the PCM with melting temperature of 326.5K was chosen as the best one among the other tested materials. The use of PCM is not effective in days with low solar radiation.

CHAPTER V:

Comparative mixed mode solutions and technical-economic study

V.1 Introduction

In this chapter and as a first part, a combination mode is presented to show the variation of the thermal performance of the solar dryer when using two techniques of heat supply in combination. As a second part of this chapter, an economic analysis of the direct solar dryer with using different techniques of heat supply is performed to show the feasibility and the viability of our dryer. The results are presented below:

V.2 Combination between PCM and heat exchanger

Fig V.1 shows the thermal performance of the solar dryer when using PCM and heat exchanger with solar water heater. It is noticed that the temperature of the drying air in the case of combining between two techniques is very high and more than that in the case without using any technique of heat supply by almost 4°C. During the day, the PCM stores the solar energy and the heat exchanger supplies the solar dryer with heat which increases the drying air temperature. After sunset till midnight, the drying air temperature remains very important (ranges between 41°C and 43°C) due to the effect of the two techniques of heat supply; the heat exchanger which becomes connected with the water storage tank and the PCM which is in progress to release the stored heat while its phase change process. The combination between these two techniques is highly improved the thermal performance of the solar dryer by maintaining a sufficient drying air temperature (more than 40°C) for 7 hours after sunset.

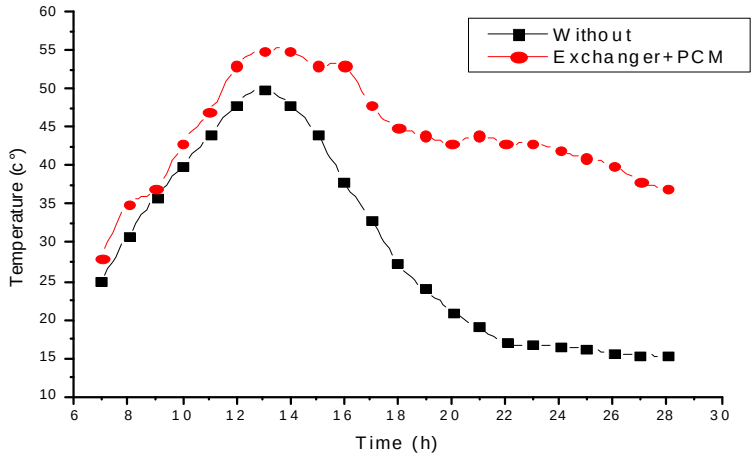

Fig V.1 Evolution of the drying air temperature in the solar dryer with combining between PCM and heat exchanger with solar water heater.

V.3 Combination between porous medium and heat exchanger

Fig V.2 shows the thermal performance of the solar dryer when combining between porous medium and heat exchanger with solar water heater. Before the midday, it is noticed that the temperature of the drying air in the case of combining between two techniques is very high and more than that in the case without using any technique of heat supply by almost 6°C. During the day, the water and the porous medium store the solar energy under the form of sensible heat. After sunset till midnight, the drying air temperature remains very important (ranges between 39°C and 43°C) due to the effect of the two techniques of heat supply; the heat exchanger which becomes connected with the water storage tank and the porous medium which is in progress to release the stored sensible heat. The combination between these two techniques improved the thermal performance of the solar dryer by ensuring a sufficient drying air temperature (more than 40°C) for 7 hours after sunset.

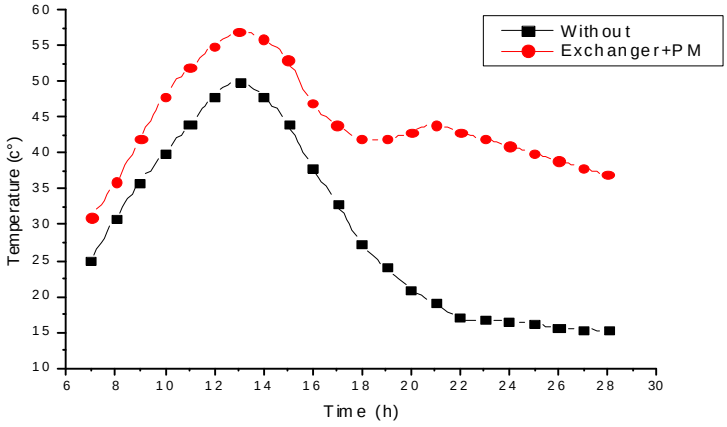

Fig V.2 Evolution of the drying air temperature in the solar dryer with combining between porous medium and heat exchanger with solar water heater.

V.4 Combination between PCM and porous medium (PM)

Fig V.3 illustrates the evolution of the drying air temperature when using PCM and porous medium as sources of heat in parallel. Before the midday, it is noticed that the drying air temperature in case of combination is less than the one in case of without using any technique. That one can be explained by the effect of PCM and porous medium which absorb the heat from the absorber plate under the conductive heat transfer which reduces the absorber temperature and consequently decreases the drying air temperature. After the midday, the

drying air temperature in the two cases of the solar dryer starts to decrease, nevertheless it is in a slow way in the case of solar dryer with combination. The obtained result shows that this combination mode in not effective comparing with the two previous modes.

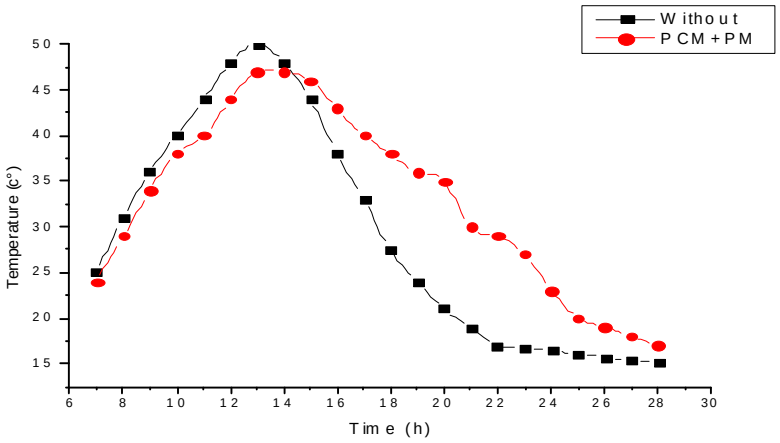

Fig V.3 Evolution of the drying air temperature in the solar dryer with combining between porous medium and PCM.

V.5 Comparison between different combinations and techniques

Fig V.4 shows the evolution of the drying air temperature of the solar dryer with using different techniques. Between the tested combinations modes, it is appeared that the combination PCM + Heat exchanger with solar water heater is the best one inasmuch to the drying air temperature which this mode provides. However, between all the used techniques of heat supply in this study, it is noticed that the one of the heat exchanger with geothermal water is the more effective technique. By using heat exchanger with geothermal water, the lowest drying air temperature was found to be 46°C, while the highest one was 58°C. After sunset and throughout the night, the drying air temperature remains important and almost steady with an average value of 48°C. The integration of the heat exchanger with geothermal water ensures the continuity of drying process at the night and even during cloudy days.

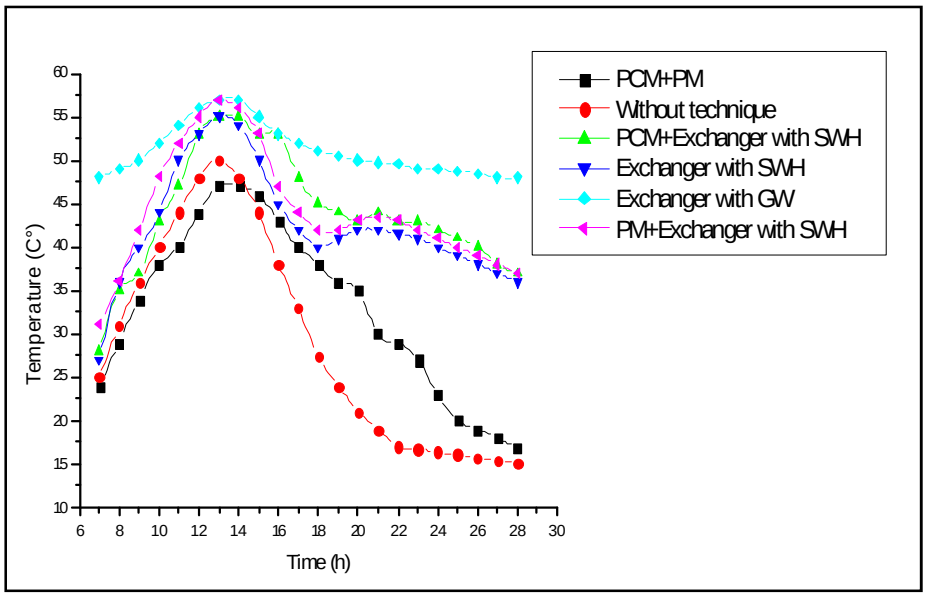

Fig V.4 Comparison between different techniques.

V.5 Economic analysis of the solar dryer

The current practice today is to report the economy of a system or a process by its return time in how much time the investment or overinvestment is amortized considering the realized savings. These criteria of investment return time as well as the possession cost are determinative assessment criteria for the customer. This will allow us to discriminate the architectures of the dryer according to the customer's needs or specifications.

Economic analysis of the dryer was carried out by computing its life cycle cost (LCC) and life cycle benefit (LCB). In addition, four economic attributes, namely, benefit-cost ratio (BCR), net present worth (NPW), annuity (A) and payback period (PBP) were also determined for judging the economic viability of the dryer.

V.5.1 Life cycle cost (LCC)

Life cycle cost (LCC) of the direct solar dryer is the sum of all the costs associated with a solar drying system over its lifetime in terms of money value at the present instant of time, and takes into account the time value of money [141]. Economics of solar dryer was calculated through life cycle cost (LCC) analysis. The procedure of life cycle cost estimation as adopted by Barnwal and Tiwari (2008) [142], Singh *et al* (2017) [142] and Sodha *et al* [143] was used.

LCC = Initial cost of unit (P_i) + P_w (O & M Costs including labor) – P_w (SV)

$$= P_i + P_w \frac{X(1-X^n)}{1-X} - SV(1+i)^{-n} \quad \text{(V.1)}$$

Where, $X = \frac{1+e}{1+i}$ =0.945

P_i = Initial investment (DA),

P_w = Operational and maintenance expenses, including replacement costs for damaged components (DA),

n = Life of the dryer (year),

P_w = Present worth of salvage value (SV) of the dryer at the end of life (DA),

e = Annual escalation in cost (4%),

i = Interest or discount rate (10%).

The table below presents the different cost values of the solar dryer system which allow us to calculate the economic attributes.

Direct solar dryer with heat exchanger cost (P_i)	15000DA+40000DA=55000 DA
Direct solar dryer with solar water heater cost (P_i)	60000DA+40000DA=115000DA
Direct solar dryer with PCM cost (P_i)	500DA/Kg*22kg+40000DA= 51000DA
Direct solar dryer with PM cost (P_i)	40000 DA
Present worth (P_w(SV))	10% of the solar dryer cost
Maintenance cost (P_w)	2.5%of the solar dryer cost
Number of functioning days in one year in case of using geothermal water heat exchanger	365 days
Number of functioning days in one year in case of using other techniques	275 days
Labor cost (P_w) (1000DA*275) or (1000DA*365)	275000 DA or 365000 DA
Life of the solar dryer	15 years
Solar dryer capacity	10kg
Buying cost of tomatoes 15DA/kg*10kg*275 Buying cost of tomatoes 15DA/kg*10kg*365	41250 DA 54750 DA
Annual benefits 500DA/kg*3kg*275 Annual benefits 500DA/kg*3kg*365	412500 DA 547500 DA

Table V.1 Cost values of the direct solar dryer.

After the numerical application on the correlation (V.1) we found that the life cycle cost of the direct solar dryer is changed from a case to another according to the technique of heat supply used:

LCC_{HE} =55000+421125(9.8)-5500(0.239) =4180707.5 DA

LCC_{SWH}=3239676.5DA

LCC_{PCM}=3161526.1DA

LCC_{PM}=3148094 DA

V.5.2 Life cycle benefits (LCB)

The annual benefit was obtained by using total drying cycle of product. Thus, the total annual benefit from dried product was estimated as adopted by Barnwal and Tiwari (2008), Singh *et al.* (2017) and Sodha *et al.* (1991).

$$LCB = R\frac{X(1-X^{n})}{(1-X)} \qquad (V.2)$$

Where: R is the annual benefit.

LCB_{HE}=5365500 DA

LCB=4042500 DA

V.5.3 Benefit cost ratio (BCR)

This ratio was obtained when the present worth of the benefit stream was divided by the present worth of the cost stream. The mathematical benefit-cost ratio (Barnwal and Tiwari, 2008; Singh et al., 2017) can be expressed as:

$$\text{Benefit cost ratio (BCR)} = \frac{\text{Life cycle benefits of hybrid solar dryer}}{\text{Life cycle cost hybrid solar dryer}}$$

$$BCR = \frac{R\frac{X(1-X^{n})}{(1-X)}}{P_i + P_w - P_w(SV)} = \frac{LCB}{LCC} \qquad (V.3)$$

BCR_{HE}=1.28

BCR_{SWH}=1.24

BCR_{PCM}=1.27

BCR_{PM}=1.28

V.5.4 Net present worth (NPW)

The NPW was determined as the difference between present worth of savings and cost of investment. It is the sum of all discounted net benefits throughout the project, and expressed as:

NPW = LCB – LCC (V.4)

NPW_{HE}=1184792.5 DA

NPW_{SWH}=802823.5 DA

NPW_{PCM}=880973.9 DA

NPW_{PM}= 894406 DA

V.5.5 Annuity (A)

The annuity (A) of the project indicates the average net annual returns. This term can be given as:

$$A = \frac{NPW}{\sum_{i=1}^{n}(1+i)^n} \quad \text{(V.5)}$$

A_{HE}=28415.46 DA

A_{SWH}=192523.62 DA

A_{PCM}=211264.72 DA

A_{PM}=214485.85 DA

V.5.6 Payback period

The payback period shows the length of time between cumulative net cash outflow recovered in the form of yearly net cash inflows. The payback period was calculated using the formula below (Neufville, 1990) [145].

$$\text{Payback period} = \frac{\text{Initial Investment}}{\text{Annual Net Undiscounted Benefits}} \quad \text{(V.6)}$$

The table below illustrates the payback period of the direct solar dryer with different techniques of heat supply:

Technique	Payback period (year)
Direct solar dryer with geothermal water heat exchanger	0.9
Direct solar dryer with solar water heater	5.4
Direct solar dryer with PCM	1.31
Direct solar dryer with PM	0.8

Table V.2 Payback period of solar dryer with different techniques.

The results presented in the table V.2 show that the payback period depends on two essential parameters; the initial cost of the solar dryer and the annual benefits which is depended on the dried product selling price. It appears that the payback period increased with increasing of the solar dryer cost and decreased with increasing of annual benefits. In our study, it is obvious that the short pay period which is 0.8 year is obtained when using the solar dryer with porous medium and that returns to the bare price of the used porous medium and which is found free of charge. While this technique (porous medium) was not recommended in thermal point of view because the daily operating time of the solar dryer obtained after using this technique was very small as compared with the other techniques and not enough to perform the drying process of such agricultural product. The second short payback period (0.9 year) was obtained with using geothermal water heat exchanger as heat supply technique. In addition to its short payback period, this kind of heat supply source is highly recommended in thermal point of view, it has given the highest drying air temperature compared with other techniques. The advantage of this technique is the possibility of performing the drying process in the whole year which gives an important value of the annual benefits. The payback period of the solar dryer with using PCM was obtained 1.31 year higher than the one of solar dryer with heat exchanger even though it costs less than it. This contradiction is explained by the role of the number of functioning day of the solar dryer which reverses its annual benefits; however, it is 275 days when using PCM and 365 days when using geothermal water heat exchanger. The highest payback period was obtained when using a solar water heater as a heat supply technique; it is 5.4 years and lower than the expected life of 15 years for the dryer.

In order to compare our dryer with the other ones, the payback period was estimated at 2.26 years, and lower than the expected life of 10 years for the dryer (Poonia et al, 2018) [141]. Barnwal and Tiwari (2008) [142] reported payback period of 1.25 years for a hybrid

PV/T greenhouse dryer for drying grapes under forced mode of operation. The payback period of a solar tunnel drier is 4 years for basic mode drier, and 3-4 years for optimum mode driers (Hossain et al, 2005) [146].

V.6 Conclusion

The design approach of the solar drying system needs to be optimized of both point of view; thermally and economically. Indeed the construction of a solar drying system is only interesting if, comparing to a conventional installation, it allows realizing profits.

General conclusion

General conclusion

Solar drying is one of the most fundamentals processes which allow increasing efficiently the storage time of the agro-alimentary products. This explains the recourse to the use of solar dryers, which have an undergone remarkable development in these recent years.

In this context, the presented work concerns an experimental and simulation study aiming to improve the thermal performance of a direct solar dryer with using different techniques of heat supply. The techniques of heat supply used in this study are: heat exchanger with geothermal water, heat exchanger with solar water heater, storage of sensible heat in a porous medium and storage of latent heat with using phase change materials. The combination between these techniques has been investigated too in this study.

Several numerical simulations using the finite volume method implemented on CFD Fluent software have been carried out. The flow is considered two-dimensional and unsteady. The solar radiation is taken for a typical day under the climatic conditions of Ouargla (Algeria).

The obtained results in this study showed a significant improvement of the thermal performance of the direct solar dryer, especially after sunset. With integration of heat exchanger with geothermal water inside solar dryer, the smallest obtained experimental value of drying air temperature was found 46°C, while the highest one was 58°C. After sunset and throughout all the night until the sunrise, the drying air temperature remains important and almost steady with an average value of 46°C and exceeds that in case of solar dryer without heat exchanger by 30°C. The integration of the heat exchanger with geothermal water inside solar dryer ensures the continuity of drying process at the night and even during cloudy days.

In addition to the importance of the obtained results relating to the improvement of the drying system with a supplementary thermal source, the present study, in case of large application, can provide tap water with satisfactory and moderate temperature as preferred by the consuming citizens. The problem of discontinuity of drying process has been resolved by using this technique.

The integration of a layer of PCM showed a marked improvement in thermal behavior, especially in the period after sunset. During non-sunny hours, liquid PCM will provide heat to the absorber; it is the useful heat of the air in circulation. Indeed,

among the tested thicknesses, the one of 4cm gave a better thermal contribution for four hours after the sunset, while the PCM with melting temperature of 326.5K was shown to be better among the other tested materials.

With integration of porous medium, the temperature of drying air increases by 4°C and extents the functioning of solar dryer by two hours after the sunset. The increase of the porous medium thickness conducts to extent the staying time of drying air inside the porous medium and leads to increase the thermal exchange area between the drying air and the porous materiel which helps to increase the temperature of drying air. The increase of the medium porosity by 10% leads to decrease the temperature of drying air by 1°C, so it is found to be non significant.

Between the tested combinations modes, it is appeared that the combination (PCM + Heat exchanger with solar water heater) is the most effective one inasmuch to the drying air temperature that this mode has provided.

Economic evaluation was done by computing life cycle cost (LCC) and life cycle benefit (LCB). In addition, four economic attributes, namely, benefit-cost ratio (BCR), net present worth (NPW), annuity (A) and payback period (PBP) were also determined for judging the economic viability of the dryer. The performed economic analysis proves the feasibility of our solar dryer; however, the heat supply technique of heat exchanger with geothermal water was chosen as the most recommended one forasmuch to the short payback period (0.9 year) obtained when using this technique.

Finally, among all the techniques of heat supply used in this study, it is noticed that the one of the heat exchanger with geothermal water is the most effective technique in thermally and economically point of view.

As perspectives, the present study needs to be improved after performing some several issues as: studying the effect of the distribution mode and the location of the PCM inside the solar dryer, taking into consideration the effect of different radiations rate according to the four seasons of the year, evaluating the thermal performance of the direct solar dryer after using an agricultural product in order to be dried and studying experimentally the using of the two other techniques of heat supply (PCM and porous medium).

References

[1] Muhlbauer W, Esper A, Muller J. Solar energy in agriculture. In: Proceedings of ISES solar world congress, Budapest; 1993, p.23–7.

[2] Mustayen AGMB, Mekhilef S, Saidur R. Performance study of different solar dryers: A review. Renewable and Sustainable Energy Reviews 34(2014)463–470.

[3] Mennouche D, Bouchekima B, Boubekri A, Boughali S, Bouguettaia H, Bechki B. Valorization of rehydrated Deglet-Nour dates by an experimental investigation of solar drying processing method. Energy Conversion and Management 84 (2014) 481–487.

[4] Chouicha S, Boubekri A, Mennouche D, Bouguetaia H, Berrbeuh MH, Bouhafs S, Rezzoug W. Valorization Study of Treated Deglet-Nour Dates By Solar Drying Using Three Different Solar Driers. Energy Procedia 50 (2014) 907 – 916.

[5] Fudholi A, Sopian K, Bakhtyar B, Gabbasa M, Othman MY, Ruslan MH. Review of solar drying systems with air based solar collectors in Malaysia. Renewable and Sustainable Energy Reviews 51(2015)1191–1204.

[6] Chouicha S, Boubekri A, Mennouche D, Berrbeuh MH. Solar drying of sliced potatoes. An experimental investigation. Energy Procedia 36 (2013) 1276 – 1285.

[7] Mekhilef S, Faramarzi S, Saidur R, Salam Z. The application of solar technologies for sustainable development of agricultural sector. Renew Sustain Energy Rev2013;18:583–94.

[8] Chauhan S, Kumar A, Tekasakul P. Applications of software in solar drying systems: A review. Renewable and Sustainable Energy Reviews 51(2015)1326–1337.

[9] Jairaj KS, Singh SP, Srikant K. A review of solar dryers developed for grape drying. Solar Energy 83 (2009) 1698–1712.

[10] Forson FK, Nazha MAA, Rajakaruna H. Modelling and experimental studies on a mixed-mode natural convection solar crop-dryer. Solar Energy 81 (2007) 346–357.

[11] Prakash O, Kumar A. Solar greenhouse drying: A review. Renewable and Sustainable Energy Reviews 29(2014)905–910.

[12] Lopez R, Vaca M, Terres H, Lizardi A, Morales J, Flores J, Lara A, Chávez S. Kinetics modeling of the drying of chickpea (Cicer arietinum) with solar energy. Energy Procedia 57 (2014) 1447 – 1454.

[13] Pirasteh G, Saidur R, Rahman SMA, Rahim NA. A review on development of solar drying applications. Renewable and Sustainable Energy Reviews 31(2014)133–148.

[14] Sangamithra A, Swamy GJ, Prema AS, Priyavarshini R, Chandrasekar R, Sasikala S. An overview of a polyhouse dryer. Renewable and Sustainable Energy Reviews 40(2014)902–910.

[15] Chauhan PS, Kumar A, Tekasakul P. Applications of software in solar drying systems: A review. Renewable and Sustainable Energy Reviews 51(2015)1326–1337.

[16] Fudholi A, Sopian K, Gabbasa M, Bakhtyar B, Yahya M, Ruslan MH, Mat S. Techno-economic of solar drying systems with water based solar collectors in Malaysia: A review. Renewable and Sustainable Energy Reviews 51(2015)809–820.

[17] Sharma VK, Colangelo A, Spagna G. Experimental investigation of different solar dryers suitable for fruit and vegetable drying. Department Enerzia, Divisione Ingegneria Sperimentale, Italy. Drying 1994;94:879–86.

[18] VijayaVenkata Ramana S, IniyanbS, Goic R. A review of solar drying technologies. Renewable and Sustainable Energy Reviews 16 (2012) 2652– 2670.

[19] Pirasteh G, Saidur R, Rahman SMA, Rahim NA. A review on development of solar drying applications. Renewable and Sustainable Energy Reviews 31(2014)133–148.

[20] Mustayen AGMB, Mekhilef S, Saidur R. Performance study of different solar dryers: A review. Renewable and Sustainable Energy Reviews 34(2014)463–470.

[21] Singh S, Kumar AGMB. Testing method for thermal performance based rating of various solar dryer designs. Solar Energy 86 (2012) 87–98.

[22] Boroze T, Desmorieux H, Méot JM, Marouzé C, Azouma Y, Napo K. Inventory and comparative characteristics of dryers used in the sub-Saharan zone: Criteria influencing dryer choice. Renewable and Sustainable Energy Reviews 40(2014)1240–1259.

[23] Pangavhane DR, Sawhney RL. Review of research and development work on solar dryers for grape drying; Energy Conversion and Management 43 (2002) 45-61.

[24] Zarezade M, Mostafaeipour A. Identifying the effective factors on implementing the solar dryers for Yazd province, Iran. Renewable and Sustainable Energy Reviews 57(2016)765–775.

[25] Sevik, S. Designing, Manufacturing and Experimental Examining of Hot Air Production System for Heating and Drying that used with Heat Pump and Solar Collector. PhD Thesis, Gazi Univ., Institute of Science and Technology, Ankara, Turkey (in Turkish).

[26] Xiao HW, Baia JW, Xiea L, Sunc DW, Gaoa ZJ. Thin-layer air impingement drying enhances drying rate of American ginseng (Panaxquinquefolium L.) slices with quality attributes considered. Food and bioproducts processing 9 4 (2015) 581–591.

[27] Sarsavadia PN. Development of a solar-assisted dryer and evaluation of energy requirement for the drying of onion. Renewable Energy 32 (2007) 2529–2547.

[28] Manaa S, Younssi M, Moummi N. Solar drying of tomato in the arid area of TOUAT (Adrar, Algeria). Energy Procedia 36 (2013) 511 – 514.

[29] Shafiq H, Eqwan MR. Experimental Study of Direct and Indirect Solar Biomass Dryer. IJSRSET. 2017. Volume 3, Issue 5.

[30] Nair KKV, Bongirwar DR. Solar dryer for agricultural products, A do it yourself solar dryer. Indian Chemical Engineering 36 (1994), 103–105.

[31] El-Sebaii AA, Abdul-Enein S, Ramdan MRI, El-Gohary HG. Experimental investigation of an indirect type natural convection solar dryer. Energy Conversion and Management 43, (2002) 2251–2266.

[32] Pangavhane R. Dilip Sawhney RL, Sarsavadia PN. Design, development and performance testing of a new natural convection solar dryer. Energy 27 (2002), 579–590.

[33] Abene A, Dubois V, Le Ray M, Ouagued A. Study of a solar air flat plate collector: use of obstacles and application for the drying of grape. Journal of Food Engineering 65 (2004) 15–22.

[34] Adolfo G. Finck-Pastrana. Nopal (Opuntia Lasiacantha) drying using an indirect solar dryer. Energy Procedia 57 (201) 2984 – 2993.

[35] Serpil S, Gulum S, Ferihan T. Usage of solar-assisted spouted bed drier in drying of pea. Food and bioproducts processing 9 1 (2013) 271–278.

[36] Lamnatou C, Papanicolaou E, Belessiotis V, Kyriakis N. Experimental investigation and thermodynamic performance analysis of a solar dryer using an evacuated-tube air collector. Applied Energy 94 (2012) 232–243.

[37] Duran G, Condorı M, Altobelli F. Simulation of a passive solar dryer to charqui production using temperature and pressure networks. Solar Energy 119 (2015) 310–318.

[38] Ringeisen B, Barrett DM, Stroeve P. Concentrated solar drying of tomatoes. Energy for Sustainable Development 19 (2014) 47–55.

[39] Stiling J, Li S, Stroeve P, Thompson J, Mjawa B, Kornbluth K, Barrett DM. Performance evaluation of an enhanced fruit solar dryer using concentrating panels. Energy for Sustainable Development 16 (2012) 224–230.

[40] Maiti S, Patel P, Vyas K, Eswaran K, Ghosh PK. Performance evaluation of a small scale indirect solar dryer with static reflectors during non-summer months in the Saurashtra region of western India. Solar Energy 85 (2011) 2686–2696.

[41] Sevik S. Experimental investigation of a new design solar-heat pump dryer under the different climatic conditions and drying behavior of selected products. Solar Energy 105 (2014) 190–205.

[42] Li Y, Li HF, Dai YJ, Gao SF, Wei L, Li ZL, Odinez IG, Wang RZ. Experimental investigation on a solar assisted heat pump in-store drying system. Applied Thermal Engineering 31 (2011) 1718-1724.

[43] Sevik S. Design, experimental investigation and analysis of a solar drying system. Energy Conversion and Management 68 (2013) 227–234.

[44] Ipliene AC, Novošinskas H, Raila A, Zvicevicˇius E. Usage of hybrid solar collector system in drying technologies of medical Plants. Energy Conversion and Management 93 (2015) 399–405.

[45] Tsamparlis, M. Solar drying for real applications. Drying Technology 8 (1990), 261–285.

[46] Amer BMA, Gottschalk K, Hossain MA. Integrated hybrid solar drying system and its drying kinetics of Chamomile. Renewable Energy 121 (2018) 539-547.

[47] Ben Salma R, Combarnous M. Study of orange peels dryings kinetics and development of a solar dryer by forced convection. Solar Energy 85 (2011) 570–578.

[48] Fudholi A, Sopian K, Alghoul MA, Ruslan MH, Othman MY. Performances and improvement potential of solar drying system for palm oil fronds. Renewable Energy 78 (2015) 561-565.

[49] Sinul V, Sharma A, Sharma N. Construction and performance analysis of an indirect solar dryer integrated with solar air heater. Procedia Engineering 38 (2012) 3260 – 3269.

[50] Mumba J. A Design and development of a solar grain dyer incorporating photovoltaic powred air circulation. Enenrgy Conuers. Mgml Vol. 37, No.5, pp.615-621, 1996.

[51] Sevik S, Aktas M, Dogˇan H, Koçak S. Mushroom drying with solar assisted heat pump system. Energy Conversion and Management 72 (2013) 171–178.

[52] Fadhel MI, Sopiana K, Dauda WRW, Alghoul MA. Review on advanced of solar assisted chemical heat pump dryer for agriculture produce. Renewable and Sustainable Energy Reviews 15 (2011) 1152–1168.

[53] Mohanraj M. Performance of a solar-ambient hybrid source heat pump drier for copra drying under hot-humid weather conditions. Energy for Sustainable Development 23 (2014) 165–169.

[54] Misha S, Mat S, Ruslan MH, Salleh E, Sopian K. Performance of a solar assisted solid desiccant dryer for kenaf core fiber drying under low solar radiation. Solar Energy 112 (2015) 194–204.

[55] Reyes A, Negrete D, Mahn A, Sepůlveda F. Design and evaluation of a heat exchanger that uses paraffin wax and recycled materials as solar energy accumulator. Energy Conversion and Management 88 (2014) 391–398.

[56] Amer BMA, Hossain MA, Gottschalk K. Design and performance evaluation of a new hybrid solar dryer for banana. Energy Conversion and Management 51 (2010) 813–820.

[57] Ouali S, Benaïssa Z, Belhamel M, Khellaf A, Baddari K, Djeddi M. Exploitation of albian geothermal water in South Algeria. Energy Procedia 6 (2011) 101–109.

[58] Reyes A, Negrete D, Mahn A, Olveda FS. Design and evaluation of a heat exchanger that uses paraffin wax and recycled materials as solar energy accumulator. Energy Conversion and Management 88 (2014) 391–398.

[59] Saibi H. Geothermal Resources in Algeria. Proceedings World Geothermal Congress 2015Melbourne, Australia, 19-25 April 2015

[60] Fekraoui A and Kedaid FZ. Geothermal Resources and Uses in Algeria: A Country Update Report. Proceedings World Geothermal Congress 2005. Antalya, Turkey, 24-29 April 2005.

[61] Etsouri S, Kaci F, Bouaziz M. The energy potential of the Albian water in Algeria : exploitation and transformation. International Journal of Scientific & Engineering Research, Volume 8, Issue 1, January-2017.

[62] Sreekumar A. Techno-economic analysis of a roof-integrated solar air heating system for drying fruit and vegetables. Energy Convers Manage 2010;51:2230–8.

[63] Sharma A, Chen CR, Vu Lan N. Solar-energy drying systems: a review. Renew Sustain Energy Rev 2009;13:1185–210.

[64] Jairaj KS, Singh SP, Srikant K. A review of solar dryers developed for grape drying. Solar Energy 2009;83:1698–712.

[65] Ekechukwu OV, Norton B. Review of solar-energy drying systems II: an overview of solar drying technology. Energy Convers Manage 1999;40:615–55.

[66] Sodha MS, Chandra R. Solar drying systems and their testing procedures: a review. Energy Convers Manage 1994;35219–267.

[67] Amer BMA, Hossain MA, Gottschalk K. Design and performance evaluation of a new hybrid solar dryer for banana. Energy Convers Manage 2010;51:820–813.

[68] Lahsasni S, Kouhila M, Mahrouz M, Idlimam A, Jamali A. Thin layer convective solar drying and mathematical modeling of prickly peel (Opuntiaficusindica). Energy 2004;29:211–24.

[69] Prasad J, Vijay VK, Tiwari GN, Sorayan VPS. Study on performance evaluation of hybrid drier for turmeric (Curcuma longa L.) drying at village scale. J Food Eng 2006;75:497–502.

[70] Lalit MB, Sanatoch S, Naik SN. Solar dryer with thermal energy storage systems for drying agricultural food products: a review. Renew Sustain Energy Rev 2010;14:2298–314.

[71] Aghbashlo M, Kianmehr MH, Arabhosseini A. Performance analysis of drying of carrot slices in a a.semi-industrial continuous band dryer. J Food Eng 2009;91:99–108.

[72] Goyal RK, Tiwari GN. Parametric study of a reverse flat plate absorber cabinet dryer: a new concept. Solar Energy 1997;60:41–8.

[73] Ertekin C, Yaldiz O. Drying of eggplant and selection of a suitable thin layer drying model. J Food Eng 2004;63:349–59.

[74] Doymaz I. Air-drying characteristics of tomatoes. J Food Eng 2007;78(4):1291–7.

[75] Prashant Singh Chauhan, Anil Kumar, PerapongTekasakul. Applications of software in solar drying systems: A review.Renewable and Sustainable Energy Reviews 51(2015)1326–1337.

[76] Afriyie JK, Nazha MAA, Rajakaruna H, Forson FK. Experimental investigation of a chimney-dependent solar crop dryer. J Renew Energy 2009;34:217–22.

[77] Gbaha P, Yobouet AH, Kouassi SJ, Kaménan KB, Touré S. Experimental investigation of a solar dryer with natural convection heat flow. Renew Energy 2007;32:1817–29.

[78] El Mokretars S, Miri R, Belhamel M. Etude du bilan d'énergie et de masse d'un séchoir de type serre- Applications au séchage des produits agro-alimentaires. Revue des énergiesRenouvelables 2004;7:23–109.

[79] Boughanmi H, Lazaar M, Guizani A. A performance of a heat pump system connected a new conic helicoidal geothermal heat exchanger for a greenhouse heating in the north of Tunisia. Solar Energy 171 (2018) 343–353.

[80] Calise F, Dentice M, Macaluso A, Piacentino A, Vanoli L. Exergetic and exergoeconomic analysis of a novel hybrid solar–geothermal polygeneration system producing energy and water. Energy Conversion and Management 115 (2016) 200–220.

[81] Bououd M, Mechaqrane A. Concentration solar dryer water-to-air heat exchanger: Modeling and parametric studies. International journal of hydrogen energy xxx (2016) 1-13.

[82] Calise F, Fraia S, Macaluso A, Massarotti N, Vanoli L. A geothermal energy system for wastewater sludge drying and electricity production in a small island. Energy (2018), doi:10.1016/j.energy.2018.08.062.

[83] Daneshipour M, Rafee R. Nanofluids as the circuit fluids of the geothermal borehole heat exchangers. International Communications in Heat and Mass Transfer 81 (2017) 34–41.

[84] Husham A, Assadi MK, Al-Kayiem H, Gitan AA, Effect of Tube Diameter on the Design of Heat Exchanger in Solar Drying system. 2018 IOP Conf. Ser.: Mater. Sci. Eng. 328 012028.

[85] Focaccia S, Tinti F, Monti F, Amidei S, Bruno R. Shallow geothermal energy for industrial applications: A case study. Sustainable Energy Technologies and Assessments 16 (2016) 93–105;

[86] Ghasemkhani H, Keyhani A, Aghbashlo M, Rafiee S, Mujumdar AS. Improving exergetic performance parameters of a rotating-tray air dryer via a simple heat exchanger. Applied Thermal Engineering 94 (2016) 13–23.

[87] Al-Hinti, Al-Muhtady A, Al-Kouz W. Measurement and Modelling of the Ground Temperature Profile in Zarqa, Jordan for Geothermal Heat Pump Applications, Applied Thermal Engineering (2017), doi: http: //dx.doi.org/10.1016/j. applthermaleng. 2017.05.107

[88] Ambriz-Dı´az VM, Rubio-Maya C, Pacheco Ibarra JJ, Galvan Gonzalez SR, Patino JM. Analysis of a sequential production of electricity, ice and drying of agricultural products by cascading geothermal energy. International journal of hydrogen energy. Vol 42, Issue 28 (2017) 18092-19002.

[89] Agra O, Erdem HH, Demir H, Atayılmaz O, Teke I. Heat capacity ratio and the best type of heat exchanger for geothermal water providing maximum heat transfer. Energy. Vol 90, Part 2 (2015) 1563-15686.

[90] Navarro AH, Gomez LC. A new approach for thermal performance calculation of cross-flow heat exchangers. Int J Heat Mass Transf 2005;48(18):3880e8.

[91] Navarro AH, Gomez LC. Effectiveness-NTU computation with a mathematical model for cross-flow heat exchangers. Braz J Chem Eng 2007;24(4):509e21.

[92] Ezzat MF, Dincer I. Energy and exergy analyses of a new geothermal–solar energy based system. Solar Energy 134 (2016) 95–106.

[93] Misha S, Mat S, Ruslan MH, Salleh E, Sopian K. Performance of a solar assisted solid desiccant dryer for kenafcore fiber drying under low solar radiation. Solar Energy 112 (2015) 194–204.

[94] Mennouche D, Bouchekima B, Boubekri A, Boughali S, Bouguettaia H, Bechki D. Valorization of rehydrated Deglet-Nour dates by an experimental investigation of solar drying processing method. Energy Conversion and Management 84 (2014) 481–487.

[95] Reyes A, Negrete D, Mahn A, Olveda FS. Design and evaluation of a heat exchanger that uses paraffin wax and recycled materials as solar energy accumulator. Energy Conversion and Management 88 (2014) 391–398.

[96] Amer BMA, Hossain MA, Gottschalk K. Design and performance evaluation of a new hybrid solar dryer for banana. Energy Convers Manage 2010; 51:820–813.

[97] Sandali M, Boubekri A, Mennouche Djamel. Thermal Behavior Modeling of a Cabinet Direct Solar Dryer as Influenced by Sensible Heat Storage in a Fractured Porous Medium. AIP Conference Proceedings 1968, 020014(2018); http://doi.org/10.1063/1.5039173.

[98] Chen W, Liu W. Numerical analysis of heat transfer in a passive solar composite wall with porous absorber. Applied Thermal Engineering 28 (2008) 1251–1258.

[99] Watmuff J, Charters W, and Proctor D. Solar and wind induced external coefficients-solar collectors. Cooperation Mediterraneenne pour l'Energie Solaire, 1977: p. 56.

[100] Swinbank W C. Long-wave radiation from clear skies. Quarterly Journal of the Royal Meteorological Society, 1963. 89(381): p. 339-348.

[101] Varun, Sunil, Avdhesh S, Naveen S. Construction and performance analysis of an indirect solar dryer integrated with solar air heater. Procedia engineering 38 (2018) 3260-3269.

[102] Mathioulakis E, Karathanos VT, Belessiotis VG. Simulation of Air movement in a dryer by computational fluid dynamics: application for the drying of fruits. J FoodEng1998; 36:183–200.

[103] Hossain M, Amer B, Gottschalk K. Hybrid solar dryer for quality dried tomato. IntJDryEnergy2008;26(12):1561–601.

[104] Sevik S, Aktas M, Dog˘an H, Koçak S. Mushroom drying with solar assisted heat pump system. Energy Conversion and Management 72 (2013) 171–178.

[105] Xiao HW, Baia JW, Xiea L, Sunc DW, Gaoa ZJ. Thin-layer air impingement drying enhances drying rate of American ginseng (Panaxquinquefolium L.) slices with quality attributes considered. Food and bioproducts processing 94 (2015) 581–591.

[106] Sarsavadia PN. Development of a solar-assisted dryer and evaluation of energy requirement for the drying of onion. Renewable Energy 32 (2007) 2529–2547.

[107] Nair KKV, Bongirwar DR. Solar dryer for agricultural products, A do it yourself solar dryer. Indian Chemical Engineering 1994; 36 (3), 103–105.

[108] Naphon P. Effect of porous media on the performance of the double-pass flat plate solar air heater. International Communications in Heat and Mass Transfer 32, pp.140–150, 2005.

[109] Sallam YI, Aly MH, Nassar AF, Mohamed EA. Solar drying of whole mint plant under natural and forced convection. Journal of Advanced Research (2015) 6, 171–178.

[110] Sopian K, Supranto, Othman MY, Daud WRW, YatimB. Double-pass solar collectors with porous media suitable for higher-temperature solar assisted drying systems.JEnergyEng2007;133(13):13–8 1.

[111] G. Tiwari, P. Bhatia, A. K. Singih, R. K. Goyal, “Analytical studies of crop drying cum water heating system”, Energy Conversion & Management 1997; 38(8):751–759.

[112] G. Tiwari, P. Bhatia, A. K. Singh, R.F. Sutar, “Design parameters of a shallow bed solar crop dryer with reflector”, Energy Conversion & Management 1994; 35(6):542

[113] P. M. Chauhan, C. Choudhury, H. P. Garg, “Comparative performance of coriander dryer coupled to solar air heater and solar air-heater-cum-rock bed storage”, Applied Thermal Engineering 1996; 16(6):475–486.

[114] http://www.cetiat.fr/fr/produits/ventilation.cfm and www.ademe.fr

[115] K.J. Russell, “Are good electrical insulators also good thermal insulators? A study of thermal conductivity”, California state science fair. Project summary (2006). Ap 02/06.

[116] S. Medvedev, S. Khomik, H. Olivier, B. Gelfand, “Effectiveness of protective covers in case of a detonation wave reflection”, Institute of chemical physics, RAS, Moscow, Russia (2003) pp 1-4.

[117] Akmak GC, Yıldız C. The drying kinetics of seeded grape in solar dryer with PCM-based solar integrated collector. Food and bioproducts processing 89 (2011) 103–108.

[118] Shalaby SM, Bek MA. Experimental investigation of a novel indirect solar dryer implementing PCM as energy storage medium. Energy Conversion and Management 83 (2014) 1–8.

[119] Jain D, Tewari P. Performance of indirect through pass natural convective solar crop dryer with phase change thermal energy storage. Renewable Energy 80 (2015) 244-250.

[120] Shalaby SM, Bek MA, El-Sebaii AA. Solar dryers with PCM as energy storage medium: A review. Renewable and Sustainable Energy Reviews 33(2014)110–116.

[121] Srivastava AK, Shukla SK, Mishra S. Evaluation of Solar Dryer/Air Heater Performance and the Accuracy of the Result. Energy Procedia 57 (2014) 2360 – 2369.

[122] Dina SF, Ambarita H, Napitupulu FH, Kawai H. Study on effectiveness of continuous solar dryer integrated with desiccant thermal storage for drying cocoa beans. Case Studies in Thermal Engineering 5(2015)32–40.

[123] Reyes A, Mahn A, Vلsquez F. Mushrooms dehydration in a hybrid-solar dryer, using a phase change Material. Energy Conversion and Management 83 (2014) 241–248.

[124] Agarwal A, Sarviya RM. An experimental investigation of shell and tube latent heat storage for solar dryer using paraffin wax as heat storage material. Engineering Science and Technology, an International Journal 19 (2016) 619-631.

[125] Ayadi M, Mabrouk SB, Zouari I, Bellagi A. Simulation and performance of a solar air collector and a storage system for a drying unit. Solar Energy 107 (2014) 292–304.

[126] Bal LM, Satya S, Naik SN. Solar dryer with thermal energy storage systems for drying agricultural food products: A review. Renewable and Sustainable Energy Reviews 14 (2010) 2298–2314.

[127] Bal LM, Satya S, Naik SN, Meda V. Review of solar dryers with latent heat storage systems for agricultural products. Renewable and Sustainable Energy Reviews 15 (2011) 876–880.

[128] S.O. Enibe. Performance of a natural circulation solar air heating system with phase change material energy storage. Renewable Energy 27 (2002) 69–86

[129] Manish K. Rathod, Jyotirmay B, Thermal stability of phase change materials used in latent heat energy storage systems: A review, Renewable and Sustainable Energy Reviews 18 (2013) 246–258.

[130] Zalba B, Jose´ MM, Luisa FC, Harald M. Review on thermal energy storage with phase change: materials, heat transfer analysis and applications. Appl Therm Eng 2003;23:251–83.

[131] Francis A, Neil H, Philip E, Mervyn S. A review of materials, heat transfer and phase change problem formulation for latent heat thermal energy storage systems (LHTESS). Renewable and Sustainable Energy Reviews 14 (2010) 615–628.

[132] Murat Kenisarin, Khamid Mahkamov. Solar energy storage using phase change materials. Renewable and Sustainable Energy Reviews 11 (2007) 1913–1965.

[133] Abhat A. Low temperature latent heat thermal energy storage: heat storage materials. Solar Energy 1983;30(4):313–32].

[134] Dan Nchelatebe Nkwetta, Fariborz Haghighat, Thermal energy storage with phase change material—A state-of-theart review, Sustainable Cities and Society 10 (2014) 87–100.

[135] Nagano K, Mochida T, Takeda S, Domanski R, Rebow M. Thermal characteristics of manganese (II) nitrate hexahydrate as a phase change material for cooling systems. Appl Therm Eng 2003;23(2):229–41.

[136] Kakuichi H, Yamazaki M, Yabe M, Chihara S, Terunuma Y, Sakata Y, et al. A study of erythrol as phase change material. In: Proceedings of the 2nd workshop IEA annex 10, phase change materials and chemical reactions for thermal energy storage, 11–13 April 1998, Sofia, Bulgaria.)

[137] Fukai J, Kanou M, KodamaY, Miyatake O. Thermal conductivity enhancement of energy storage media using carbon fibers. Energy Convers Manag2000;41: 1543–56.

[138] Zhong Y, Guo Q, Li S, Shi J, Liu L. Heat transfer enhancement of paraffin wax using graphite foam for thermal energy storage. Sol Energy Mater Sol Cells 2010;94:1011–4.

[139] Morisson, Abdel-Khalik. Effects of phase-change energy storage on the performance of air-based and liquid-based solar heating systems. Solar Energy 1978;20:57–67.

[140] Ghoneim A. Comparison of theoretical models of phase-change and sensible heat storage for air and water-based solar heating systems. Solar Energy 1989;42(3):209–20.

[141] Surendra P, A K Singh and Dilip J. Mathematical Modelling and Techno-economic Evaluation of Hybrid Photovoltaic-thermal Forced Convection Solar Drying of Indian Jujube (Zizyphus mauritiana). Journal of Agricultural Engineering. Vol. 55 (4): October-December, 2018.

[142] Barnwal P; Tiwari G N. 2008. Grape drying by using hybrid photovoltaic–thermal (PV/T) greenhouse dryer: an experimental study. Sol. Energy, 82, 1131–1144.

[143] Singh D; Singh A K; Singh S P; Poonia S. 2017. Economic analysis of parabolic solar concentrator based distillation unit. Indian J. Eco. Dev., 13(3), 569-575.

[144] Sodha M S; Chandra R; Pathak K; Singh N P, Bansal N K. 1991. Technoeconomic analysis of typical dryers. Energy Convers. Manage., 31(6), 509-13.

[145] Boughali S, Benmoussa H, Bouchekima B, Mennouche D, Bouguettaia H, Bechki D. Crop drying by indirect active hybrid solar‐Electrical dryer in the eastern Algerian Septentrional Sahara. Solar Energy 83 (2009) 2223‐2232.

[146] Hossain M A, Woods J L, Bala B K. Optimization of solar tunnel drier for drying of chili without color loss. Renew. Energy, 30(5) 2005, 729-742.

Scientific valorization

- Messaoud Sandali, Abdelghani Boubekri, Djamel Mennouche, Noureddine Gherraf. Improvement of a direct solar dryer performance using a geothermal water heat exchanger as supplementary energetic supply. An experimental investigation and simulation study. Renewable Energy 135 (2019) 186-196.
- Messaoud Sandali, Abdelghani Boubekri, Djamel Mennouche. Improvement of the Thermal Performance of Solar Drying Systems Using Different Techniques: A Review. Journal of Solar Energy Engineering. 2019. doi:10.1115/1.4043613.
- Messaoud Sandali, Abdelghani Boubekri, Djamel Mennouche. Thermal behavior modeling of a cabinet direct solar dryer as influenced by sensible heat storage in a fractured porous medium. AIP Conference Proceedings 1968, 020014 (2018); doi: 10.1063/1.5039173.

- Messaoud Sandali, Abdelghani Boubekri, Djamel Mennouche. Numerical Study of the Thermal Performance of a Direct Solar Dryer with Integrated Geothermal Water Heat Exchanger. International Jornal of Scientific Research & Engineering Technology –IJSET Vol.5 pp31-38.

- Messaoud Sandali, Abdelghani Boubekri, Abderrahmane Benhamza, Belkhir Settou, Daoud Halassa, and Djamel Mennouche. Etude de l'influence des paramètres géométriques sur le comportement thermique du capteur solaire plan à air, 1st International Seminar on the Apport of the Simulation in Technological Innovation, Ghardaïa (Algeria), March, 07-08, 2017.

- Messaoud Sandali, Abdelghani Boubekri, Djamel Mennouche and Abderrahmane Benhamza. Etude du comportement thermique d'un séchoir solaire direct influencé par l'intégration d'un milieu poreux non consolide, 6ème Séminaire Maghrébin sur les Sciences et les Technologies de Séchage (SMSTS2018) Matmata (Tunisie) 19-21 Mars 2018.

- Messaoud Sandali, Abdelghani Boubekri, Said Mansouri, Bachir Zengui and Djamel Mennouche. Etude de l'effet de l'intégration d'une couche MCP sur les performances d'un séchoir solaire direct. Le 5ème Séminaire International sur les Energies Nouvelles et Renouvelables. Unité de Recherche Appliquée en Energies Renouvelables, Ghardaïa – Algeria 24 - 25 Octobre 2018.

- Messaoud Sandali, Abdelghani Boubekri, Abderrahmane Benhamza, Belkhir Settou, Daoud Halassa, and Djamel Mennouche. A simulation study of a solar collector using phase change materials for air heating application needs. AIP Conference Proceedings 1814, 020010 (2017); doi: 10.1063/1.4976229.